 31X

Russian Original Vol. 46, No. 5, May, 1979

November, 1979

LS - File

~~[illegible]~~

SATEAZ 46(5) 351-426 (1979)

SOVIET ATOMIC ENERGY

АТОМНАЯ ЭНЕРГИЯ

(ATOMNAYA ÉNERGIYA)

TRANSLATED FROM RUSSIAN

CONSULTANTS BUREAU, NEW YORK

SOVIET ATOMIC ENERGY

Soviet Atomic Energy is a cover-to-cover translation of *Atomnaya Énergiya*, a publication of the Academy of Sciences of the USSR.

An agreement with the Copyright Agency of the USSR (VAAP) makes available both advance copies of the Russian journal and original glossy photographs and artwork. This serves to decrease the necessary time lag between publication of the original and publication of the translation and helps to improve the quality of the latter. The translation began with the first issue of the Russian journal.

Consultants Bureau journals appear about six months after the publication of the original Russian issue. For bibliographic accuracy, the English issue published by Consultants Bureau carries the same number and date as the original Russian from which it was translated. For example, a Russian issue published in December will appear in a Consultants Bureau English translation about the following June, but the translation issue will carry the December date. When ordering any volume or particular issue of a Consultants Bureau journal, please specify the date and, where applicable, the volume and issue numbers of the original Russian. The material you will receive will be a translation of that Russian volume or issue.

Subscription (2 volumes per year)
Vols. 44 & 45: $130 per volume (6 Issues) — Single Issue: $50
Vols. 46 & 47: $147.50 per volume (6 Issues) — Single Article: $7.50

Prices somewhat higher outside the United States.

CONSULTANTS BUREAU, NEW YORK AND LONDON

227 West 17th Street
New York, New York 10011

Published monthly. Second-class postage paid at Jamaica, New York 11431.

Soviet Atomic Energy is abstracted or indexed in *Applied Mechanics Reviews, Chemical Abstracts, Engineering Index, INSPEC—Physics Abstracts and Electrical and Electronics Abstracts, Current Contents,* and *Nuclear Science Abstracts.*

SOVIET ATOMIC ENERGY

A translation of *Atomnaya Énergiya*

November, 1979

Volume 46, Number 5 May, 1979

CONTENTS

CONTENTS

(continued)

The Russian press date (podpisano k pechati) of this issue was 4/21/1979. Publication therefore did not occur prior to this date, but must be assumed to have taken place reasonably soon thereafter.

Declassified and Approved For Release 2013/02/12 : CIA-RDP10-02196R000800010005-1

THE PEACEFUL ATOM IN THE SOCIALIST COUNTRIES

A. F. Panasenkov

UDC 621.039(103)

In 1979 the Council for Mutual Economic Aid (COMECON) completed its 30th year of activity as the first international economic, scientific, and technical organization of socialist governments.

In January 1949 representatives of Bulgaria, Hungary, Poland, Rumania, the Soviet Union, and Czechoslovakia met in Moscow. The participants in this meeting to organize broader economic cooperation recognized the need to create COMECON. In April of the same year the first meeting of the COMECON Session was held and began the practical activity of the organization. Now the members of COMECON include 10 socialist governments: Bulgaria, Hungary, Vietnam (since 1968), the GDR (since 1950), Cuba (since 1972), Mongolia (since 1962), Poland, Romania, the Soviet Union, and Czechoslovakia. The member-nations of COMECON, with a population of 437 million, are developing relations on the principles of socialist internationalism, complete equality, mutual advantage, and friendly assistance to one another. During the three decades, the countries of the socialist community have made impressive advances in developing their economies and jointly solving the large-scale problems of scientific–technical progress. Their national income in 1978 was 10 times that of 1948 and industrial production has increased by 17 times. The member-countries of COMECON, occupying 18.7% of the territory and having 10.4% of the population, now produce about one-third of the world's industrial output, including generating 21% of its electricity, extracting 19% of its oil and 27% of its natural gas, and making 30% of its steel. With joint efforts involving the participation of more than 3000 scientific-research and design-construction organizations, more than 14,000 theoretical and applied projects have been completed, many of which have found practical application and have had a significant economic effect.

The year 1979 also marks the 25th anniversary of the peaceful use of atomic energy (startup of the first nuclear power plant in the world at Obninsk) and the start of national scientific centers in the member-nations of COMECON. By organizing such centers with the technical aid of the Soviet Union they have been able to begin nuclear research and train scientific staff in a comparatively short time. Thus, already in 1957–1958 research reactors were built and put into operation in Romania, Czechoslovakia, the GDR, and Poland, and later in Hungary and Bulgaria. These centers are equipped with other modern experimental equipment as well: charged-particle accelerators, and apparatus and equipment for nuclear physics and radiochemical research. The staffs (physicists, chemists, energy experts) needed for these purposes were trained in Soviet institutes.

The creation of their own scientific-research base in the socialist countries has led to a need for exchange of scientific–technical achievements, and the expansion of communication, coordination, and cooperation with regard to scientific developments on a multilateral basis. The first major step in the organization of multilateral collaboration was the creation of the Joint Institute for Nuclear Research (JINR) at Dubna in 1956. The entire world now knows of the great scientific achievements of this international collective of scientists who are successfully carrying out experimental and theoretical research in elementary particle physics, nuclear and neutron physics, biophysics, and solid-state physics. In 1976 the Institute was awarded the Order of Friendship among Peoples for advances in fundamental research and on the occasion of its 20th anniversary. Two further major achievements at the Institute in recent years should be noted: the startup of the powerful U-400 isochronous heavy ion accelerator in December, 1978 and the physical startup of the IBR-2 pulsed fast reactor and the LIU-30 high current injector in the same year.

The second important step in multilateral collaboration was the organization in 1960 of the Permanent Commission of COMECON on the Peaceful Uses of Atomic Energy, in which the participants are Bulgaria, Hungary, Vietnam, the GDR, Cuba, Poland, Romania, the Soviet Union, and Czechoslovakia. Its operating experience has shown that the Commission's activity is of considerable help in developing and strengthening collaboration among the member-nations of COMECON and in creating the prerequisites for efficient entry of nuclear technology into the national economy. The working organs (on reactor technology and nuclear power, on the processing and decontamination of radioactive wastes, on apparatus and installations for nuclear technology, and on radiation safety) of the Commission, meetings of specialists on various problems in nuclear

---

Director, Department for the Peaceful Uses of Atomic Energy of the Secretariat of COMECON. Translated from Atomnaya Énergiya, Vol. 46, No. 5, pp. 299-309, May, 1979.

0038-531X/79/4605-0351 $07.50

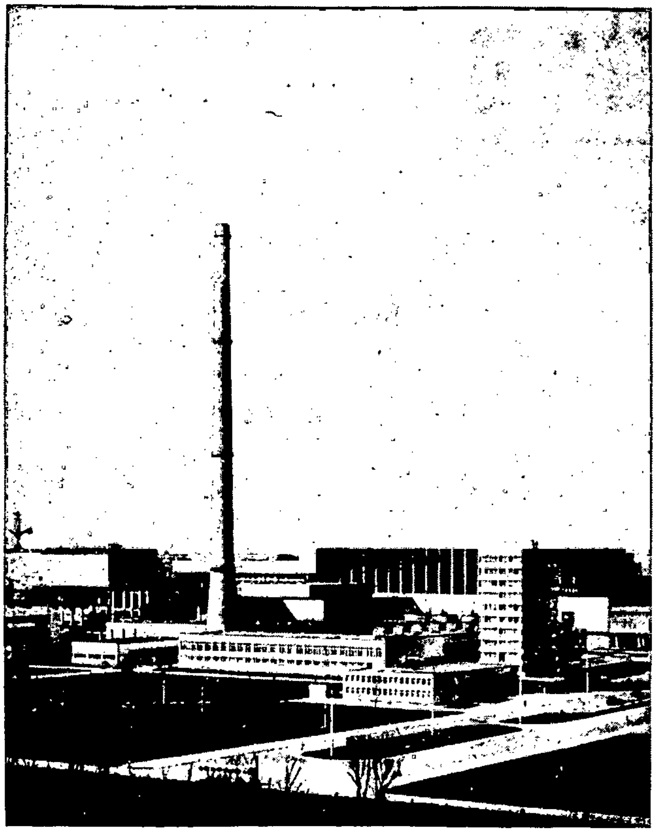

Bulgaria. The Kozlodui nuclear power station.

science and technology, and the Secretariat of COMECON (the Department for the Peaceful Uses of Atomic Energy) play an important role in the main activities of the Commission.

The multilateral scientific–technical collaboration in the framework of the commission encompasses broad areas of reactor science and technology, of nuclear power and its fuel cycle, of the construction of nuclear equipment, of the production and application of nuclides and sources of ionizing radiation, of radiation protection technology, of radiation safety, and of standardizing components for nuclear technology. The collaboration is realized on the basis of five-year plans, working plans on individual topics, 2-yr organizational–technical plans for the Commissions operations, and annual plans in the area of standardization. The most important work is included in the operating plans of the Executive Committee and in the combined documents on interdisciplinary problems of COMECON.

The Commission develops and coordinates prospective plans for cooperation. Thus, the five-year plan for scientific–technical cooperation in 1976–1980 envisions work on 15 major problems which presently cover more than 80 themes. About 90 scientific-research, construction, and industrial organizations are involved in this work. The delegation of the Soviet Union plays an invaluable role in the work of the Commission.

The most perceptible results achieved by the member-nations are in the development of reactor technology and nuclear energy. The discussion on the design engineering materials for an 880-MW nuclear power plant with two VVÉR-440 reactors prepared by the Soviet delegation, the collaboration on the VVÉR-1000 reactor, and the results of joint work on the reliability and safety of nuclear power plants, on the reprocessing and decontamination of radioactive waste, and other problems have had a significant effect on the formation of national programs for the development of nuclear power in the member-nations of COMECON. The results of this work are graphically obvious. While in 1960 only the Soviet Union had nuclear power stations, in 1979 they exist in Bulgaria, the GDR, and Czechoslovakia, one is being built in Hungary, and preliminary work for building nuclear power plants is being done in Cuba, Poland, and Romania. The growth in nuclear power plant output is also indicative: 1960 – 105 MW (USSR), 1965 – 465 MW (USSR), 1970 – 1100 MW (GDR and USSR), 1978 – 12,000 MW (Bulgaria, GDR, USSR, Czechoslovakia). To ensure this output, the Soviet has given the necessary design and technical documentation to the member-nations of COMECON, constructed the basic technological equipment, and provided technical help in building the nuclear power station, in startup and repair work, and in training the necessary staff.

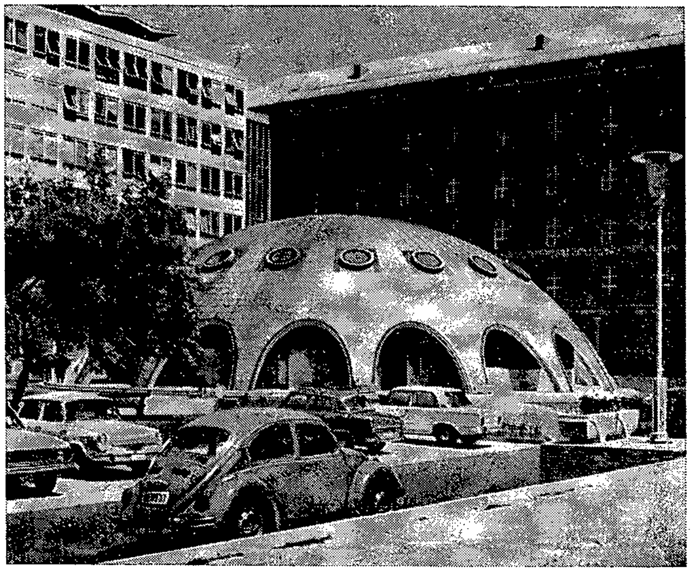

Hungary. The teaching reactor building at the Central Institute for Physical Research.

The Overall Program for Socialist Economic Integration adopted at the 25th meeting of the COMECON Session in 1971 is of considerable importance for the accelerated development of nuclear power. This program envisions the further development and effective entry of nuclear energy into the national economies. In accordance with this program, in recent years multilateral cooperation has concentrated on building and utilizing high power reactors using thermal and fast neutrons. Here the most important task is completion of work on the development and introduction into commercial use of a plant with an output of 1000 MW (the VVÉR-1000) which employs thermal neutrons and the accelerated development of a 1600-MW fast reactor (the BN-1600). In the current five-year plan the member-nations of COMECON have spent 200 million convertible rubles on scientific-research and engineering experimental work on these problems. Important developments have been realized in the course of this work: in Hungary a boron concentration meter has been developed and is being tested in the Kozlodui nuclear power station in Bulgaria and at the NVAES; in the GDR cluster systems for controlling the core of the VVÉR-1000 have been developed and are being tested jointly with the Soviet Union, a test version of an apparatus for determining the moisture content of steam has been constructed, and methods and apparatus have been developed for noise diagnostics of reactors; a device for monitoring inside a reactor and for monitoring the neutron flux of high power reactors has been constructed in Poland and the Soviet Union and is undergoing tests at the Kozlodui and Bruno Leuschner (GDR) nuclear power stations, at the NVAES, and at the Kolskaya nuclear power station (USSR); and, in Czechoslovakia modular steam generators for fast reactor nuclear power stations, high-capacity high-speed pumps for the primary loop of power stations using the VVÉR reactor, and a system for monitoring the metal of the vessel by acoustic emission as the reactor is operated have been developed. In accordance with the program for cooperation in the area of fast reactors, joint efforts have been undertaken by specialists from the member-nations of COMECON on fundamental studies on physics and hydrodynamics, programs for computing the complex physics of a breeder reactor, including a calculation of the burnup and refuelling, have been developed, an automatic plug indicator of impurities in the sodium coolant has been developed and tested, methods and devices have been developed for studying the dynamics of reactors using the oscillator method, neutron spectra have been measured, and so on.

The Commission determines the questions which are to be worked on under the agreements. They include the development of a system for obtaining and processing information on the working state of a power reactor, cluster regulators for the VVÉR-1000, and a system for monitoring the metal in the reactor vessel by an acoustic emission method, as well as experimental and computational studies on the heat transfer crisis in bunches of rods with a perforated barrier. Equipment will be built for an experimental prototype nuclear power station with a 300-MW fast reactor with a dissociating coolant. Also to be built are a high-power steam generator, prototype hydrogen, oxygen, and carbon monitors for the sodium loop, systems for acoustically detecting water and sodium flows in steam generators, and an experimental loop for the Maria reactor in Poland for studying emergencies in the cooling loop of the VVÉR. Radiation tests will be made of the fissile and construction materials and tests will be made of the fuel elements in the midst of the dissociating coolant in the Mariya reactor. Experimental and computational studies are to be made of the heat-transfer crisis in

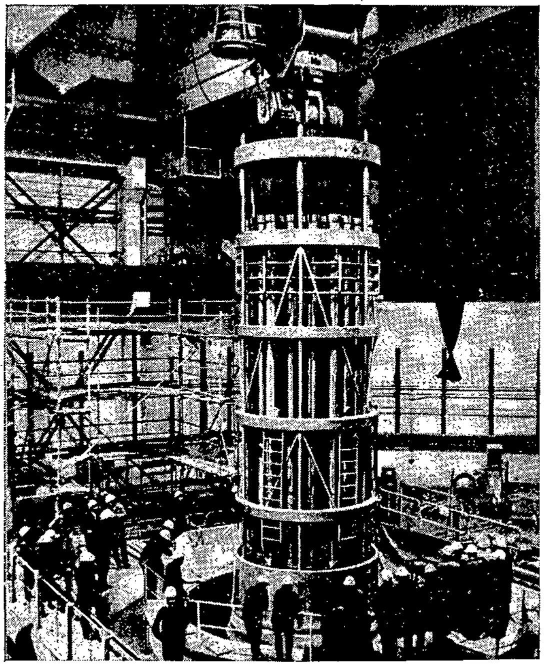

GDR. Installing the core of the Bruno Leuschner nuclear power station.

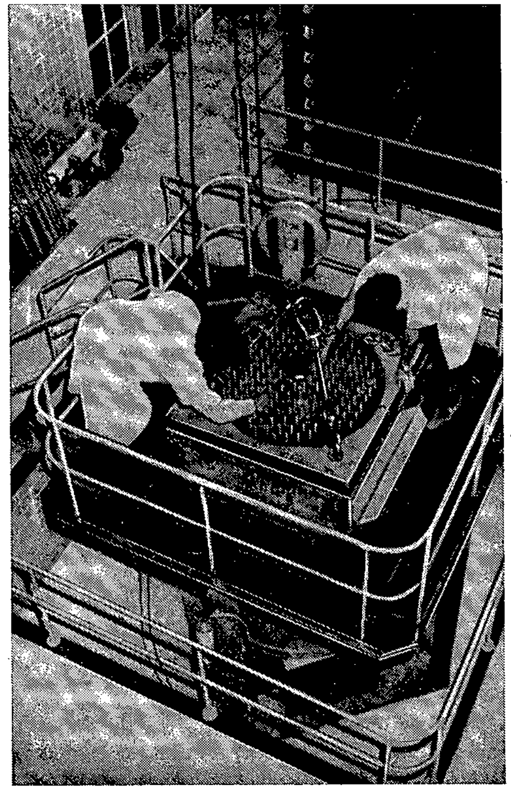

Cuba. A subcritical assembly at the Institute for Nuclear Research.

bunches of rods in nonstationary regimes including loss of coolant emergencies. Some of these tasks have already been completed.

An important step in the collaboration among the member-nations of COMECON and in the activity of the working units was the development of long-term cooperative program goals which are a further extension and realization of the complex Program. About 250 measures have been specified, including some providing for the economic requirements of the member-nations of COMECON for the basic forms of energy, fuel and raw materials and on the development of mechanical engineering based on specialization and cooperation in production, including the manufacture of equipment for nuclear power. The following problems are included in the subprogram of the Commission on Electric Power:

the construction and utilization of power plants with water-cooled—water-moderated (VVÉR) reactors with electrical power outputs of 1000 MW and the further improvement of this type of reactor;

the development of high-power fast reactors (with sodium or dissociating gases as a coolant); and,

the development of reactors for nuclear thermal power stations and for nuclear heat supply installations to produce industrial steam and provide central heating.

The delegations of the member-nations of COMECON to the Commission participate in working out the measures for realizing the Program for the maximum possible development of nuclear engineering production in the member-nations of COMECON. This Program is a composite part of the Long-Term Program for developing mechanical engineering on the basis of specialization and cooperation in production.

The fuel and energy problem is crucial to the collaboration among the member-nations of COMECON. Thus, at the 32rd meeting of the Session of COMECON (June, 1978), which took place at the level of heads of government, the Long-Term Goal Program for cooperation in energy, fuels, and raw materials, was established as a program of primary importance. This program envisions the accelerated development of nuclear power, an increased yield and improved utilization of the countries' own reserves of solid fuels, a provision for the further development of Combined Electrical Energy Systems, etc.

The construction in the European member-nations of COMECON and in Cuba of nuclear power plants with a total power of 37 GW with the technical assistance of the Soviet Union by 1990 and the joint construction by interested countries of the Khmelnitskaya nuclear power station with a power of 4 GW from VVÉR reactors

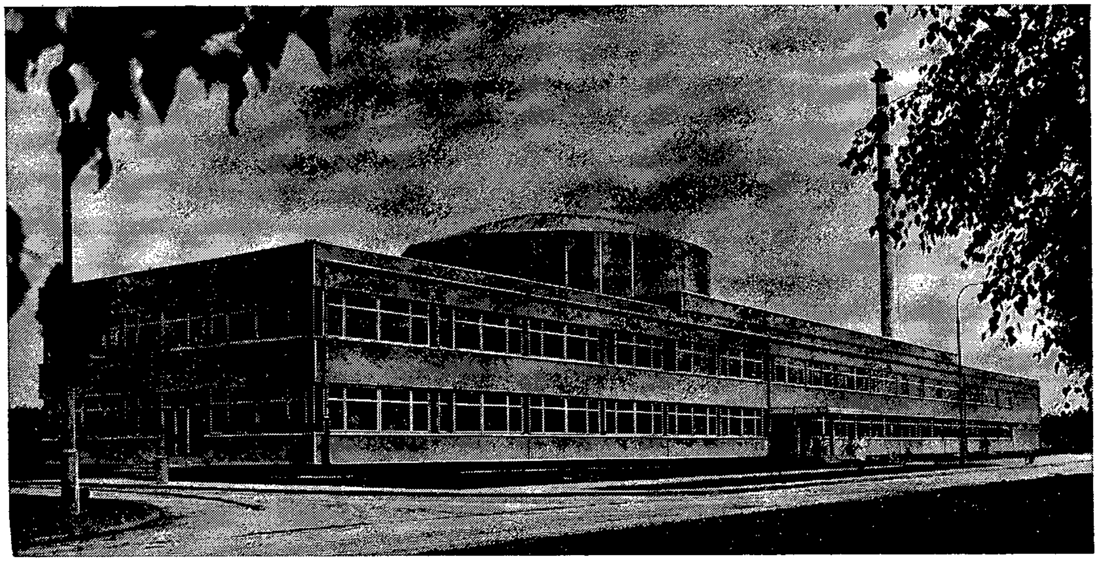

Poland. The building for the Maria research reactor at the Institute for Nuclear Research at Swierk.

to deliver energy to these countries will play a significant role in solving the energy problem.

Realization of the prospective program for the development of nuclear power requires efforts to create a nuclear engineering industry and to speed up the introduction of nuclear reactors with individual powers of 1000-1500 MW. At this time the member-nations of COMECON and the organs of the Council together with the "interatomenergo" organization are completing the preparation of an agreement on multilateral international specialization and cooperation in the production and mutual deliveries of nuclear power station equipment for the periods until 1990. This will also be aided by the electric transmission line (LÉP 750 kV) constructed in 1978 by the joint efforts of the member-nations of COMECON, which will make it possible to reliably build large nuclear power stations with powers of 4-5 GW at a single site.

The large-scale development of nuclear power requires substantial financial, material, and labor expenditure. The maximum economic efficiency can be achieved by correct choice of the optimum development paths. In this regard work on forecasts occupies an important place in the Commission's activity. Planning studies have shown that the best way of solving the fuel problem is the introduction of fast breeder reactors which makes it possible to improve the structure and fuel consumption levels of the nuclear power system.

The Commission devotes considerable attention to collaboration on improving and efficiently using research reactors. Work done for this purpose is of practical importance in the development and utilization of nuclear power reactors. Of these results the following should be noted:

mastering the techniques of manufacturing threshold detectors for determining the energy spectra of fast neutrons (in the Soviet Union);

the development of criteria for comparing the methods and equipment used for measurements inside reactors in order to standardize them within the COMECON framework;

the development of nondestructive methods for determining the burnup of nuclear fuel (in Poland and Romania);

the development of continuous detectors for measuring the neutron flux density (in several countries); and

the creation of calorimeters for determining the energy release in fuel elements and construction materials. Work has been done on monitoring and controlling research reactors by means of computers, an effort which is of great practical interest for creating automatic monitoring and control systems for nuclear power stations.

In recent years there has been a considerable expansion in the experimental prospects for research reactors in Hungary, the GDR, Poland, Romania, the Soviet Union, and Czechoslovakia as they have been rebuilt and their powers have been increased. New high-power research reactors have been built. This makes it possible to carry out a broad program of research in nuclear physics, solid-state physics, and the radiation

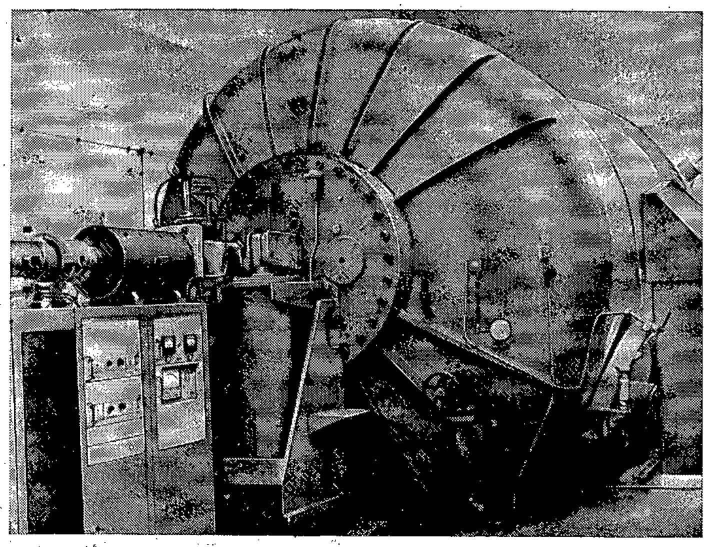

Romania. The electrostatic charge exchange accelerator
at the Institute of Physics and Nuclear Technology.

properties of materials and to obtain valuable data for the design and utilization of nuclear power plants.

One efficient form of collaboration is the activity of the Provisional International Scientific-Research Collective in reactor physics research on a VVÉR type critical assembly (at the Central Institute for Physical Research of the Hungarian Academy of Sciences in Budapest) which was organized on the Commissions' initiative in 1972. Work on improving available and developing new computational programs and measurement techniques for water-cooled–water-moderated (VVÉR) reactors is an important contribution to the creation and modernization of the cores of VVÉR-type reactors.

The development of nuclear power is inseparably coupled to improvements in the fuel cycle and the solution of complex problems in the reprocessing of spent nuclear fuel and the decontamination and burial of radioactive wastes. Scientific–technical collaboration in this area is characterized by cooperation and sharing of work, the carrying out of technical tasks, and the systematic presentation to the member-nation of annotated reports for discussion at the sessions of the working unit of the Commission.

A scheme has been developed for reprocessing nuclear fuel using tributyl phosphate and a heavy noncombustible diluent and is intended for reprocessing fuel elements with uranium burnup of about 30,000 MW days / ton. A further improvement of this scheme will make it possible to use it for fast reactor fuel element reprocessing with a burnup of roughly 100,000 MW days / ton of uranium. The apparatus and process have been developed for reprocessing nuclear fuel by a fluoride method which is used for finishing off the optimum variant of the gaseous fluoride method for recovery of fast reactor fuel elements, including BOR-60 fuel elements. The optimum capacity of a radiochemical plant has been determined and criteria have been established for choosing its site. Apparatus have been developed for the engineering design of nuclear fuel reprocessing schemes: small-scale fluctuation, turbine, and centrifugal extractors of various sizes and types (Poland and the USSR), a screw dissolver made of stainless steel, electromagnetic batchers, mixing and settling tanks, fluctuating columns (USSR), and others. The technology and apparatus have been created for removal of fuel-element jacket materials by thermal dissection; this method makes it possible to remove both the stainless steel shell (from the fuel elements of fast reactors) and the zirconium shells from the oxide fuel for the VVÉR. For monitoring and controlling the reprocessing of spent nuclear fuel, devices have been made for radiometric determination of uranium and plutonium and for the simultaneous determination of uranium and free nitric acid. Also a neutron method for measuring the levels of solutions and an acoustic method for monitoring the location of the phase interfaces in chemical apparatus, as well as neutron level meters and thermal flowmeters, have been developed. In order to increase the efficiency of fuel, use in nuclear power plants and to increase the accuracy of determinations of the amount of valuable components in spent nuclear fuel, specialists from the GDR, Poland, Romania, the Soviet Union, and Czechoslovakia are comparing measurements of the amounts of these components in solutions of spent nuclear fuel from VVÉR reactors (the SROK experiment).

An important link in the fuel cycle is the transport of spent fuel from a nuclear power station to the reprocessing site. Extensive work has been done on the construction and unification of transport, the technical conditions for the assembly of spent VVÉR-440 fuel elements have been worked out, and a special container

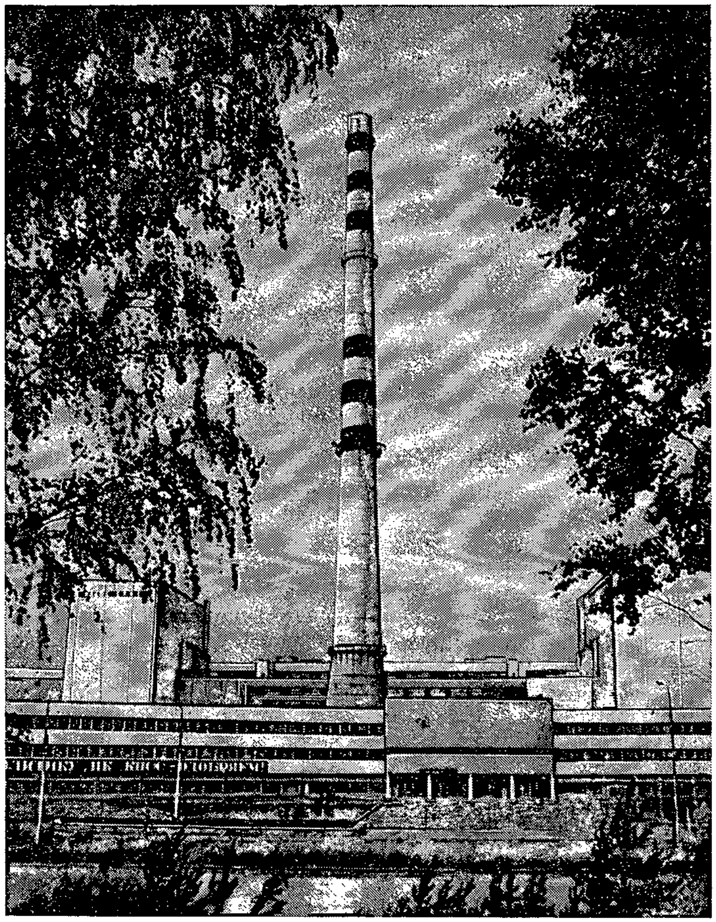

Soviet Union. The V. I. Lenin Nuclear Power Station in Leningrad.

has been developed for safe transport of fuel from a nuclear power plant based on a VVÉR reactor. As a result of this collaboration, rules for the safe transport of spent nuclear fuel from power stations in the member-nations of COMECON have been developed which regulate technical and legal matters.

One of the determining factors in the development of nuclear power is the rational and safe decontamination and removal of radioactive wastes produced by nuclear power stations. In recent years research and experimental work has been done in the member-nations of COMECON which will serve as a basis for the safe burial of solidified radioactive wastes. In Bulgaria, the GDR, Poland, the Soviet Union, and Czechoslovakia a large amount of data has been obtained on the rate of leaching of radionuclides from blocks made by adding various radioactive wastes to bitumen. In the GDR a process has been developed for solidifying liquid radioactive waste with concrete and ash from filters at thermal power stations. In Poland research has been done on reducing the rate of leaching of cesium and strontium and recommendations have been developed for the use of condensate resins and bentonite for this purpose. In the Soviet Union the mechanism of the radiation processes occurring in bitumen blocks of various composition and specific activity have been studied. In Czechoslovakia additives for increasing the degree of bonding of strontium and cesium isotopes in bitumen blocks have been studied. In the Soviet Union and Czechoslovakia a combination of equipment for bitumenizing nuclear power plant waste has been tested which demonstrates that standard equipment from other branches of industry (film apparatus, extruders, roller driers) can be adapted for bitumenizing radioactive wastes.

In the course of the collaboration, much work has been done on methods of burying radioactive wastes in geological formulations. The possibility of creating burial sites in various layers on the earth's surface has been studied: in surface levels (Hungary and Czechoslovakia), in deep aquiferous strata (USSR), and in salt formations (GDR). As a result, a technological basis has been created and experimental tests are being made of centralized underground burial sites for liquid, solid, and solidified radioactive waste of low and medium activity.

Because nuclear power plants have been in use in the Soviet Union, Bulgaria, and the GDR for a long time, experience has been gained in organizing and carrying out work on the decontamination of surfaces and equipment in nuclear power stations. This experience has made it possible to jointly develop a standard apparatus for decontamination of equipment in nuclear power stations with VVÉR-440 reactors.

The use of nuclear energy in industry, agriculture, and medicine has brought a new technology into being: nuclear and radioisotope instrument manufacture. Originally the instruments and apparatus of nuclear technology were developed and made in the scientific centers and pilot plants of the member-nations of the COMECON. Later, as cooperation developed and with the technical aid of the Soviet Union, this equipment has gained a secure place at such well-known firms as the "Electron" company in Sofia, the "Gamma" firm and the EMG factory in Budapest, the VEB "Otto Schön" in Dresden, the "Polon" works in Warsaw, and the "Tesla" firm in Prague.

The scientific–technical and industrial potential which has been created has made it possible to organize multilateral collaboration among the member-nations of COMECON in the area of nuclear instrument manufacture, taking into account the future development of power reactors and the need to develop and manufacture the instrumentation system for nuclear power plants. Thus, a group of instruments have been created for nuclear power plants using VVÉR reactors which monitors for radiation safety at the plant site and for fulfillment of the norms for emission of radioactive aerosols, and also provides for individual dosimetric monitoring of the personnel. This group of instruments is included in the design of the fifth unit of the NVAES (nuclear power station), in the third and fourth units of the Bruno Leuschner nuclear power station, and in the Dukovany nuclear power station in Czechoslovakia. In 1976-1978 a large amount of work was done in the GDR to determine the location of the regulator units in a VVÉR-440 reactor with a computer readout, and instruments for diagnosing the reactor were constructed. Specialists from the GDR, Poland, and Czechoslovakia have been involved in work to construct an instrument for measuring reactivity. In Hungary a second draft was prepared on the technical requirements for instruments for continuous monitoring of the concentration of boric acid in the coolant of a VVÉR. The technical specifications for promising new types of scintillation and gas-filled counters are being worked out in Czechoslovakia and Poland, respectively. The delegation of the Soviet Union to the Commission has prepared a proposal on the development of an analysis and forecast of the development and improvement of equipment for the manufacture of nuclear power plant instrumentation through 1995 and the Polish delegation heads the collaboration among the member-nations of COMECON and CAMAC instrumentation. The important contribution of Hungary, especially the "Gamma" firm, in organizing collaboration and directly working on systems of instruments, apparatus, and installations for nuclear medicine, including mastering the production of the MV-190 gamma camera for radioisotope diagnostics with an extensive data analysis system, should be noted.

In order to enhance the effectiveness and practical yield of the collaboration in the area of nuclear instruments and apparatus, the International Economic Union for Nuclear Instrument Manufacture "Interatominstrument" was created in Warsaw in 1972. The goal of this organization is to satisfy completely the needs of the member-nations of COMECON for high-quality nuclear instruments and apparatus at the world scientific–technical level. "Interatominstrument" now includes 15 manufacturing and foreign trade organizations from Bulgaria, Hungary, the GDR, Poland, the Soviet Union, and Czechoslovakia.

The principal problem of "Interatominstrument," given the large variety and small production runs of the nuclear instrument manufacturing industry, was to organize specialization and cooperation in the items produced. Already in 1976 an Agreement on Multilateral Specialization in Production was signed and in 1977 a supplement was added to it to cover 70 items with an overall volume of deliveries of about 65 million convertible rubles over the period until 1981. The inventory of specialized products includes equipment for radiographic laboratories, nuclear medical apparatus, radiometers and dosimeters, flaw detectors, automatic probe positioners, etc.

The economic activity of the Union is expanding on the basis of a statutory fund of 2,100,000 rubles. An important stage in this activity was the organization in 1975-1976 of three service affiliates in Bulgaria (Pleven), Poland (Zelena Gura), and the Soviet Union (Dubna) for technical service on their own and imported nuclear instrumentation. A significant profit was realized because of the success of these affiliates, which, together with income obtained from work on the economic agreements, made it possible to cover current expenses from the firm's own income without receiving supplementary payments from the members of "Interatominstrument"; i.e., they were able to become self-sufficient. One of the important tasks of "Interatominstrument" until 1990 is organizing work on specialization and cooperation on instruments and apparatus for monitoring and control of nuclear power stations using modern computer techniques.

In 1974 the Agreement on Multilateral International Specialization and Cooperation in the Production of Isotope Goods was concluded. This agreement has had a noticeable effect on the growth of goods exchange

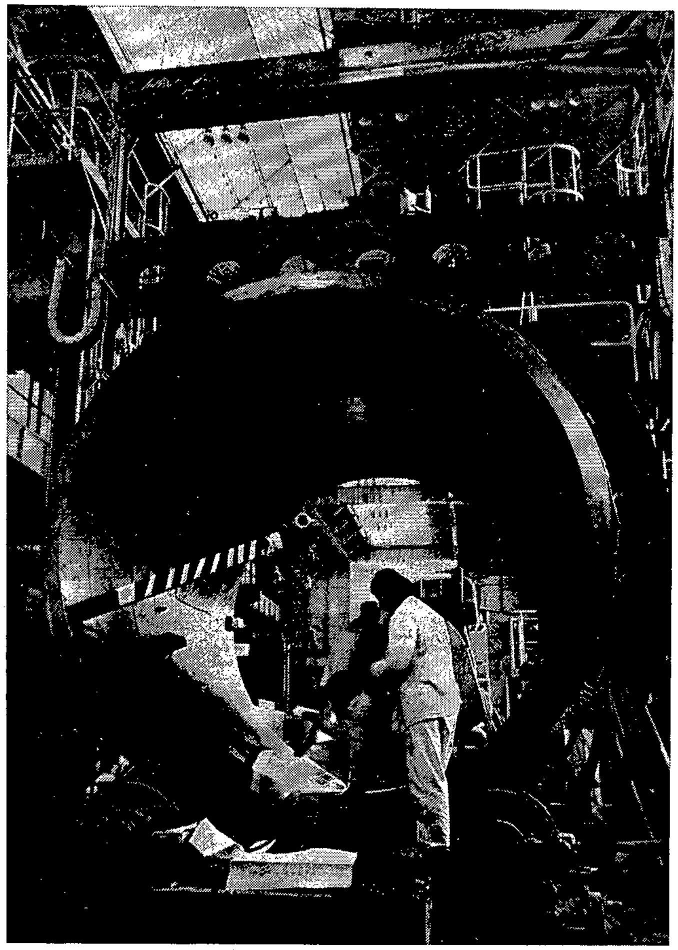

Czechoslovakia. Welding the vessel of a VVER-440 reactor at the Skoda works.

among the member-nations of COMECON, on the growth of foreign trade collaboration, and on improving the quality of isotope production. The inventory now includes 1463 items including 74 specialities from Hungary, 316 from the GDR, 87 from Poland, 113 from Romania, 714 from the Soviet Union, and 159 from Czechoslovakia. One result of the collaboration in this area was the Forecast of Production and Needs for Isotopes until 1990, which indicates that the production and use of radioisotope items in the member-nations of COMECON over the next 12-15 years will tend to increase by about 3 times.

As a result of the collaboration within the framework of the Commission on Radiation Technology, standards have been produced which determine a single approach to the construction, use, and economics of radiation technology equipment intended for obtaining materials with new useful properties, for increasing agricultural yield, for the fight against damage to food products, for sterilization of medical materials, and for environmental protection. The Forecast of Basic Radiation Technology and Radiation Equipment Development until 1990 and other specific technical proposals for organization in the member-nations of COMECON of industrial production of items from radiation modified wood, of radiation treated insulators for the electrical industry, and of radiation sterilized medical production have been developed.

In the area of radiation protection technology, cooperation is aimed at unifying and standardizing protective equipment and operational technological equipment used in work with radioactive materials and sources of ionizing radiation. Standards have been worked out for furniture and packaging assemblies as well as boxes, chambers, exhaust hoods, and manipulators. Work is under way on standardizing the manufacture of these items.

Collaboration on radiation safety is concentrated on such important topics as radiation monitoring of the environment, especially near nuclear power stations, the creation of standards needed for design, construction, and safe use of nuclear power stations, the development of measures for prevention of accidents at nuclear power stations and the liquidation of their consequences, working out measures for the reduction of exposure by nuclear power station personnel during normal operation, and providing safe working conditions with differents kinds of ionizing radiation sources. In this area the standards used in the member-nations of COMECON in their own national efforts have been developed.

Much work has been done on the standardization of nuclear technology equipment. The transition to devising COMECON standards covering the following four complex themes has been completed: "nuclear instrument manufacture," "isotpes and tracer compounds," "radiation protection technology," and "radiation technology." It is intended to develop 47 COMECON standards.

The radiation environments of the basins of the Danube River and of the Black and Baltic seas are being systematically studied. In this regard it is important to note the successful completion in August-September, 1978 of a joint expedition by specialists of the member-nations of COMECON to study the radioactivity of the Danube. During the expedition samples were taken at specified points and quick analyses were made of samples of soil, bottom sediments, fish tissue, and algae. The results of the analyses made it possible to conclude that the Danube had not been contaminated by radionuclides.

Multilateral scientific—technical cooperation is continually expanding and improving as it encompasses all the new areas of possible application of nuclear methods and materials. Besides the above-mentioned areas, cooperation has recently been organized on the technical utilization of superconductivity and controlled thermonuclear fusion.

The Commission and Secretariat of COMECON support constant contact with the Joint Institute for Nuclear Research (JINR). Representatives of the Institute regularly participate in the meetings of the Commission and its working organs and in many scientific—technical measures. Members of the COMECON Secretariat participate in meetings of the Scientific Council of the JINR. There is a wide exchange of information and materials between the COMECON Secretariat and the JINR.

With each year the contacts between the COMECON and the IAEA expand and are strengthened. Representatives of the IAEA are systematically invited to the Commission's activities and representatives of the COMECON Secretariat also participate in IAEA activities. In September 1975 an agreement was signed between the COMECON and the IAEA to enable further expansion of cooperation in the spirit of fulfilling the economic and scientific statues of the final act of the Conference on Security and Cooperation in Europe (Helsinki, 1975).

The international economic cooperation among the member-nations of COMECON is an historically based natural process in the development of a world-wide socialist system. It can be said that V. I. Lenin's assertion, made even before the victory of the Great October, that, as a counterweight to imperialism which alienates nations from one another, socialism will create "new, higher forms of human society when the legitimate needs and progressive hopes of the working masses of every nationality are first satisfied in international unity" [V. I. Lenin, Poln. Sobr. Soch. (Complete Collected Works), Vol. 26, p. 40], has been realized.

The Soviet Union makes a prominent contribution to the development of international economic relations of a new type and to the strengthening of the position of world socialism. Its successes in the building of communism, its consistent internationalist policy, and its fight to strengthen peace and for the relaxation of international tension have a deep influence on the course of world events. The Twenty-Fifth Congress of the Communist Party of the Soviet Union devoted great attention to the development of external economic links between the Soviet Union and other countries. Primary emphasis will be given in the future to developing and strengthening cooperation with the socialist countries in COMECON. At the Congress the General Secretary of the Central Committee of the Communist Party of the Soviet Union and Chairman of the Presidium of the Supreme Soviet of the USSR, Comrade L. I. Brezhnev said:

"Together with the fluorishing of every socialist country and the strengthening of the sovereignty of socialist states, their mutual ties become ever closer, more common elements appear in their policies, economics, and social life, and there is a gradual equalizing of their levels of development. This growing closeness of the socialist countries is now occurring most certainly as a natural law."

LITERATURE CITED

1. "30 Years of the Council for Mutual Economic Aid," Kommunist, No. 3, 15 (1979).
2. Atomic Science and Technology in the USSR [in Russian], Atomizdat, Moscow (1977).
3. I. Barbur et al., At. Energ., 43, 402 (1977).
4. Communique on the Thirty-Third Meeting of the Session of the Council for Mutual Economic Aid, Pravda (June 30, 1978).

ARTICLES

SAFETY PROBLEMS OF SODIUM – WATER STEAM GENERATORS AND THEIR SOLUTION IN THE USSR

V. M. Poplavskii, Yu. E. Bagdasarov, F. A. Kozlov, L. A. Kochetkov, and V. F. Titov

UDC 621.039.534.63

Sodium–water steam generators occupy an important position in the scheme of nuclear power stations (NPS) using fast reactors. This has been shown by the experience of operating the Enrico Fermi (U.S.A.), BN-350 (USSR), Phoenix (France), and PFR (Great Britain) NPS. As the various designs of steam generators for fast reactors were being developed, the opinion was expressed that first, no matter what the construction of the steam generator, it is necessary to consider the possibility of an emergency situation due to the entrance of water into the sodium and in view of this to develop an appropriate system of stand-by shielding of the steam generator; second, with the existing level of technology one can expect that steam generators with a single wall separating the water and sodium can be built whose construction meets the requirements of safety.

Because of its economic advantages, it was decided to separate the water and the sodium in the steam generator by a single wall when the BN-350 industrial NPS was being designed. Later, a similar principle of construction was also adopted in the BOR-60 installation. The application of single-wall construction in the sodium–water steam generator made it necessary to study a whole complex of problems related to the safety of these systems. Such studies, which began in the USSR in 1960, included the experimental and design-theoretical study of breakdown effects originating from various leaks of water into sodium, the creation of methods for making numerical estimates of accidental states of the sodium loop, and the development of schemes and the elements of a system for the stand-by shielding of a steam generator. In this review, we present the main results of a study of this set of problems, and also the approach adopted in the USSR for assuring the safety of the steam generators under discussion.

Experimental Study of Malfunctions and the Numerical Methods for Analyzing Accidental Situations. The first experimental studies made in the USSR of effects accompanying the integration of sodium with water under steam-generator conditions were intended to demonstrate the possibility, in principle, of creating a construction which would resist the contact of the coolant when substantial leaks develop.

A cycle of studies on various models from those having the simplest content to those repeating the fundamental features (material, geometry, weakening process, hydrodynamics) of the BN-350 and BOR-60 steam generator tube bundles [1-3] made it possible to expose the processes accompanying large leaks of water into sodium. The studies determined the characteristics of the pressure and temperature variation in the reaction zone and the hydrodynamical phenomena in the sodium loop (the deformation characteristics of the construction elements), while methods were developed for holding the damage parameters within allowable limits. By 1969 these studies had made it possible to formulate the principles of stand-by shielding for BN-350 NPS steam generator [4, 5]. Methods were developed for making numerical estimates of the main parameters (pressure, temperature, coolant flow rates) of the sodium loop in an emergency condition.

At the present time several methods are used to calculate these parameters with appropriate computer programs. Thus, in constructing steam generators with large sodium capacity, a method is used whose main assumptions reduce to the following [5]:

a) the only reaction used in the calculation is that involving the formation of a hydroxide and hydrogen;

b) the interaction reaction occurs instantly. The rate of accumulation of the reaction products is determined by an assigned rate of discharge of water into the sodium, and the quantity of the discharge is not affected by the pressure in the sodium cavity;

c) the distribution of the parameters (temperature and pressure) in the volume of the reaction products is uniform;

Translated from Atomnaya Énergiya, Vol. 46, No. 5, pp. 311-316, May, 1979. Original article submitted April 17, 1978.

d) the maximum possible theoretical values of pressure and temperature develop (under adiabatic conditions) in the zone of the reaction products at the initial instant;

e) the heat exchange of the interaction zone containing the reaction products with the surrounding medium is neglected.

The assigned discharge rate of water into sodium and its time dependence are determined from a postulated maximal breakdown in the steam generator assumed to be an instantaneous break equal to the total cross section of one tube. This choice was made after a special analysis of the effect of the type of postulated accident on the developing pressure and temperature in the steam generator and second loop. It was shown that this type of accident has more dangerous (from the standpoint of dynamical loads) consequences than any other sequence of gradual opening of even several tubes at the maximum rate that can be predicted from practice, experiments, or calculations.

The calculated maximum pressure in BN-350 or BN-600 steam generators under an accidental condition involving instantaneous rupture of the complete cross section of one heat-transfer tube amounts to $9 \cdot 10^5$ or $2 \cdot 10^6$ Pa, respectively. The acoustical approximation is used to take the compressibility of sodium into account. A simplified calculational program which neglects the compressibility of sodium can be used in an approximate analysis of the hydrodynamical effects in the elements of the sodium loop and in the determination of the time-varying pressure field. A calculation method based on a quasistationary view of the processes is used in preliminary multivariate calculations for determining the maximum pressure in the reaction zone.

For steam generator construction where the sodium moves in separate channels (e.g., the "inverse" type), a method has been developed in which the rate of discharge of the water into the sodium is determined by the drop in pressure between the steam and sodium chambers in the damage zone, and the interaction rate of the reagents is determined by the process of mass exchange between the sodium and the water through the hydrogen vapor look formed in the sodium channel and also by the interaction of the water reaching the channel with the sodium film remaining on the walls of the channel.

The first studies of the characteristics of malfunctions involving small leaks of water into sodium were made in 1962 [1]. It was discovered that as the water enters the sodium in the intertube space at rates of up to several hundredths of a kilogram per second through a calibrated opening 0.5-1.5 mm in diameter, a zone of higher temperature is formed (the reaction flare), followed by arcing over through the adjacent tube wall. Extensive investigations were subsequently undertaken in order to show the main effects associated with small leaks, using experiments both on targets and on models simulating the steam generator junctions.

The effect of leak sizes and spacing between specimens on the rate of failure of various materials [6] was studied on targets at sodium temperatures of up to 500°C and steam discharge rates in the range 0.001-0.011 kg/sec, using pearlite (1Kh2M), ferrite (0Kh12N2M), austenite (1Kh18N10T), and high-nickel (sanicro-31) steels. It was found that the maximum rate of corrosion—erosion damage obtains when the ratio of the target-nozzle distance to the nozzle diameter is 25.

The resistance to failure of the high-nickel steel is $\approx$2.5, 3.5, and 6 times as high, respectively, as that of 1Kh18N10T, 0Kh12N2M, and 1Kh2M steels (according to the rate at which the mass of steel is carried out in the zone of influence of the reaction products).

The study of the effect of temperature, phase, and geometric factors on the failure rate of a material in the zone of small leaks as applied to the conditions which were obtained in a BN-350 steam generator provided a means to explain the nature and rate of development of breakdowns in steam generators. It was also found that irrespective of the temperature regime, a small leak in a gas cavity is not accompanied by appreciable self-development and corrosion—erosion damage of the elements of the tube bundle.

Special investigations were devoted to the evolution of leaks. It was shown that the sodium temperature has a decisive effect on the self-development of leaks in pearlite (1Kh2M), austenite (Kh18N10T), and high-nickel (Kh20N40V) steels. A reduction in temperature from 450 to 300°C is associated with a drop in the rate of self-development of the leak by almost an order of magnitude, irrespective of the type of steel. Self-development of the leak is observed when water containing up to 5% by mass of sodium hydroxide is discharged into the air through an opening in 1Kh2M steel. On the basis of this, it can be assumed that the controlling factor affecting the growth in the size of the leak as a function of time is the penetration of the alkali formed from the reaction of the sodium with water in the discharge channel.

In the case of the BN-350 steam generator, a model study was made of the dynamics of the susceptibility of the tubes to damage at the onset of a small leak. The typical behavior of the development in time of a small leak was found for this type of construction. The analysis of the breakdown situations observed in the steam generators and the comparison of the results obtained with experiment confirmed the possibility of predicting the dynamics of the breakdown processes by studying them on steam generator models.

Investigations of small leaks in tube panels [7, 8] showed that failure of materials occurs only when local radiation jets are formed, and failure does not occur if the leak is observed along the perimeter of the junction of the tube with the tube panel. Metallographic studies of the specimens showed that along with the leaks in tubes, the failure which occurs is frontal for the pearlite steels and along the grain boundaries in the austenite steels.

Experimental studies of the leaks of water into sodium were also made on models having inverted construction (sodium in the tubes, water in the intertube space). It was found that if the sodium flow rate through the stand-by channel is maintained during a malfunction in an inverted-construction steam generator, the abrasion rate of the steel in the channel approaches the rate found in the usual construction at leak rates above 0.001 kg/sec. For leaks in the range 10^{-4}-10^{-3} kg/sec, the abrasion rate in the material in the inverted-construction steam generator is almost an order of magnitude less than that found in the usual construction.

If a "stopped-up" regime is established while the water is leaking into the sodium in a stand-by channel, the rate of corrosion–erosion failure at the location of the leak drops as the flow rate of the water increases, in contrast to the increased abrasion found in the uninverted construction.

Regimes were observed in which the failure rate of the material in a steam generator using inverted construction was the same whether the coolant flow was stopped up or not. However, the rate still remained less than the rate under the conditions of the uninverted steam generator construction.

Up to now, the design-theoretical investigations in the USSR in the field of small leaks of water into sodium have been made to develop methods for calculating the parameters in the flare of the reaction in order to obtain additional data (along with experimental data) that would explain the mechanism of failure of materials. A method based on the behavior of the turbulent heat and mass transfer was proposed for the purpose of calculating the field of concentrations, temperatures, and velocities in the region of the reaction flare [9].

At the present time there have been developed criteria and methods for analyzing experimental data in order to establish requirements for a stand-by shielding system of a steam generator in the "small leak" regime. The characteristics of a system of stand-by shielding of a steam generator are considered as satisfactory if the time required for an opening to develop in the wall between the neighboring and the current tube is less than the overall time required for detecting the leak and evacuating the steam–water cavity. Two methods are used to obtain this overall time as applied to the conditions of the steam-generator construction being analyzed. The first method is based on two experimental relationships: the behavior of the increase of the leak in time (self-development) and the dependence of the rate of damage of the material on the size of the leak (at each point of this functional relationship, the leak is constant in time). The required parameters which characterize the malfunction and the requirements for the shielding systems of natural steam generators are found by jointly analyzing the above data. It was in this way that small-leak malfunctions were studied as applied to the BN-350 steam generator installation.

The second method is based on the assumption that the leak which originally developed stays constant throughout the whole time of the damage process in the adjacent tube wall. The experimentally determined relation between the size of the initial leak and the time interval from the moment a small leak starts to the time it suddenly begins to increase (the experiments were done with a minimum amount of water entering into the sodium) was used as a starting relationship, as well as the relationship between the size of the unvarying (in time) leak and the rate of failure of the adjacent tube material. If the time that such a leak exists at a constant level is larger than the time required for the tube wall to fail during the process, the failure time is used as the maximum allowable. The time of existence of the leak at a constant level is used as the controlling quantity with an inverse relationship.

A similar method was used to analyze the small-leak regime for a BN-600 steam generator.

Steam-Generator Construction and Breakdown Processes. Requirements for a System of Stand-By Shielding and the Development of Its Elements. It is well known that shell-type steam generators were the first types of sodium–water steam generators constructed in the USSR (at the BOR-60 and BN-350 nuclear power stations). With this type of construction it is almost impossible to localize the zone of failure or the damaged element, and therefore the whole steam generator is taken out of service in case any leak of water into the sodium develops in a malfunction. An appropriate stand-by shielding system (SSS) was developed, which was linked to the construction characteristics. This system must also form an emergency signal at the proper time for any size of the initial leak of water into sodium (so that small leaks that arise are not allowed to become large ones), and also to ensure the safety of the construction after the emergency signal is received. The main characteristics of the SSS (compensated volumes, quick operation of the equipment in water, number and nature of the safety devices, and the hydraulic characteristics of the run-off lines, separating devices, expanders, etc.) must satisfy the previously stated requirements with due regard for a possible "large-leak" regime.

As shown by the experience of operating the BN-350 steam generator, the SSS which was developed satisfactorily handled the problems of preventing the failure of the elements of the sodium loop in the presence of large leaks. However, when the steam generator was operated in the small-leak regime at high temperatures, the stand-by shielding system did not prevent the small leaks from becoming large. This is mainly due to the fact that at the time the BN-350 was being developed and installed (1965-1971) the characteristic self-development time of small leaks was not yet known.

The tendency to limit the reaction zone of the sodium—water interaction to within the confines of a small element comprising only part of the steam generator and also considerations of a technological nature subsequently led to the creation of structures whose heat-exchange surfaces are placed in small modules connected in a unit (sectioned steam generators) [10]. As is known, a sectioned steam generator is being proposed for use in the BN-600 nuclear power station [11]. The main operating regime of the SSS of this steam generator on the appearance of a leak in one of the sections is a disabling of the whole steam generator. The cut-off fittings in the steam—water and sodium channels of each section make it possible to detach the stand-by section after a shutdown of the steam generator and then starting it up using the effective elements. The algorithm of excluding the damaged section while the equipment is in operation is proposed for use as an auxiliary regime of the SSS (in case a section is discovered in time at the small-leak level).

A system of stand-by shielding of sectioned steam generators is now being developed in the USSR, based on the stipulation that the stand-by section is disconnected without shutdown of the steam generator for any leak, with the main requirements for the SSS being [12]:

a) at the moment a signal is received indicating the presence of a leak in the steam generator by means of a subsystem forming a malfunction signal, there must be provided an assured selectivity (identification of the stand-by section);

b) after detection of the stand-by section, it must be isolated at the proper time from the main loop and from the remaining effective sections of the steam generator (i.e., until the time the maximum allowable corrosion—erosion deterioration of the construction elements is reached or until reaching the maximum allowable contamination of the coolant of the main loop by the reaction products);

c) the criterion of quick operation in disconnecting the damaged section in the sodium and steam—water channels must be the prevention of the entrance of the reaction products from the stand-by section into the main circulating loop in the "large-leak" regime (instantaneous and total failure of one tube);

d) the shielding system must prevent the pressure from rising above the maximum permissible value not only in the main sodium loop, but also in the excluded section, i.e., to ensure the safety of the stand-by element;

e) irrespective of the size of the leak, the coolant of the isolated section must be totally drained at the proper time along the steam—water and sodium loops and the spaces filled with an inert atmosphere.

The required characteristics of the SSS elements (sensitivity and time constant of the system for indicating large and small leaks, quick operation of the fittings, etc.) which satisfy the above requirements are determined with allowance for corrosion—erosion failure of the material in the leak zone, and also with allowance for the parameters of the sodium and steam—water channels of the steam generator [12]. The experience in operating the steam generator of the BN-350 installation confirmed the need for draining the coolant with the reaction products at the proper time, since the duration of stay of corrosive products within the confines of the stand-by zone led to considerable secondary corrosive failure of the tube bundle elements.

As shown by analysis, the use of sectioned steam generators with appropriate SSS makes it possible to shorten the time the reaction products act on the structural elements of the stand-by section, and to decrease the total contamination of the sodium loop even allowing for the growth of the leak with time (the small volumes of sodium and water within the confines of the stand-by section and the use of fast-acting mechanisms leads to a rapid drainage of the section with respect to both loops and to its isolation from the effective elements). In view of this, it appears to be possible in principle to simplify the system for indicating small leaks through the application of quick-acting devices with a certain reduction of the requirements for their sensitivity (the use of simplified acoustic systems, magnetic flow gauges, etc.).

The development of the elements of a system of emergency shielding for sodium–water steam generators in the USSR is proceeding in several directions at the present time. Systems for measuring hydrogen concentration in sodium and in gas cavities are being introduced as a way of indicating small leaks. The concentration-measuring devices involve diffusion membranes (in sodium or a gas) combined with a magnetic discharge pump. Allowing for possible signal overshoots, the sensitivity of the system for indicating hydrogen in sodium which was obtained in a test lasting 1000 h was $5 \cdot 10^{-6}$% by mass. A group of experiments on the BN-350 shows that it is possible to reach a sensitivity of ~(1-2) $\cdot 10^{-6}$% by mass under industrial conditions. The sensitivity of the devices for indicating hydrogen in gas is 10^{-3}% by volume, which can be considered as completely acceptable with existing background concentrations. A group of studies of instrumentation noise in the BP-10, BOR-60, and BN-350 reactors was used for developing acoustic systems, plus an analysis just of the noises of the leaks of water into sodium with models. Devices that record the change of pressure in gas cavities as well as the flow of sodium in the sections (for sectioned construction) are used to indicate large leaks in steam generators. Membranes that undergo spontaneous or forced rupturing in the gas cavities are used as safety devices in steam-generator SSS. Hydraulically driven equipment with action times as low as 5 sec was used for emergency drainage of the steam–water loop. Fast-acting sodium equipment is being developed for the sectioned construction. Systems for the discharge and separation of the reaction products use a design for two-stage separation by changing the direction and velocity of the gas–liquid mixture. Cycle-type devices are not used.

Conclusions. From the results of experimental studies on models, computer investigations based on methods which have been developed, and the analysis of malfunctions in BN-350 steam generators, it is now possible to give a fairly complete description of the evolution of breakdown processes for various leaks of water into sodium (large and small leaks). The experience of the BN-350 is of fundamental importance from the point of view of the possibility of combining sodium and water in an NPS scheme and the validity of separating them by one wall in industrial steam generators. It was shown that even when considerable water enters the sodium, it is possible to contain the breakdown processes within the sodium circuit without it disintegrating.

The presently available information about breakdown processes associated with a leak of water into sodium makes it possible to formulate the main requirements for a steam generator and its stand-by shielding system (the sensitivity of leak-indicating instruments, the response speed of protective devices, the characteristics of the discharge and separation devices, etc.) which would not only ensure the safety of the NPS, but also to reduce to a minimum the size of the failure of the steam-generator elements and the extent of contamination of the coolant by the reaction products in a breakdown regime. In view of this, a steam generator with sectioned construction and an appropriate shielding system has certain advantages which make it possible to contain the breakdown effects within the confines of the damaged section and to ensure (when necessary) the continuous operation of the steam generator on the effective sections no matter what the size of the initial leak of water into the sodium.

LITERATURE CITED

1. V. M. Poplavskii et al., Teploenergetika, 6, 70 (1966).
2. A. I. Leipunskii et al., At. Energ., 22, No. 1, 13 (1967).
3. Yu. E. Bagdasarov et al., Technical Problems of Fast Neutron Reactors [in Russian], Atomizdat, Moscow (1969).
4. B. I. Lukasevich et al., in: Proc. Study Group Meeting on Steam Generators for LMFBR's, Bensberg, Oct. 14-17 (1974), p. 239.
5. V. M. Poplavskii et al., At. Energ., 30, No. 2, 191 (1971).
6. A. S. Mazanov et al. [4], p. 129.
7. F. I. Kozlov et al., in: Proc. US/USSR Seminar on the Development of Sodium-Cooled Fast Breeder Reactor Steam Generators, Los Angeles, Dec. 2-4 (1974), p. 367.
8. V. M. Poplavskii et al., in: State and Perspectives of Work on Creating NPS Using Fast Breeder Reactors [in Russian], Vol. II, FEI, Obninsk (1975), p. 518.
9. V. V. Petukhov et al. [7], p. 540.
10. V. F. Titov et al. [8], Vol. I, p. 608.
11. V. F. Titov et al. [7], p. 243.
12. V. M. Poplavskii et al. [7], p. 488.

ACCURACY OF NEUTRON FIELD REGULATION IN NUCLEAR REACTORS

L. P. Plekhanov

UDC 621.039.515

One way to improve the performance of a nuclear power reactor is to increase the accuracy of three-dimensional regulation of its neutron field. The problem is solved by designing field regulation systems equipped with several sensors and regulators. The problem has been the topic of several works [1-5] which discussed system design and stability as well as the theoretical and experimental behavior of complete systems.

Unfortunately, certain important aspects of the problem have been somewhat neglected. One is the dependence of steady-state regulation accuracy on the number and location of sensors and control devices, on the sensor accuracy, on the regulator dead zone, etc.

In this article we discuss the relationships that govern the steady-state accuracy of neutron field regulation.

Formulation of the Problem. Let the deviation $\Delta\Phi(r)$ of the field from the rated steady-state distribution taking into account internal feedbacks be described by the linear boundary problem

$$\begin{aligned} &L(\Delta\Phi)=f(\Delta\alpha);\\ &B[\Delta\Phi(r)]=0, \quad r\in\Gamma, \end{aligned} \tag{1}$$

where Γ is the core boundary; L and B, linear operators; f, an operator; and $\Delta\alpha(r)$, change in the neutron multiplication constant (the perturbation).

The perturbation is assumed to be bounded by one of the following two inequalities with known right-hand sides:

$$|f[\Delta\alpha(r)]|\leqslant F(r); \tag{2a}$$

$$\int\{f[\Delta\alpha(r)]\}^2\,dV(r)\leqslant A^2. \tag{2b}$$

Here and in the following all integrals are taken over the entire core volume.

The regulation system is defined by the following data. N_s sensors with an error δ_i are located at points r_i ($i = 1, 2, \ldots, N_s$) of the reactor core. After being compared with the rated value, the signal of sensor i is applied to the k-th regulator with a weight factor c_{ki}. The total number of regulators is N_r. A regulator with number k controls one control device (e.g., a rod) located at the point ξ_k ($k = 1, 2, \ldots, N_r$) and has a regulation error (or dead zone) Δ_k.

It is assumed that the regulation system is stable and that the shape of control rods (CR) in the geometry of (1) remains practically unchanged. We have to find the steady-state regulation error $\Delta\Phi(r)$ at any point r of the reactor core as a function of the regulator errors Δ_k, the sensor errors δ_i, and the perturbation $\Delta\alpha$.

Basic Equations. Let us assume that the homogeneous problem corresponding to (1) has no nontrivial solution. This is true of most reactors operating under power-generating conditions (otherwise, see note at the end of the article). The desired regulation error can be written as

$$\Delta\Phi(r)=\sum_{k=1}^{N_r} G(r,\xi_k)\,f(\Delta\alpha_k)+\int G(r,\xi)\,f(\Delta\alpha(\xi))\,dV(\xi), \tag{3}$$

where $G(r, \xi)$ is Green's function of (1), $\Delta\alpha_k$ is the change in the neutron multiplication constant caused by the k-th CR. The regulator equation is

$$\sum_{i=1}^{N_s} c_{ki}\,[\Delta\Phi(r_i)+x_i]=y_k, \tag{4}$$

Translated from Atomnaya Énergiya, Vol. 46, No. 5, pp. 316-319, May, 1979. Original article submitted November 23, 1977.

 0038-531X/79/4605-0366$07.50

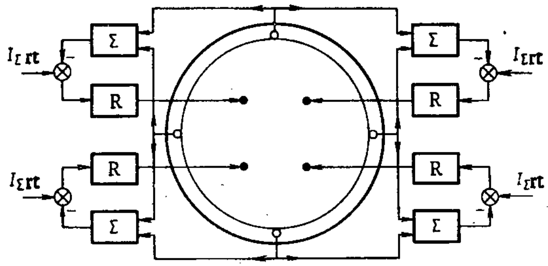

Fig. 1. Regulation system structure in which the CR location is not uniquely determined (here and in Fig. 3 – O) sensors; ●) control rods; and R) regulators.

where x_i and y_k are uncontrolled signals of the i-th sensor and k-th regulator that do not exceed the respective errors:

$$|x_i| \leqslant \delta_i; \quad |y_k| \leqslant \Delta_k. \tag{5}$$

Let us introduce the following notation: C, matrix of the factors c_{ki}; Δp, vector of CR effects with the elements $f(\Delta\alpha_k)$; G, static transfer matrix of an object whose elements $G(r_i, \xi_k)$ are changes of the field at the point of location of the i-th sensor caused by a single action of a k-th CR; $g(\xi)$, a vector function with elements $G(r_i, \xi)$ representing the change of field at points r_i caused by a single perturbation at point ξ; d(r), a vector function whose elements $G(r, \xi_k)$ represent field changes at points r due to a single effect of the k-th CR under the assumption that the matrix G and functions d(r) and $g(\xi)$ can be measured experimentally; x, the vector of x_i signals; and y, the vector of y_k signals.

In this notation, the regulator equation for Δp can be written as

$$CG\Delta p + \int Cg(\xi) f[\Delta\alpha(\xi)]\, dV(\xi) + Cx = y. \tag{6}$$

System Structure Demands. For Eq. (6) to be uniquely solvable for Δp it is necessary and sufficient that the matrix CG has a nonzero determinant. Otherwise, whenever det (CG) = 0, each Δp_k effect will depend on one or more arbitrary variables. In a practical system (e.g., such as the one shown in Fig. 1) this will cause great differences in CR operating times and result in large neutron field inhomogeneities. In fact, if in the system shown in Fig. 1 two opposite rods are pulled up for a certain distance, and the other two pushed down for the same distance, the system will not return to its former state. A system with such properties is unsatisfactory and the demand

$$\det(CG) \neq 0 \tag{7}$$

is obligatory in the selection of system structure, and of the sensor and CR locations. In the following discussion, the condition (7) is assumed to be satisfied.

Estimation of Regulation Accuracy. Substituting into (3) the expression for Δp obtained from (6), we get an expression for the regulation error:

$$\Delta\Phi(r) = d'(r)(CG)^{-1}y - d'(r)(CG)^{-1}Cx + \int f(\Delta\alpha(\xi))[G(r, \xi) - R(r, \xi)]\, dV(\xi), \tag{8}$$

in which a stroke denotes transposition. The function $R(r, \xi) = d'(r)(CG)^{-1}Cg(\xi)$, called the regulator nucleus, indicates what partial field is created at point r in the core by the regulation system in response to a single perturbation at the point ξ.

The first term of the regulation error in (8) is due to regulator errors (dead zones); the second, to sensor errors; and the third, to the effect of perturbations. Since these terms are independent, we will consider them individually denoting them by $\Delta\Phi_r$, $\Delta\Phi_s$, and $\Delta\Phi_p$. Thus, denoting the elements of vector function $d'(r) \times (CG)^{-1}$ by $q_k(r)$, we have from (8) and (5):

$$|\Delta\Phi_r(r)| \leqslant \sum_{k=1}^{N_r} |q_k(r)|\Delta_k; \tag{9}$$

$$|\Delta\Phi_s(r)| \leqslant \sum_{i=1}^{N_s} \left|\sum_{k=1}^{N_r} q_k(r) c_{ki}\right| \delta_i. \tag{10}$$

For practical purposes it is often more desirable to calculate the corresponding mean-square regulation errors $\sigma_r(r)$ and $\sigma_s(r)$. Assuming that x_i and y_k are independent random signals with dispersions a_i and b_k, respectively, we have from (8)

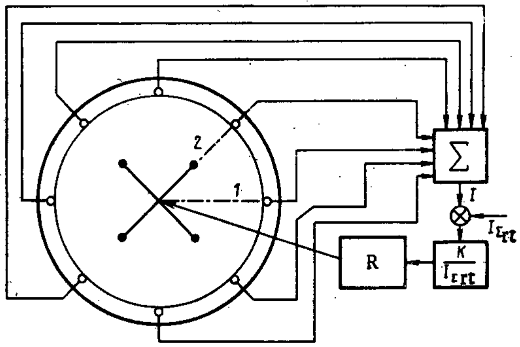

Fig. 2

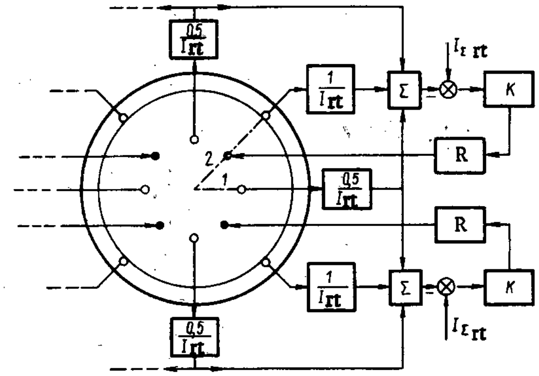

Fig. 3

Fig. 2. Integral regulation system (here and in Fig. 3 K denotes the amplification factor).

Fig. 3. Regional regulation system.

$$\sigma_{r}^{2}(r)=\sum_{k=1}^{N_r} q_k^2(r)\, b_k; \tag{11}$$

$$\sigma_s(r)=\sum_{i=1}^{N_s}\Big(\sum_{k=1}^{N_r} q_k(r)\, c_{ki}\Big)^2 a_i. \tag{12}$$

For the regulation error due to perturbations, we have estimates obtained from (2) and (8) using the Cauchy–Bunyakovskii inequality:

$$|\Delta\Phi_p(r)| \leqslant \int F(\xi)\,|G(r,\xi)-R(r,\xi)|\,dV(\xi), \tag{13a}$$

$$|\Delta\Phi_p(r)| \leqslant A\left\{\int [G(r,\xi)-R(r,\xi)]^2\,dV(\xi)\right\}^{1/2} \tag{13b}$$

The right-hand sides of (9)-(13) are distributed estimates of the respective errors expressed through known problem parameters.

All regulation errors depend on the location of sensors and control rods, and on the interdependence factors c_{ki}. Since these dependences are very complex, it is possible to make only some general conclusions. The regulation error due to the regulator dead zones (9) and (11) decreases when all c_{ki} factors increase; other errors do not possess this property.

To reduce the regulation error $\Delta\Phi_p(r)$ due to the effect of perturbations, the regulator nucleus $R(r, \xi)$ must be made to approximate Green's function $G(r, \xi)$ as closely as possible. Expansion of Green's function $G(r, \xi) = \sum_{k=1}^{\infty} \frac{\psi_k(r)\bar{\psi}_k(\xi)}{\lambda_k}$, where $\psi_k(r)$ and $\bar{\psi}_k(\xi)$ are eigenfunctions (harmonics) of (1) and of its conjugate, respectively, indicates that the regulator must first of all compensate the perturbation harmonics corresponding to eigenvalues λ_k with the smallest moduli. It should be however born in mind that the regulation system also adds field distortions at the remaining uncompensated harmonics.

The calculated estimates allow to take measures to reduce the overall neutron field regulation error, to compare alternative sensor and control rod locations and regulator structures, etc. The results obtained by calculating the regulation error estimates for two systems shown in Figs. 2 and 3 are given below. The systems implement the "integral" and the "regional" regulation principles, respectively [4].

The object of regulation is a cylindrical reactor with a core having a 6-m radius, a 1-m-thick reflector, and a 1-m-thick enrichment zone. The power feedback is $0.5\beta/100\%$, where β is the effective delayed neutron fraction.

The mathematical model of the object is a one-group diffusion equation in which the reflector is allowed for by an effective increment of 0.65 m. The errors of sensors in the reflector and in the reactor, and of the

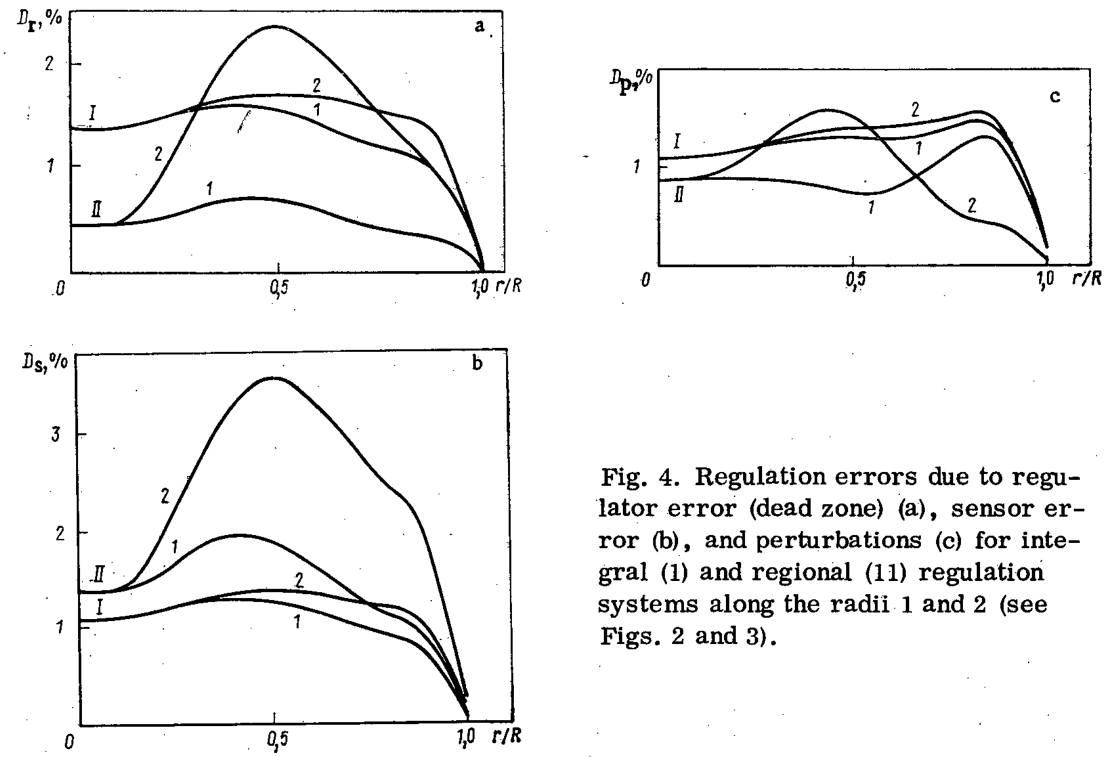

Fig. 4. Regulation errors due to regulator error (dead zone) (a), sensor error (b), and perturbations (c) for integral (1) and regional (11) regulation systems along the radii 1 and 2 (see Figs. 2 and 3).

regulator dead zone were taken as 1%, 2%, and 1%, respectively. The value A in the constraint (2b) was assumed to be 0.01. In Fig. 4 D_r, D_s, and D_p denote, respectively, the right sides of inequalities (9), (10), and (13b) in percent of rated field at the core center.

An analysis of the curves indicates that on the whole regional regulation gives a lower field regulation error due to regulator error and to perturbations than integral regulation. The regulation error due to sensor errors is greater in regional regulation as a result of the lower accuracy of sensors used in the reactor. In addition, the regional regulation system shows considerable local field distortions near the control rods.

Note. If the homogeneous problem (1) has a nonzero solution $\Phi^0(r)$, the term $\gamma\Phi^0(r)$ must be added to Eq. (3), and for $G(r, \xi)$ one must take the modified Green function orthogonal to $\Phi^0(r)$. To find the factor γ the system (3) and (4) must be supplemented with the equation for the perturbed-state criticality:

$$\sum_{k=1}^{N_r} \Phi^0(\xi_k) f(\Delta\alpha_k) + \int \Phi^0(\xi) f[\Delta\alpha(\xi)]\, dV(\xi) = 0.$$

The structural demand (7) remains valid and the estimates (9)-(13) are slightly corrected.

LITERATURE CITED

1. I. Ya. Emel'yanov et al., At. Energ., 37, No. 2, 118 (1974).
2. G. B. Usynin and V. K. Chirkov, At. Energ., 37, No. 2, 123 (1975).
3. B. N. Seliverstov, N. P. Rudov, and F. F. Voskresenskii, At. Energ., 38, No. 5, 329 (1975).
4. I. Ya. Emel'yanov et al., At. Energ., 41, No. 2, 81 (1976).
5. A. N. Kosilov, P. T. Potapenko, and E. S. Timokhni, At. Energ. Za Rubezhom, No. 7, 17 (1975).
6. L. P. Plekhanov, At. Energ., 42, No. 4, 268 (1977).

AN INVESTIGATION OF THE DYNAMICS OF NUCLEAR POWER FACILITIES UPON DETERIORATION OF HEAT EXCHANGE

G. G. Grebenyuk and M. Kh. Dorri

UDC 621.039.553.34

The use of plants operating at high specific thermal fluxes, high steam contents, and high pressures has led to the organization of a large number of investigations of heat-exchange processes and the conditions of motion of two-phase flows. Investigations of these processes have been conducted especially actively for the purpose of studying the physics of crisis phenomena of heat exchange, refining the limiting values of the parameters at which crises arise, and determining the heat-transfer coefficients in these cases [1-5].

We note that the aftereffects of the appearance of crises involving the heat-exchange are discussed mainly from the point of view of a pulsation of the temperature of the heat-exchanger pipes and the onset of critical loads and are not connected with the structure of the control system of nuclear power plants (NPP) as a whole This fact stems from the practice of performing careful static calculations in the development of NPP designs to guarantee conditions which exclude a heat-exchange crisis.

Factors may accumulate in the operation of NPP which affect the limiting values of the parameters which cause heat-exchange crises. Such factors are variation of the hydrodynamic characteristics of the plants, the appearance of pulsations of the flows in parallel pipes of the heat exchangers, and nonuniformity in the distribution of thermal flows in them. These factors can cause crisis processes in NPP. The development of the dynamical process associated with a crisis is determined by the action of the specific control system of the plant.

In this article we investigate the effect of the control system structure on the nature of the development of the dynamical processes upon a deterioration in the heat exchange. It is shown that the structure of the control system can result in an instability in the operation of the NPP when the neutron power is set independently of the thermal mode.

Such a structure is encountered in power plants both with water and with liquid-metal coolant. The type of steam generator affects the nature of the dynamical processes. Plants with steam generators of once-through and repeated circulation are considered in this paper.

The investigations are carried out with the use of a mathematical model of a nuclear plant. The model takes into account the distributed nature of the parameters in the separate units and a number of peculiarities of the heat exchange and the water dynamics, aspects which have received inadequate attention in earlier analyses of the control processes. In the first place the variation in the density of the steam—water medium of the second loop of the steam generator as a function of the thermal flux and the associated variation in the flow rate of this medium are among these peculiarities.

The indicated phenomena are taken into account by a mathematical description of an opposed heat exchanger, which is carried out on the assumption of the flow of a homogeneous two-phase equilibrium steam—water medium of the second loop and an incompressible coolant of the first loop. The description contains difference analogs of the conservation equations for

energy:

$$\frac{\partial t}{\partial \tau} - \frac{G}{(S\gamma)_{\rm I}} \frac{\partial t}{dx} = \left(\frac{\Pi\alpha}{c\gamma S}\right)_{\rm I} (\theta - t);$$

$$\frac{\partial \theta}{\partial \tau} + (\alpha\Pi)_{\rm I} (\theta - t) + (\alpha\Pi)_{\rm II} (\theta - \vartheta) = 0;$$

$$\frac{\partial (\gamma i)_{\rm II}}{\partial \tau} + \frac{1}{S_{\rm II}} \frac{\partial (iD)_{\rm II}}{\partial x} = (\alpha\Pi)_{\rm II} (\theta - \vartheta),$$

Translated from Atomnaya Énergiya, Vol. 46, No. 5, pp. 320-324, May, 1979. Original article submitted May 29, 1978.

Declassified and Approved For Release 2013/02/12 : CIA-RDP10-02196R000800010005-1

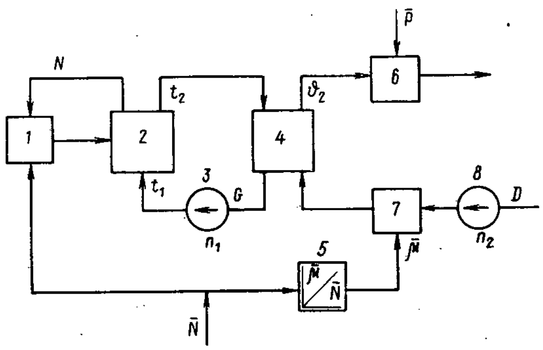

Fig. 1

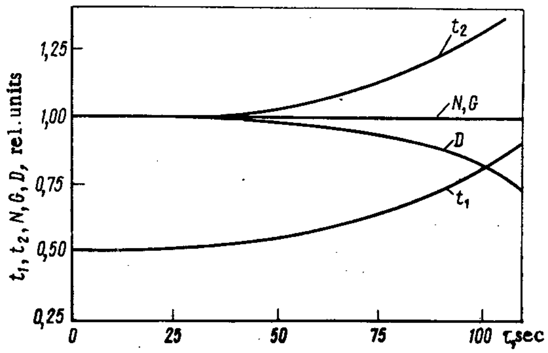

Fig. 2

Fig. 1. Structure of the control system of an NPP with a once-through steam generator; 1) neutron power regulator; 2) reactor; 3) circulating pump of the first loop; 4) steam generator; 5) functional unit; 6) pressure regulator; 7) valve position regulator; and 8) supply pump.

Fig. 2. Variation of the parameters upon self-heating of an NPP.

momentum:

$$\frac{\partial D}{\partial \tau}+\frac{1}{S_{II}}\frac{\partial}{\partial x}\left(\frac{D^2}{\gamma}\right)_{II}=-Sg\frac{\partial P}{\partial x}-(\gamma S)_{II}\,g-\left(\frac{\xi}{2S\gamma}\right)_{II}|D|D,$$

continuity:

$$\frac{\partial \gamma_{II}}{\partial \tau}+\frac{1}{S_{II}}\frac{\partial D}{\partial x}=0$$

and the equations of state:

$$\gamma_{II}=\Phi_1(i,\ P),$$
$$\vartheta_{II}=\Phi_2(iP),$$

where G and D are the mass flow rates of the coolants of the first and second loops, respectively; i and P, enthalpy and pressure of the coolant of the second loop; t, ϑ, θ, temperatures of the coolants of the first and second loops and the wall separating them, respectively; α, heat-transfer coefficient between the middle of the wall and the coolant; γ, c, specific mass and the heat capacity of the coolant; ξ, hydraulic drag coefficient; Π, pipe perimeter wetted by the coolant; S, straight-through cross section of the coolant; g, gravitational acceleration; and I and II, subscripts that determine whether the parameters belong to the first or second loop.

One Form of the Instability of a Double-Loop Facility with a Once-Through Steam Generator. Let us consider a double-loop NPP with a once-through steam generator and the control system illustrated in Fig. 1.

The neutron power N of the reactor, the position of the valve of the supply water μ, and the steam pressure P at the exit from the steam generator are kept equal to the assigned values $\bar{N}$, $\bar{\mu}$, and $\bar{P}$ by regulators. The flow rate of the coolant of the first loop is constant. The position of the valve of the supply water is in agreement with the power setting.

One of the variants of the scheme of Fig. 1 is the control of the flow rate of the second loop by regulation of the revolutions of the shaft of the supply pump of this same loop as a function of the neutron power level.

The structure of the control system of Fig. 1 is unstable in this and the other case. The mean temperature of the coolant of the first loop begins to vary in the facility after its coordinates are brought out into the nominal state and in the absence of any external perturbations at all. The transitional process is shown in Fig. 2.

In this process the temperature difference $t_2 - t_1$ of the coolant in the reactor remains constant, since the neutron power of the reactor is constant. However, the specific mass of the steam–water medium of the second loop varies, which causes a decrease in the flow rate of the supply water.

The amount of heat removed by the second loop is determined by the flow rate of the supply water; when it decreases, the removal of heat from the first loop is reduced. A lower removal of heat leads to an increase in the temperature t_1 of the coolant at the entrance to the reactor and at constant power N – to an increase in

TABLE 1. Nonuniqueness of the Parameters of an NPP

Version	N	n_1	n_2	t_1	t_2	G	D
1	1	1	1	1	1	1	1
2	1	1	1	1,16	1,1	1	0,94
3	1	1	1	1,33	1,2	1	0,9

the mean temperature of the coolant of the first loop. This process causes in its turn a decrease in the specific mass of the steam–water medium of the second loop, the flow rate of the supply water, etc.

We note that measures for the stabilization of the flow rate of the second loop are taken in operating control systems of water–water reactors with a once-through steam generator by maintaining a pressure difference at the supply valve. This step also makes such systems stable. The reactor power is not kept constant, but it is corrected depending on the temperature conditions, e.g., keeping the mean temperature of the coolant flowing through the active zone constant.

It is characteristic that movement of a system from the point of view of phase space both in the direction of an increase in the mean temperature of the first loop and in the direction of its decrease is possible. In other words, the assigned neutron power, revolution rate of the pump shaft, and degree of opening of the supply water valve do not uniquely determine the statics of the entire facility as a whole.

Alternative sets of NPP parameters for one and the same nominal neutron power and revolution rates of the pump shafts of the first and second loops n_1 and n_2 are given in Table 1. The parameters are given in relative units.

The "Shaibovaniya" coefficient of the steam generator exerts a large effect on the limiting levels of the parameters of a facility. The larger this coefficient is, the less is the scatter of the parameters. The system becomes stable upon stabilization of the flow rate of the second loop by special measures, e.g., by virtue of holding the pressure difference at the supply valve constant or controlling the flow rate of the second loop with a separate regulator. Nevertheless, this measure is insufficient for high-quality regulation of a nuclear facility, since the system remains sensitive to a variation in the flow rate of the second loop D. This circumstance is confirmed by the static calculation presented in Fig. 3.

A Heat Exchange Crisis in an NPP with a Recirculation Steam Generator. Let us consider the control system of an NPP in which the structure illustrated in Fig. 1 is applied. A heat exchanger with forced recirculation is used instead of a once-through steam generator. This structure is shown in Fig. 4.

The number of revolutions n_2 of the shaft of the pump for forced recirculation in the power range of operation of the facility and the pressure at the exit from the steam reheater are held constant.

The control system illustrated in Fig. 4 is stable under normal conditions. When a zone of deteriorated heat exchange appears in the evaporator section of the steam generator, a tendency is detected towards unstable operation and an increase in the mean temperature of the coolant of the first loop.

In contrast to the facility illustrated in Fig. 1, the temperature of the water in the second loop (the steam generator–separator loop) is not raised above the saturation temperature. Any heating of the first loop results in an increase of the heat transferred to the second loop and to the establishment of a steady state. A variation of the mass flow rate of the supply water has an insignificant effect on the heat balance through the wall of the steam generator. Since this variation is insignificant of itself, it depends on a variation in the specific mass of the steam–water medium of the second loop, i.e., on the temperature attained by this medium (at constant pressure).

Analyzing the causes responsible for instability in facilities with the once-through steam generator of Fig. 1, and comparing the stable structure of the control system illustrated in Fig. 4 with them, we arrive at the following qualitative explanation of the difference in the transitional processes.

Let us arbitrarily divide the steam generator into m sections along its length. The heat flux Q from the first loop to the second in the j-th section depends on the difference in the temperatures of the coolants of the first and second loops $t_j - \vartheta_j$ and the heat-transfer coefficient k_j:

$$Q = \sum_{1}^{m} k_j (t_j - \vartheta_j).$$

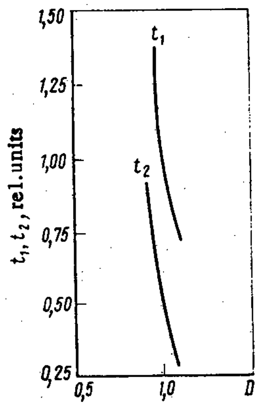

Fig. 3

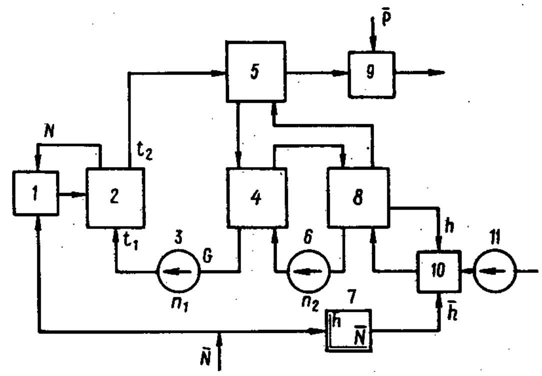

Fig. 4

Fig. 3. Static characteristics of the coolant temperature versus the flow rate of the supply water.

Fig. 4. Structure of the control system of an NPP with a recirculation steam generator: 1) neutron power regulator; 2) reactor; 3) circulating pump of the first loop; 4) steam generator; 5) steam reheater; 6) recirculation pump; 7) functional unit; 8) separator; 9) pressure regulator; 10) regulator of the wave level (h) in the separator; and 11) supply pump.

The oscillations of this flux are caused on the one hand by the variation of the coefficient k_j, and, on the other hand, by the variation of the difference $t_j - \theta_j$. The coefficient k_j depends on the rate of movement of the steam–water medium in the economizer and steam-reheating zones and on the amount of heat Q transferred to the second loop in the evaporator zone. If the parameters of the facility are such that a decrease (increase) in the overall product $\sum_j^m k_j(t_j - \vartheta_j)$ occurs upon a random increase (decrease) of the temperatures t_j of the first loop, the facility is unstable.

The above explanation is of a qualitative nature, since the additional couplings among the heat-transfer coefficient, the heat flux, the coolant velocity, etc. were not taken into account here.

A decrease in the total amount of heat transferred to the second loop in a structure with a once-through steam generator causes heating of the first loop, an increase of the steam-reheating zone, and a decrease in the mass flow rate of the second loop. The latter event causes a deterioration in the heat exchange, a decrease in the heat transferred to the second loop, heating of the first loop, etc.

The heating of the first loop in the structure of the facility in Fig. 4 is compensated by an increase in the total heat flux from the first to the second loop, and the facility is stabilized. However, the structure of the control system (see Fig. 4) can result in heating of the first loop. The cause involves the possibility of the appearance of zones of deteriorated heat exchange or crisis phenomena in the steam generator. A heat exchange crisis (of the first and second kind) causes a decrease of the heat-transfer coefficient k. A decrease in the amount of heat transferred in a section results in an increase in the mean temperature of the coolant of the first loop and in the propagation of the zone of deteriorated heat exchange along the length of the steam generator.

This situation is especially relevant to a crisis of the first kind. In this case a steam generator with recirculation behaves like a once-through one, and the facility illustrated in Fig. 4 heats itself up. With these same parameters the application of a different structure of the control system, e.g., holding back the temperature of the coolant at the reactor exit, leads to satisfactory control of the facility and the absence of self-heating. A heat-exchange crisis of the second kind causes a somewhat more moderate propagation of the zone of deteriorated heat exchange and an increase in the mean temperature of the first loop.

The recirculation of the water of the second loop is of great interest. A heat-exchange crisis reduces the recirculation, and this facilitates propagation of the zone of deteriorated heat exchange to other sections of the steam generator.

A heat-exchange crisis in the facility of Fig. 4 was simulated by replacing the "precrisis" heat-transfer coefficient when the steam content x reaches the limiting value $X^0_{\lim}$ by a "postcrisis" small heat-transfer

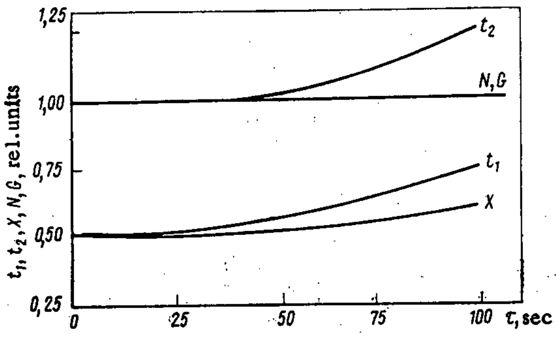

Fig. 5

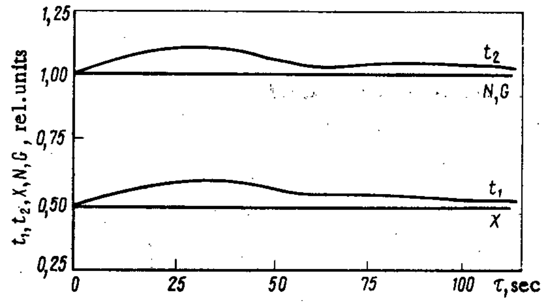

Fig. 6

Fig. 5. Variation of the parameters in the case of a heat-exchange crisis in a steam generator with $\alpha \sim 1\%$ of the precrisis value.

Fig. 6. Variation of the parameters upon a heat-exchange crisis in a steam generator with $\alpha \sim 20\%$ of the precrisis value.

coefficient. After elimination of the crisis conditions, i.e., after the relationship

$$X_j < (X^0_{\text{lim}})_j,$$

is established, instantaneous recovery of the precrisis value of the heat-transfer coefficient occurred.

Plots of the transitional processes upon operation of the facility in the steady-state mode with the steam content of the coolant at the exit from the evaporating zone equal to X = 0.5 are illustrated in Fig. 5. A heat-exchange crisis of the second kind was simulated by lowering the limiting value of the steam content to $X^0_{\text{lim}} <$ 0.5. The nature of the transitional process depends strongly on the postcrisis heat-transfer coefficient. If it is small and equal to ~1% of the precrisis heat-transfer coefficient, appreciable heating up of the first loop occurs (see Fig. 5). If this coefficient is equal to 20% of the precrisis value, the mean temperature of the coolant of the first loop increases inappreciably and then stabilizes at some level (see Fig. 6).

The data of [4, 5] were used to calculate the postcrisis heat-transfer coefficient. The processes illustrated in Figs. 5 and 6 are obtained with values of the heat-transfer coefficient corresponding to its lower and upper limits.

Conclusions. The structure of a control system with independent setting of the neutron power and the revolution rate of the pump of the second loop directly from a controller without additional measures for stabilization is unstable in facilities with a once-through steam generator.

A similar structure in facilities in which a steam generator with recirculation is used is stable under normal operating conditions and gives a satisfactory quality of the transitional processes. However, one should bear in mind that such a structure is unstable in facilities in which thermal loads are close to the critical ones when a heat-exchange crisis arises in the steam generator. In order to eliminate the cited instability, it is necessary to introduce relations into the structure of the control system which form a law for controlling the reactor power as a function of directly measurable variables which depend on the temperature conditions in the reactor.

LITERATURE CITED

1. A. M. Kutepov, L. S. Sterman, and N. G. Styushin, Hydrodynamics and Heat Exchange in Connection with Steam Formation [in Russian], Vysshaya Shkola, Moscow (1977).
2. V. E. Doroshchuk, Heat Exchange Crises upon the Boiling of Water in Pipes [in Russian], Énergiya, Moscow (1970).
3. G. F. Hewitt and N. S. Hall-Taylor, Annular Two-Phase Flow, Pergamon (1974).
4. Z. L. Miropol'skii, Teploenergetika, No. 5, 49 (1963).
5. S. S. Kutateladze, Fundamentals of Heat Transfer, Academic Press (1964).

RADIATIONAL SWELLING OF TWO-PHASE AUSTENITIC – FERRITIC STAINLESS STEELS

Yu. A. Utkin, V. A. Nikolaev, O. N. Zhukov, I. A. Kuz'mina, and L. G. Egorov

UDC 621.039.531

It is of practical interest to investigate the radiational swelling of the metal of welded joints of Kh18N9 and Kh16N11M3 steels, recommended for fast-reactor construction [1]. Distinctive feature of the weld-joint metal include the possibility of forming a two-phase $\alpha + \gamma$ structure, the associated microinhomogeneities of the alloying-element distribution, and the presence of internal stress. The presence of ferrite, with no tendency to swelling [2], would seem likely to facilitate a reduction in the swelling of the material. At the same time, tensile stress may cause the opposite effect [3]. Therefore, it is difficult to reach any a priori conclusions on the radiational swelling of weld-joint metal.

Method of Investigation

The investigation was carried out for the metal of a weld seam made by means of an argon arc using Sv-02Kh17N10M2-VI welding material without subsequent thermal treatment. The content of α phase in the molten material was ~5%. For variation of the α-phase content over a wider range, Kh20N8M2 steel was melted in laboratory conditions.* An ingot of mass 16 kg was hammered on a rod, and then heated at 1100°C, with subsequent cooling in air. In this case there was no stress of the first kind in the metal. For comparison, Kh20N2 steel with a single-phase ferrite structure prepared by an analogous technology and also commercial Kh16N11M3 austenitic steel were taken.

The α-phase content was estimated by x-ray-structural and magnetic methods, while chemical and micro-x-ray methods were used for the analysis of the alloying elements in the γ and α phases (Table 1). The presence of stress of the second kind may be evaluated indirectly by measuring the halfwidth of the lines on the x-ray photographs for the investigated materials. The recordings were made on a DRON-1,5 apparatus, using the K_β line of chromium radiation.

The investigated materials were irradiated in the form of samples of diameter 3 mm and length 27 or 55 mm in the active zone of BR-10 and BOR-60 reactors. In the BR-10, the samples were irradiated in sodium at T_{rad} = 500-550°C. The neutron flux (E > 0.1 MeV) was $(1.6-1.8) \cdot 10^{22}$ neutrons/cm^2. In the BOR-60, the samples were irradiated in a medium of argon at T_{rad} = 500-600°C and in a sodium flow at T_{rad} = 380-480°C at a flux of up to $(1-3.3) \cdot 10^{22}$ neutrons/cm^2.

The change in density was determined from the change in sample length Δl. After irradiation, $\Delta V/V = 3\Delta l/l$. The length was measured using an IZV-2 vertical length-measuring instrument and an MIG meter with an error of 1-2 μ. The swelling was also estimated by the method of transmission electron spectroscopy (TES). To determine the volume fraction of pores, 10-15 microstructure photographs were used. The blanks taken for thinning down were cut from samples from which preliminary measurements of the change in length had been made. The absolute error of the TES measurements was ~80%. To monitor the density changes of the investigated samples due to phase transitions, some of the samples were held at temperatures of 500 and 550°C for 8000 and 10,000 h, respectively.

*The materials for investigation were supplied by A. Ya. Madorskii, N. I. Zakhodska, and A. K. Guro, to whom many thanks are due.

Translated from Atomnaya Énergiya, Vol. 46, No. 5, pp. 324-329, May, 1979. Original article submitted March 13, 1978.

Declassified and Approved For Release 2013/02/12 : CIA-RDP10-02196R000800010005-1

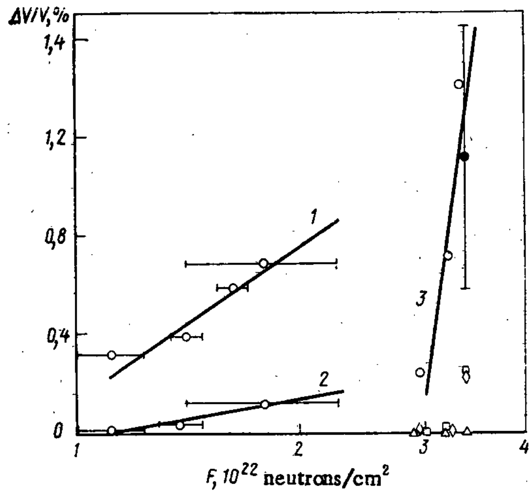

Fig. 1

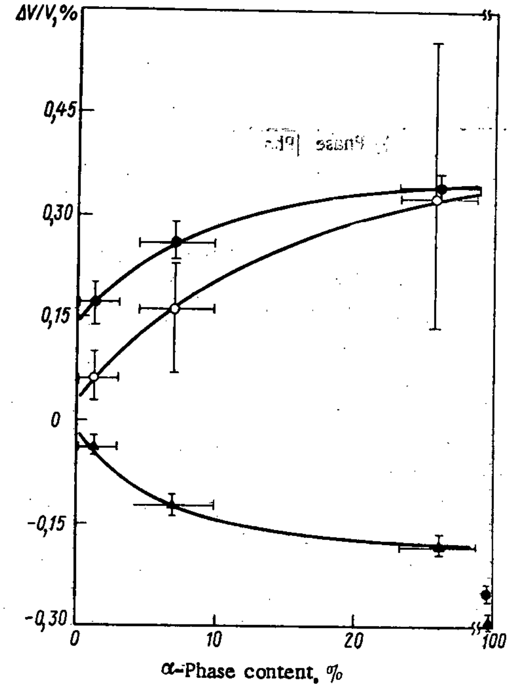

Fig. 2

Fig. 1. Swelling of austenitic steels with a molten recrystallized structure at different neutron fluxes: 1, 2) weld-seam metal and Kh16N11M3, respectively, at T_{rad} = 380-430°C; 3) weld-seam metal at T_{rad} = 500-600°C; the filled circle corresponds to TES; △, ◇, □) Kh16N11M3, Kh18N10T, and Kh18N9 steels, respectively, at T_{rad} = 500-600°C.

Fig. 2. Effect of α-phase content on the change in density of Kh20N8M2 steel as a result of neutron irradiation and thermal holding: ●) by measuring linear dimensions; ○) by TES, F = (1.6-1.8) · 10^{22} neutrons/cm^2 at T_{rad} = 500-550°C; ▲) holding at 550°C for 10,000 h.

Experimental Results

The change in density of the weld-seam metal with F = (1-3.3) · 10^{22} neutrons/cm^2* is shown in Fig. 1, together with data on the swelling of Kh18N9, Kh18N10T, and Kh16N11M3 austenitic steels [4] irradiated with the weld-seam-metal samples. The ratio of alloying elements in these steels is such that, like the weld-seam metal, they may contain up to 5% α phase in the molten state. After hot plastic deformation and austenization, their structure was completely austenitic. It follows from Fig. 1 that in Kh16N11M3 and in weld-seam metal at T_{rad} = 380-430°C the swelling increases with increase in neutron flux from 1 · 10^{22} to 2.25 · 10^{22} neutrons/cm^2. The maximum swelling of Kh16N11M3 steel in these conditions does not exceed 0.13%. In the weld-seam metal, the swelling becomes pronounced (0.31%) even at a flux of 1 · 10^{22} neutrons/cm^2, while at F = 2.25 · 10^{22} neutrons/cm^2 it reaches 0.7%. Qualitatively similar behavior is observed for the investigated materials with irradiation in the temperature range 500-600°C. In the weld-seam metal at F = (2.9-3.3) · 10^{22} neutrons/cm^2, a change in density from 0.23 to 1.4% was observed. In Kh18N9 and Kh18N10T steels, small swelling was observed (0.2-0.25%) only at F = 3.3 · 10^{22} neutrons/cm^2, and in Kh16N11M3 no swelling was observed at all.

The effect of the α-phase content on the swelling of Kh20N8M2 steel at F = 1.7 · 10^{22} neutrons/cm^2 is shown in Fig. 2, from which it is evident that increase in the α-phase content of steel from 1 to 26% leads to increase in the swelling by a factor of 2-2.5. In steel with a ferrite structure (Kh20N2), on the other hand, the density increases by ≈0.25%.

The change in the density of steel as a result of thermal holding (Fig. 2) indicates a reduction in volume, increasing with increase in the amount of α phase in Kh20N8M2 steel and reaching a maximum (0.28%) in Kh20N2 steel. In Kh16N11M3 steel and weld-seam metal, no pronounced changes in density as a result of thermal holding are observed. It must be assumed that the reduction in volume of the steel is associated primarily

*Data on the swelling of the weld-seam metal evidently reflects not only the dependence on the flux but also certain differences in T_{rad} for the samples, over the range 500-600°C.

TABLE 1. Ferrite Content and Chemical Composition of the Phases of the Investigated Steels

Material	α-Phase content, %	Phase analyzed	Elementary composition, mass %: Cr	Ni	Mo
Kh16N11M3 steel	< 0,05	γ	15,8	11,4	1,97
Weld seam	5±3	α+λ	18,4	8,45	1,59
Kh20N8M2 steel	< 3	γ	19,4	7,9	1,75
	7±3	γ	22,0	7,0	2,21
		α	23,7	4,6	3,05
	26±3	γ	24,3	6,9	2,1
		α	28,5	4,3	3,2
Kh20N2	100	α	18,9	2,25	—

Note. The content of P and S was in the range 0.006-0.014% of Si 0.25-0.37%, of Mn 1.0-1.8%, of C 0.04-0.07%.

TABLE 2. Change in Peak Halfwidth of the (311) Austenite Line on Heat Treatment

Material	α-Phase content, %	Heat treatment	Peak halfwidth, 10^{-4} rad
Weld seam	5±3	No treatment	218±6
	5±3	500 °C — 8000 h, air	266±6
	< 3	1100 °C 1 h, air	177±6
Kh20N8M2 steel	< 3	The same	166±6
	7±3	"	183±6
	26±3	"	209±6

with the precipitation of chromium carbides. It is well known that the breakdown of a solid solution supersaturated with carbon (ferrite and austenite) is associated with a decrease in specific volume. Because of the smaller solubility and larger diffusional mobility of carbon, the precipitation of carbides in ferrite would be expected first, which is confirmed by the results of electron-microscope analysis. Therefore, the reduction in volume is intensified with increase in α-phase content in the steel.

The structure of weld-seam metal and Kh20N8M2 steel consists of an austenite grains surrounded by ferrite layers, in which, after holding at 500 and 550°C, carbide particles and polygonizational dislocation grids appear. After irradiation at 500-600°C, the structure of the weld-seam metal is characterized by the presence of porosity in the austenite grains. The visible pores range from 6 to 60 nm in size. In α-phase regions no pores are observed, but a large number of carbide particles are present (Fig. 3). A similar picture – the presence of pores in austenite and a considerable amount of carbide phase in the ferrite grains – is observed in investigating the structure of irradiated Kh20N8M2 steel.

Comparing the result of sample-length measurements and of TES determinations of the specific pore volume shows (see Figs. 1 and 2) that the two methods are in sufficiently good agreement. This offers confirmation that the change in sample length as a result of irradiation is mainly due to the change in density of the austenitic phase.

Electron-microscope investigation also reveals features of the structure of the irradiated weld-seam metal such as nonuniformity of the porosity distribution over the austenite grain. The formation of regions with reduced density and smaller pore size close to the grain boundaries, which serve as sinks for point defects, is well known [5], which also confirms the investigations made of the austenite–austenite boundaries. A different picture is observed close to the austenite–ferrite boundary, where the pore size is greated than in the body of the grain. For five different sections of austenite bordering on the α phase, and also for a section of large-angle austenite–austenite boundary, curves were plotted for the distribution of pore volume fraction with increasing distance from the phase boundary (Fig. 4). It follows from Fig. 4b that in the layer directly adjacent to the austenite–austenite boundary, swelling is minimal (0.6-0.7%), while at a distance of around 600 nm it reaches a value characteristic for the grain body (1.4%). In austenite layers close to the boundary with ferrite, on the other hand, an increase in the swelling by a factor of 4-20 in comparison with the inner regions of the grain is observed (Fig. 4a). However, the position of the maximum given by the data of different experiments is not the same. With increase in the distance from the boundary up to 300 nm, the swelling decreases, but thereafter it remains practically unchanged. Increase in the swelling of austenite at the boundary with ferrite may be observed on photographs of the microstructure of uranus-50 steel [2].

Discussion of the Results

The experimental results clearly indicate that austenitic–ferritic steel show an enhanced tendency to radiational swelling in comparison with austenitic steels of similar composition. This is the more remarkable in that the ferritic phase itself under the same conditions experiences a reduction in volume as a result of structural transformations. It may be suggested that the tendency to swelling of two-phase steels is associated with their chemical composition, and in particular the reduced content of elements such as carbon, nickel, and molybdenum, the presence of which in solid solution diminishes swelling [2, 6, 7]. This explanation, however, runs contrary to the observation that the swelling of weld-seam metal is more pronounced than that of Kh18-N10T steel, which contains no molybdenum and carbon mainly in the form of titanium carbide. In Kh20N8M2

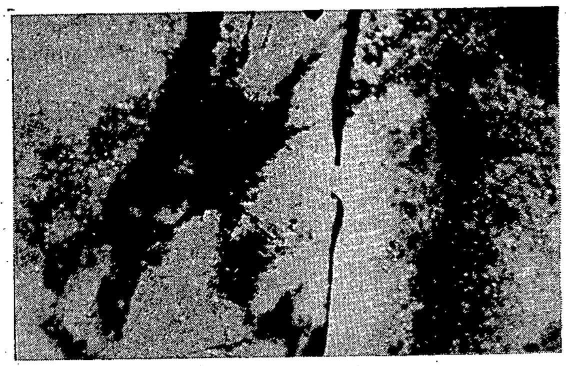

Fig. 3

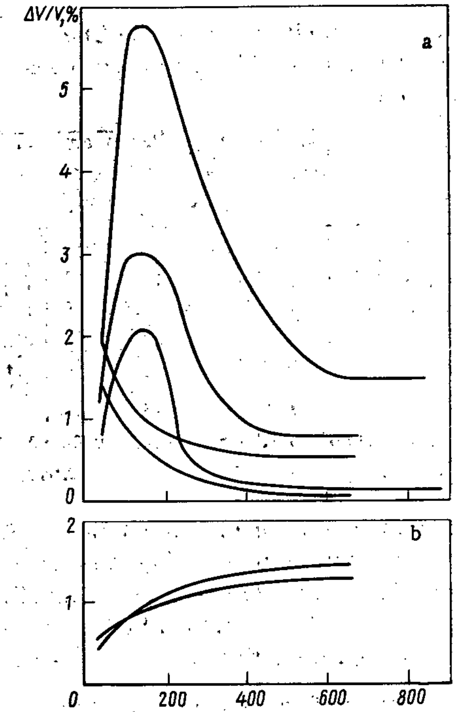

Fig. 4

Fig. 3. Structure of weld seam after irradiation at $F = 3.3 \cdot 10^{22}$ neutrons/cm^2 and T_{rad} = 500-600°C (×40,000).

Fig. 4. Dependence of the specific pore fraction in the austenite of weld-seam metal on the distance to the phase boundary with $F = 3.3 \cdot 10^{22}$ neutrons/cm^2 and T_{rad} = 500-600°C.

steel, with a different amount of α phase, the austenite composition differs practically only in the chromium content (Table 1), which is not found to have any effect on the swelling of steel with a nickel content of 8-12%. Features of the chemical composition cannot, therefore, explain the increased tendency to swelling of the two-phase steel.

It may be suggested that the observed effect is due to the presence of ferrite and, more precisely, the appearance of tensile stress in its presence. X-ray structural investigations confirm that in the investigated steel stress of the second kind increases with increase in the α-phase content, since the halfwidth of the austenite line likewise increases (Table 2).

The source of stress of the second kind in two-phase steel subjected to homogenizing heat treatment is the difference in linear-expansion coefficients of austenite and ferrite ($1.8 \cdot 10^{-5}$ and $1.2 \cdot 10^{-5}$), and also the reduction in specific volume of ferrite in the precipitation of chromium carbides. This circumstance may explain [3] both the total increase in swelling of the austenite grains under the influence of tensile stress and the local increase close to the austenite–ferrite boundary. The reason for the appearance of dislocations in Kh20N8M2 steel close to the austenite–ferrite boundary after prolonged thermal holding also becomes clear. The presence of dislocations provides evidence of relaxational processes in the region of interphase-stress concentration.

The formation of vacancy pores in austenite irradiated in the stressed state may be regarded, generally speaking, as a unique mechanism of stress relaxation. It is evident that, when a swelling which compensates the elastic deformation is reached, the stress factor ceases to act. At present it remains unclear whether the structure of the material formed up to a given moment has an effect on the kinetics of the subsequent swelling. Such an effect would be expected if the role of stress is to increase the number of pores in the austenite. It follows from the results obtained, however, that the increase in their mean size is more rapid in the presence of α phase. It may therefore be assumed that the increased tendency to swelling of two-phase materials is associated with a reduction in the incubation time for the initiation of vacancy pores. This hypothesis, of course, requires experimental verification. It is not the only possible explanation of the effect observed. In particular, it cannot be ruled out as a possibility that vacancy transfer between austenite and ferrite occurs at radiation temperatures of 400-600°C, the resultant vacancy flux through the interphase boundary being directed from the ferrite phase to the austenite.

These suggestions as to the causes of the enhanced swelling of steel containing α phase allow an approach to the suppression of this effect to be formulated. Above all, for a metal of welded components, it is important to ensure the correct administration of austenitization, which should usually prevent local failure in the near-weld region. Decrease in α-phase content in the weld-seam metal as a result of such heat treatment may serve as the main means for the reduction in swelling in those cases when the presence of α phase is unavoidable. Decrease in structural stress may be achieved by heat treatment facilitating the occurrence of relaxational processes in the material, e.g., stabilizing tempering. Specific heat-treatment conditions should be chosen so as to take into account not only radiational swelling but also other factors, in particular change in mechanical properties.

LITERATURE CITED

1. G. I. Kapyrin et al., in: Proceedings of the Scientific–Engineering Conference on Atomic Energy, Fuel Cycles, Radiational Metals Science [in Russian], Vol. 3, Atomizdat, Moscow (1971), p. 310.
2. W. Johnston, I. Rosolowski, and A. Jurkalo, J. Nucl. Mater., 54, No. 1, 24 (1974).
3. J. Bates and E. Gilbert, J. Nucl. Mater., 59, No. 2, 95 (1976).
4. V. V. Andreev et al., in: Shipbuilding Problems, Metals-Science Series [in Russian], No. 22, Leningrad (1976), p. 34.
5. Yu. V. Konobeev et al., in: Problems of Atomic Science and Technology, Fuel- and Structural Materials Series [in Russian], No. 1(4), VNIINM, Moscow (1976), p. 39.
6. J. Leitnaker et al., J. Nucl. Mater., 49, No. 1, 57 (1973).
7. P. Murray, React. Technol., 15, No. 1, 16 (1972).

ELECTRON-SPECTROSCOPIC ANALYSIS OF NEUTRON-IRRADIATED PYROGRAPHITE

A. N. Baranov, A. G. Zelenkov,
V. M. Kulakov, V. P. Smilga,
Yu. A. Teterin, V. I. Karpukhin,
Yu. P. Tumanov, and O. K. Chugunov

UDC 539.184:546.26-162

The radiation resistance of reactor-grade graphite subjected to the constant action of neutron fluxes [1] has held the constant attention of researchers.

Pyrographite (PG), which is close in structure and properties to graphite single crystals, is a good model material. Changes induced in the structure of pyrographite by irradiation were studied earlier [2-4]. It is therefore desirable to study the radiation damage to graphite by electron spectroscopy for chemical analysis (ESCA).

Experimental Part. Pyrographite obtained by depositing carbon from the gaseous phase and treated at 3200°C was irradiated in the MR reactor at the I. V. Kurchatov Institute of Atomic Energy at various fluences and temperatures. The technique used to irradiate the specimens and the annealing procedure were described in earlier papers [2, 3]. In our studies we used four series of specimens:

A (T_{irr} = 200°C, $F = 6 \cdot 10^{20}$ neutrons/cm^2);

B (T_{irr} = 100°C, $F = 4 \cdot 10^{20}$ neutrons/cm^2);

C (T_{irr} = 450°C, $F = 4.1 \cdot 10^{20}$ neutrons/cm^2);

D (T_{irr} = 100°C, $F = 0.26 \cdot 10^{20}$ neutrons/cm^2),

Translated from Atomnaya Énergiya, Vol. 46, No. 5, pp. 329-331, May, 1979. Original article submitted April 8, 1977; revision submitted August 21, 1978.

0038-531X/79/4605-0379$07.50

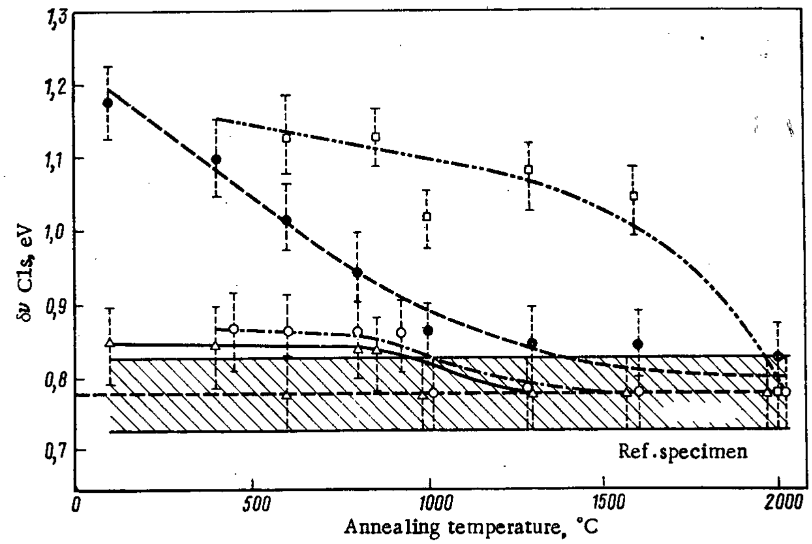

Fig. 1. Effect of annealing temperature on half-width $\delta\nu$ of C1s line of irradiated PG for specimens A (□), B (●), C (○), and D (Δ) (here and in Figs. 3 and 4 the shaded area denotes the region of the error of the reference specimen).

where F is the fluence of neutrons with E > 0.18 MeV. After irradiation, the specimens of each series were annealed at different temperatures in a vacuum furnace for 2 h.

The x-ray electron spectra were obtained with an electrostatic spectrometer built by Hewlett-Packard (HP 5950 A) by using monochromatized Al Kα (1486.6 eV) x rays with a vacuum of no worse than $1 \cdot 10^{-9}$ mm Hg. The resolution of the instrument, as determined from the full width at half-maximum of the Au $4f_{7/2}$ line, was 0.6 eV.

The position, area, half-width, and separation of the satellite line from the principal line were found by computer (HP 2100 A) from a proposed algorithm [5]. The accuracy of determination of the position of the satellite line relative to the principal line was ± 0.2 eV, that of the half-width ±0.05 eV, and that of the area ~10%. To calibrate the spectra we used the Au $4f_{7/2}$ line (83.8 eV) and the C1s-electron line of carbon from a pyrographite reference specimen (284.1 eV). For our reference we used an unirradiated pyrographite specimen annealed at 3200°C. All of the specimens were studied at room temperature. The reduced areas of the satellites are given as percentages of the principal line of C1s electrons of carbon.

Results and Discussion. The x-ray photoelectronic spectrum of C1s electrons of pyrographite consists of a principal line (284.1 eV) and an additional satellite line of low intensity (see Table 1), shifted relative to the principal line toward higher binding energies by roughly 6.5 eV.

In the spectra of irradiated pyrographite the fundamental C1s-electron line is broadened considerably, but does not change its position within the limits of the error of measurement. As can be seen from Fig. 1, an increase in the fluence leads to broadening of the C1s line and raising the annealing temperature compresses this line. Under irradiation of specimens A and B, the width of the C1s line approaches that observed for amorphous graphite (see Fig. 1 and Table 1).

X-ray structural analysis of the pyrographite used (T_{irr} = 3200°C) showed that the lattice constant (3.354 Å, the distance between layers, and 1.420 Å, the distance between neighboring atoms in layers [3]) is in good agreement with known data for crystalline graphite. Neutron irradiation results in the disruption of the regular structure of pyrographite and the formation of various radiation-induced defects [2-4]. As a result, there is a change in the electronic structure of some carbon atoms, e.g., atoms knocked out of the regular lattice and interstitials between graphite layers or atoms near lattice defects.

In the C1s-electron spectra of irradiated specimens of pyrographite separate lines are not observed for the various electronic states of carbon atoms; there is one common symmetrically broadened line, characterizing the entire totality of carbon atoms in the volume of the specimen studied. Analysis of the broadening of the C1s-electron line makes it possible to estimate the relative fraction of carbon atoms with a changed electronic structure.

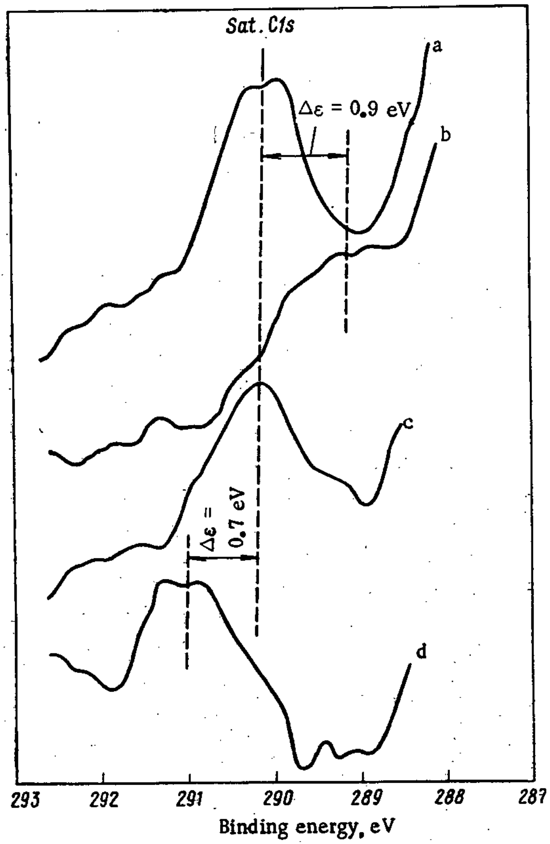

Fig. 2. Satellite lines in ESCA spectra of C1s electrons of carbon: a) pyrographite reference specimen; b) irradiated unannealed specimen B; c) specimen B, annealed at 2000°C; d) aniline sulfate.

TABLE 1. Shift $\Delta\varepsilon_{sat}$ of Satellite Line Relative to Principal Line, Area S_{sat} of Satellite, and Half-Width $\delta\nu$ of Line of C1s Electrons of Carbon

Specimen	$\Delta\varepsilon_{sat}$, eV	S_{sat}, %	$\delta\nu$, eV
C_6H_6 gaseous [8]	7,0	10	1,35
$C_6H_5NH_2 \cdot H_2SO_4$	7,2	5	1,64
PG (T_{irr} = 3200 °C)	6,5	1,6	0,78
PG (T_{irr} = 2800 °C)	6,2	1,5	0,78
PG (T_{irr} = 2100 °C)	6,4	1,5	0,86
Amorphous graphite	4,0	0,5	1,4

Indeed, since the C1s-electron line in the spectrum of irradiated pyrographite does not change its position but merely becomes broader symmetrically, it is natural to assume that the undamaged lattice of pyrographite gives a line of standard width coinciding with the C1s-electron line of the reference specimen. Therefore, the difference in the areas of these two lines characterizes the relative number of atoms with changed electronic structure.

The estimate made for irradiated and unannealed specimens B (T_{irr} = 100°C, F = $4 \cdot 10^{20}$ neutrons/cm^2) and D (T_{irr} = 100°C, F = $0.26 \cdot 10^{20}$ neutrons/cm^2) showed that the fraction of such atoms is ~40 and ~9%, respectively.

It is seen from Fig. 1 that with a rise in temperature of irradiation at the same fluence less disruption of the pyrographite structure is observed. Thus, raising this temperature from 100 to 450°C at F = $4 \cdot 10^{20}$ neutrons/cm^2 (specimens B and C) results in fewer atoms with a changed electronic structure. At a fluence of $4 \cdot 10^{20}$ neutrons/cm^2 (specimen B) heating to 450°C is already sufficient for almost complete restoration of the regular structure of pyrographite as the result of relaxation processes. Thus, it follows from these data that the degree of regularity of the structure and the fraction of atoms with changed electronic structure can be qualitatively estimated from the width of the C1s-electron line.

Irradiation of pyrographite also changes the position and intensity of the satellite in the spectrum of C1s electrons. It is known that this satellite is not due to impurities but is the result of multielectron excitation occurring during photoionization of carbon atoms and reflects the structure of graphite and other cyclic molecules [6-8]. A similar satellite is observed in the spectrum of aniline sulfate (Fig. 2 and Table 1) as the result of the presence of cyclic π-bonds.

It is seen from Figs. 2-4 that with an increase in the neutron fluence the satellite decreases in intensity and shifts towards the principal C1s-electron line, the shift approaching that observed in the case of amorphous graphite (see Table 1). Raising the annealing temperature of irradiated pyrographite specimens to 2000°C leads

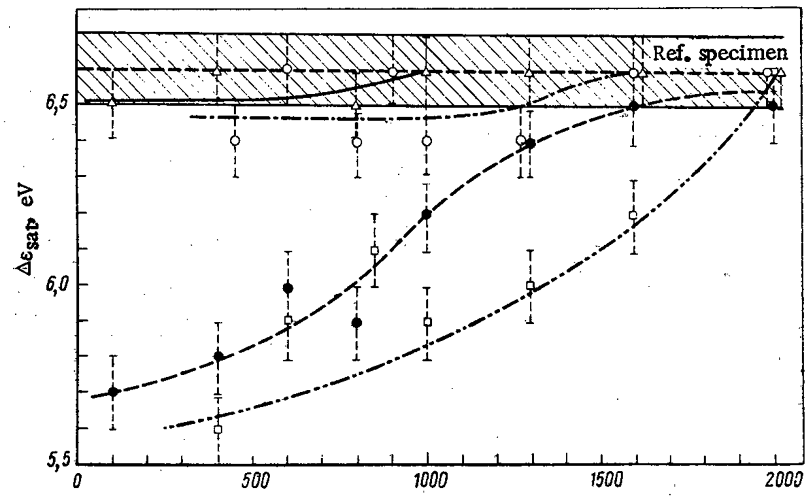

Fig. 3. Change in position of satellite relative to C1s line in irradiated PG with rise in annealing temperature for different series of specimens (notation as in Fig. 1).

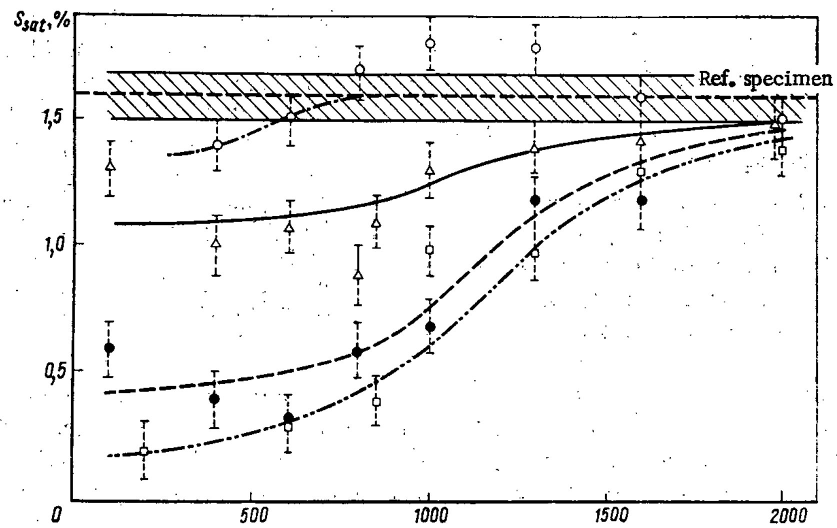

Fig. 4. Dependence of area of satellite on annealing temperature of irradiated PG for different series of specimens (notation as in Fig. 1).

to an increase in the intensity and a shift of the satellite (for all series of specimens) to practically the same position that it occupies in the spectrum of the pyrographite reference specimen (see Figs. 2-4). Figure 3 shows the dependence of the position of the satellite on the annealing temperature of the irradiated specimens. It is seen that increasing the fluence results in the growth of the number of defects and raising the temperature of irradiation from 100°C (specimen B) to 450°C (specimen C) reduces the residual radiation damage.

A similar conclusion may be made upon following the change in the intensity of the satellite as the annealing temperature is increased along with the fluence and irradiation temperature (Fig. 4). The drop in the intensity of the satellites indicates the breaking of bonds between carbon atoms. With the specimen at the same temperature during irradiation, an increase in the fluence results in a decrease in the intensity and a shift of the satellite as well as broadening of the C1s line. For example, after irradiation at 100°C to a fluence of $0.26 \cdot 10^{20}$, $2.3 \cdot 10^{20}$, and $4 \cdot 10^{20}$ neutrons/cm^2 the intensity of the satellite was 1.3, 1, and 0.6%, respectively, and the line half-width was 0.86, 1.10, and 1.17 eV, respectively.

It follows from the data obtained that at an annealing temperature of 2000°C the structure of pyrographite is almost completely restored and its spectral characteristics correspond to those obtained for the pyrographite reference specimen. An increase in the irradiation temperature of the pyrographite is accompanied by a reduction in the number of residual radiation-induced defects. Raising the temperature of the heat treatment above 2500°C does not cause any significant changes in the ESCA spectrum, which indicates that a quite ordered pyrographite structure is formed (see Table 1). These results are in good agreement with those obtained by x-ray structural analysis [3].

LITERATURE CITED

1. J. Simmons, Radiation Damage in Graphite, Intern. Series of Monographs in Nuclear Energy, Vol. 102, Pergamon Press, Oxford (1965).
2. P. A. Platonov et al., Rad. Effects, 25, 105 (1975).
3. P. A. Platonov et al., IAE Preprint 2247, I. V. Kurchatov Institute of Atomic Energy, Moscow (1972).
4. P. A. Platonov et al., IAE Preprint 2266, I. V. Kurchatov Institute of Atomic Energy, Moscow (1973).
5. V. I. Mikhailenko, B. I. Kucherenko, and M. V. Kotov, Zh. Prikl. Spektrosk., 19, No. 2, 361 (1973).
6. V. I. Nefedov, Molecular Structure and the Chemical Bond [in Russian], Vol. 1, VINITI, Moscow (1973).
7. A. Bradshaw, J. Phys. C, Solid State Phys., 7, 4503 (1974).
8. T. Ohta, T. Fujikawa, and P. Kuroda, Chem. Phys. Lett., 32, 369 (1975).

MATHEMATICAL SIMULATION OF PROCESSES OF EXTRACTION PROCESSING OF NUCLEAR FUEL FLUXES

6. EFFECT OF FLUX OSCILLATIONS ON THE ACCUMULATION OF PLUTONIUM

A. M. Rozen and M. Ya. Zel'venskii

UDC 621.039.59.001.57

It was shown in [1, 2] that an internal accumulation of plutonium occurs in the extraction stage in the first cycle of the scheme for extraction regeneration of the fuel of a type water-cooled—water-moderated (VVÉR) reactor upon a decrease in the flux ratio and the approach of conditions to the limiting ones. This accumulation can be appreciable and can create a threat to nuclear safety [3, 4]. It was found that appreciable accumulation of plutonium is possible only in a very narrow range of conditions close to the limiting ones [4, Fig. 8] upon extended operation at a "dangerous" flux ratio. Meanwhile, oscillations of the fluxes are unavoidable in practice, and one could expect that oscillations which take the system beyond the range of the narrow danger region strongly reduce the internal accumulation of plutonium. This problem is investigated in this paper by comparing the accumulation of plutonium in the extractor in the case of a transitional process from nominal conditions in the absence of oscillations of the flux ratio and with them.

It is known that saturation with uranium of an organic phase (the extract) emerging from the extractor is an important technological characteristic of the extraction process. On the one hand, it is desirable to increase the saturation, since purification of the extract of fission products is improved and the productivity of the apparatus is increased; on the other hand, internal accumulation of plutonium and losses of valuable components in what is refined out increase [5]. The second problem of this article is to establish a region of saturations which are permissible from the standpoint of nuclear safety as a function of the engineering parameters and characteristics of the flux oscillations.

Layout of the Extractor and Method of Investigation. The extractor of the first cycle of the extraction (with tributylphosphate — TBP) layout of the reprocessing of a fuel solution from a Type VVÉR reactor [6] was selected as the object of our investigation. It was assumed that the extractor has 10 steps in the extraction and five steps in the rinsing sections (Fig. 1). The stay time of the water phase in the mixing chamber of a step is $\tau_X^m = 0.025$ h and in the settling chamber — $\tau_X^S = 0.05$ h.

A mathematical model of the extraction process performed in a cascade of mixing and settling tanks and the computational computer algorithm described in detail in [4] were used for the investigation.

Translated from Atomnaya Énerigya, Vol. 46, No. 5, pp. 333-336, May, 1979. Original article submitted March 27, 1978.

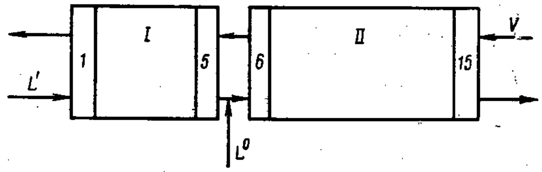

Fig. 1. Layout of the extractor, the input fluxes, and the concentrations under nominal conditions: I is the rinsing section (steps 1-5, $n_w = V/L'$), II is the extraction section (steps 6-15, $n_e = V/L^0 + L'$), L' is the rinsing solution (L' = 0.6 liter/h, x'_{HNO_3} = 3 moles/liter), L^0 is the initial water solution (L^0 = 1 liter/h, x^0_U = 300 g/liter, x^0_{Pu} = 3 g/liter, $x^0_{HNO_3}$ = 3 moles/liter), V is the extract (V = 3.3 liters/h, $y^0_O = 0$, S_0 = 1.09 moles/liter ≈ 30% TBP), and x, y are the concentrations in the water and organic phases.

Effect of Oscillations on Plutonium Accumulation. In order to take oscillations into account, the model of [4] was supplemented by equations describing two types of oscillations of the flux ratio – sinusoidal and pulse-type, respectively:

$$n_i = \bar{n}_i \left\{ 1 + A \sin \frac{2\pi \left[t - (N-1)\left(\tau_x^m + \tau_x^s/\bar{n}_i\right)\right]}{T} \right. ; \tag{1}$$

$$n_i = \bar{n}_i \left\{ 1 + A \,\mathrm{sign}\left[\sin\left(\frac{2\pi}{T}\right) \right] \right\}, \tag{2}$$

where $\bar{n}_i$ is the mean flux ratio in the i-th step; A, oscillation amplitude, rel. units; T, oscillation period in hours; t, instantaneous time; and N, number of steps in the cascade.

The gradual advance of the perturbation front through the extractor (it was assumed that a perturbation is introduced by the flow of the organic phase) was taken into account [see Eq. (1)] in a series of calculations for sinusoidal oscillations* of the flux ratio; the amplitude of the oscillations varied from 1 to 15%, and the period of oscillation from 1 to 6 h. It turned out that these oscillations of the flux ratio have practically no effect on plutonium accumulation. The second series of calculations was performed on the assumption of a rectangular (pulse-type) shape for the oscillations [see Eq. (2)]. One could anticipate that these oscillations are more similar to the actual ones and at the same time have a comparatively strong effect on the accumulation process. Oscillations about the mean values $\bar{n}^0$ = 3.3, 3.2, 3.1, 3.0, and 2.9 (the limiting value was $\bar{n}^0$ = 2.98) with an amplitude in the 2.5-15% range and a period of 1-6 h were investigated.

The calculations showed that in the first place the extractor reaches steady-state conditions comparatively rapidly (in 1-3 h) for flux ratios far from the limiting value (n^0 = 3.3-3.1); as the amplitude and period of the oscillations increases, the accumulation of plutonium increases (Fig. 2a); secondly, conditions close to the limiting ones (n^0 = 3.0) differ in that a steady state does not have time to be established in 24 h even in the absence of oscillations, and concentration oscillations arise at T ≥ 3 h which for A = 10% become asymmetrical and very significant (Fig. 2b).† One can conclude that both sinusoidal and pulse-type oscillations of the flux ratio not only do not reduce the plutonium accumulation in comparison with the process in the absence of oscillations, but on the contrary, they lead to its increases. In a region far from the limiting conditions this is explained by the fact that the extractor reaches a steady-state condition comparatively rapidly which corresponds to the "plus" or "minus" deviations from the mean value of the flux ratio. An increase in the accumulation naturally gives a minus phase of the oscillations, and with an increase in A and T the conditions approach the limiting ones during a more prolonged time. Near to the limiting conditions a plus phase is already not in a state to cut off the accumulation arising in the minus phase; the mean value of the accumulation becomes two

*As in the previous papers [3-5], it was assumed that the transitional process for the concentrations is appreciably longer than the transitional process for the flow rates; therefore, the latter was not taken into account in the calculations.

†At T = 1 h the concentration oscillations are not shown in order not to confuse the figure.

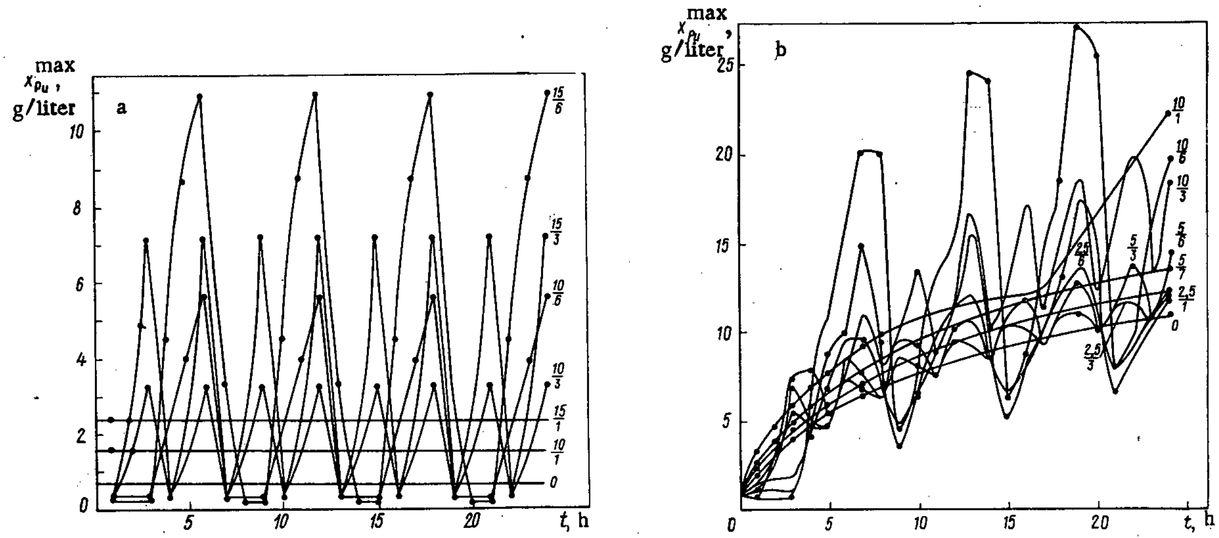

Fig. 2. Plutonium accumulation in the case of oscillations of the flux ratio (the numbers next to the curves have the following meaning: the numerator is the amplitude in %; the denominator is the period in hours): a) $\bar{n}^0 = 3.3$; b) $\bar{n}^0 = 3.0$.

times larger than in the absence of the oscillations.

Representation of the Data with the Help of Accumulation–Saturation Diagrams. In [1-4] plutonium accumulation was represented as a function of the flux ratio. It is more convenient for analysis of the process to represent the data with the help of accumulation (of plutonium)–saturation (of the organic phase with uranium) diagrams, especially when all the parameters of the process except the flow rates are sufficiently stable. Such diagrams (Fig. 3) have two sections: (a) weak effect of saturation and (b) sharp increase of the accumulation. Conditions lying in region a are desirable (from the standpoint of nuclear safety), and conditions in region b are undesirable, even if the plutonium concentration is permissible, since very high accuracy of the regulation is required in this region; deviations can result in a violation of the nuclear safety conditions (for the concentration of fissionable material).

The results of the investigation of the effect of flux oscillations on plutonium accumulation were presented in an accumulation–saturation diagram (Fig. 4a, b, c). It is evident that the oscillations shift only slightly the boundary of the danger region b (see Fig. 3) practically independently of the amplitude and period of the oscillations; the process occurs in region a up to $y_V^{out} \leq 95$ g/liter, and the plutonium accumulation remains less than 2 g/liter.

Effect of the Parameters of the Operating Conditions on Plutonium Accumulation. The effect of the acidity of the rinsing solution and the concentration of the extracting agent (TBP) in the organic phase on the plutonium accumulation and the permissible saturation of the extract with uranium was also investigated: the acidity was varied within the range of 2-5 M HNO_3 and the TBP concentration within the 30-40% range; it was assumed that part of the plutonium (20%) in the original solution is present in the hexavalent state. As is evident from Figs. 5 and 6, the variation of these parameters has an appreciable effect on plutonium accumulation and the permissible saturation of the extract with uranium. The permissible saturation (for 30% TBP) amounts to 88, 92, and 96 g/liter, respectively, for an acidity of the rinsing solution of 2, 3, and 5 M. An increase of TBP leads

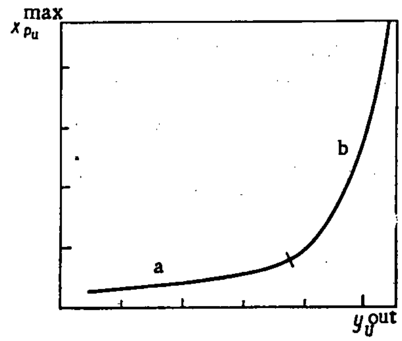

Fig. 3. Accumulation–saturation diagram.

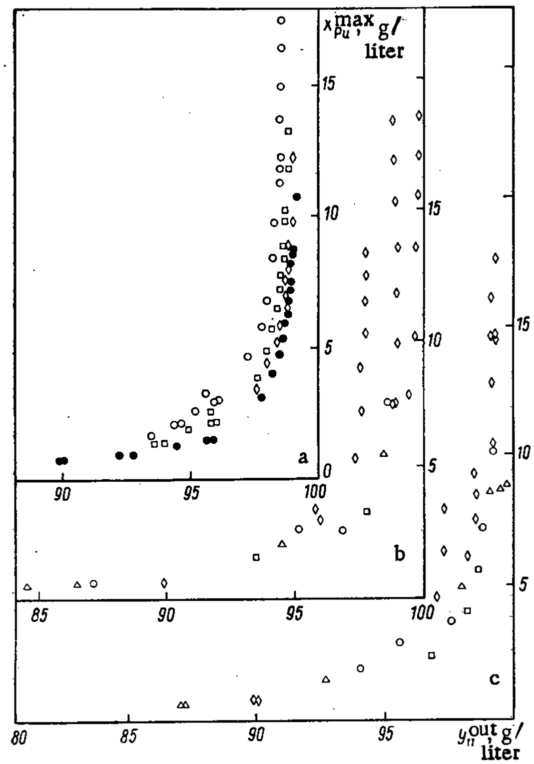

Fig. 4

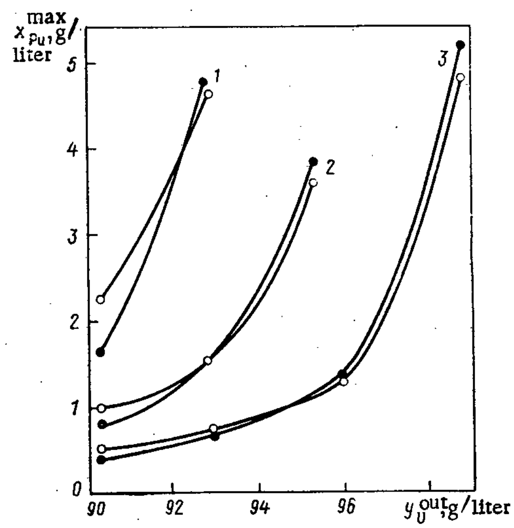

Fig. 5

Fig. 4. Dependence of plutonium accumulation on saturation of the extract with uranium for different amplitudes A and periods T of the oscillations of the flux ratio: a) T = 1 h and A = 10% (○), 5% (□), 2.5% (◇), and 0% (●); b, c) T = 3 and 6 h, respectively, and A = 10%, $n^0 = V/L^0 = 3.3$ (□), 3.2 (○), 3.1 (△), and 3.0 (◇).

Fig. 5. Dependence of plutonium accumulation on the saturation of the extract with uranium for an acidity of the rinsing solution of (1) 2, (2) 3, and (3) 5 M: ○ – Pu (IV); ● – Pu (VI).

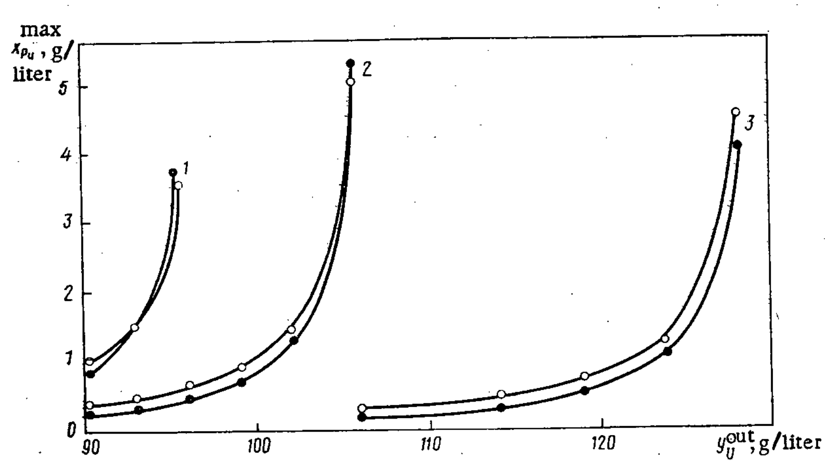

Fig. 6. Dependence of plutonium accumulation on saturation of the extract with uranium for a concentration of the TBP extracting agent of (1) 30, (2) 33, and (3) 40% (the notation is the same as in Fig. 5).

to a proportional increase in the permissible saturation (for 30, 33, and 40% TBP it amounts to 92, 100, and 120 g/liter in the case of a rinsing solution acidity of 3 M). The data for all concentrations of TBP are described well by a single accumulation–saturation percentage diagram (Fig. 7), and the permissible percentage is ~70%.

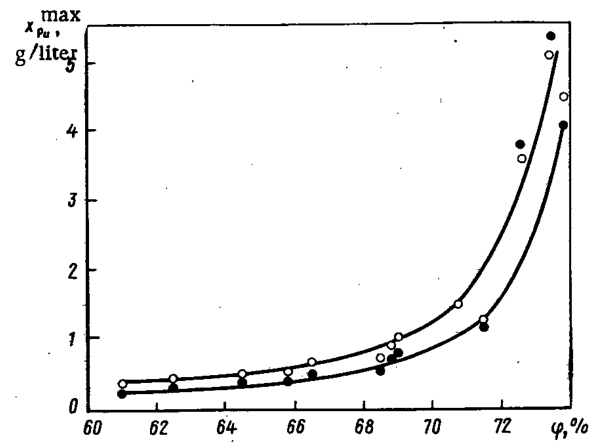

Fig. 7. Dependence of the plutonium accumulation on the relative saturation of the extract with uranium φ for an acidity of the rinsing solution of 3 M HNO_3 (the notation is the same as in Fig. 5).

LITERATURE CITED

1. A. M. Rozen, At. Energ., 7, No. 3, 277 (1959).
2. A. M. Rozen et al., Third Geneva Conference, USSR Lecture No. 346 (1964).
3. A. M. Rozen, Yu. V. Reshet'ko, and M. Ya. Zel'venskii, At. Energ., 37, No. 3, 194 (1974).
4. A. M. Rozen and M. Ya. Zel'venskii, Radiokhimiya, 18, No. 4, 572 (1976).
5. A. M. Rozen and M. Ya. Zel'venskii, At. Energ., 37, No. 3, 187 (1974).
6. V. B. Shevchenko et al., Fourth Geneva Conference, USSR Lecture No. 435 (1971).

LINEAR ELECTRON ACCELERATOR FOR 1-mA AVERAGE CURRENT

G. L. Fursov, V. M. Grizhko,
I. A. Grishaev, B. G. Safronov,
L. K. Myakushko, V. S. Balagura,
V. I. Beloglazov, F. S. Gorokhovatskii,
A. I. Martynov, and A. P. Rudenko

UDC 621.384.644.3

The growing need of the national economy in elementary particle accelerators for use in nondestructive quality control, activation analysis, sterilization of medical products, in agriculture, etc. requires the design of efficient acceleration facilities. The efficiency of an accelerator is to a large extent determined by the intensity of the particle beam it produces. A linear electron accelerator (LEA) for medium energies generating current pulses of 10-μsec duration and 1-mA average has been designed at the Kharkov Physics Institute of the Academy of Sciences of the Ukrainian SSR. Such an accelerator can be effectively used in applied research and as the initial stage of a multisection facility.

The accelerator and results of its testing are described below.

Accelerator Structure

The structural diagram of the accelerator is shown in Fig. 1. The electron source is a two-electrode gun with a lanthanum hexaboride cathode. The cathode is heated by bombardment from an auxiliary gun. The cathode thickness and diameter are 2 and 17 mm, respectively. The source current is controlled by a variable collimator and beam focusing, by two axisymmetric lenses. The injection voltage is 80 kV. Beam modulation is obtained by partial discharge of a storage capacitor through the primary winding of a pulse transformer with a transformation ratio of 4. High-voltage pulse top stability of 1.5% for a pulse duration of 10 μsec is obtained by connection of a diode correction circuit in the pulse transformer secondary. The injector accelerator section [1] is an iris waveguide 300 cm long whose main portion (270 cm) is a uniform structure with a wave phase

Translated from Atomnaya Énergiya, Vol. 46, No. 5, pp. 336-340, May, 1979. Original article submitted March 22, 1978.

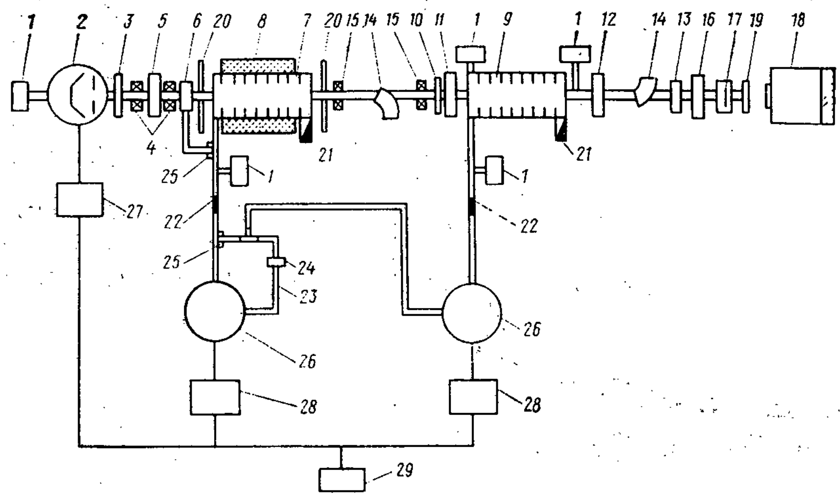

Fig. 1. Structural diagram of accelerator: 1) vacuum pumps; 2) electron gun; 3) variable collimator; 4) axisymmetric focusing lenses; 5) gun Faraday cylinder; 6) resonator-buncher; 7) injector section; 8) solenoid; 9) accelerator section; 10) transit current detector; 11, 12, 16) Faraday cylinders with retractable end covers; 13) beam admittance meter; 14) magnetic spectrometers; 15) magnetic beam corrector; 17) beam spreader; 18) two-layer absorber; 19) titanium exit foil; 20) magnetic shield; 21) HF load; 22) vacuum separating window; 23) KIU klystron oscillator feedback; 24) stabilizing resonator; 25) directional power coupler; 26) KIU klystrons; 27) source modulator; 28) klystron modulators; 29) synchronization and starting unit.

velocity equal to the velocity of light. The initial section of the injector accelerator (30 cm) in which electrons are preliminarily grouped into clusters with a 30° phase length is an integral part of the main section. In the initial section the phase velocity changes stepwise from 0.7 to 0.95c and the field intensity, from 40 to 70 kV/cm. The injector section is located inside a focusing solenoid and is mounted on a rigid nonmagnetic frame. The focusing solenoid provides longitudinal magnetic fields of up to 1000 Oe. The possible alignment error of the injector section with respect to the accelerator section is compensated by a system of correctors that control beam deviation in horizontal and vertical directions.

Power passing through the injector section is absorbed in the terminal load. The standing wave ratio of this section at an operating frequency of 2797 MHz is 1.12 and does not exceed 1.2 within a frequency band of ±3 MHz around the center frequency. The operating temperature of the injector section is +40°C. The injector is built so that it can be used as an independent accelerator for operation in the energy range from 8 to 20 MeV.

The accelerating section 318 cm long has a continuous structure and a wave phase velocity equal to the velocity of light. The shunt resistance of the section $R_{sh} = 42.7$ MΩ/m, the damping factor $\alpha = 0.74 \cdot 10^{-3}$ cm^{-1}. The section consists of five subsections with different radial cross sections of the accelerating disks [2]. The critical current of this section is 1.6 A for a 10-μsec pulse and 2 A for a 2-μsec pulse.

High-frequency power is applied to the injector and accelerator sections by two type KIU-53 power klystrons [3] operating with a pulse power of 10 MW and an off-duty factor equal to 1000. The klystron anode voltage of up to 250 kV is generated by modulators [4] based on the discharge of a storage capacitance. The stability of the klystron voltage pulse top is 2.2% at full pulse duration and 0.5% at 8 μsec. The klystron hf power is applied to the section inputs through rectangular waveguides with a cross section of 90 × 45 mm and an overall length of about 12 m [5]. A 4.2-m section of the waveguide is fulled with compressed nitrogen at a pressure equal to 6 kgf/cm^2; the remaining waveguide section is in vacuum at 10^{-7} mm Hg. The pressurized and vacuum portions of the waveguide are separated by ceramic separating windows. Power loss in the waveguide is about 5%. The injector klystron amplifier operates in a self-excited mode [6]. For frequency stabilization the oscillator has a feedback loop with a waveguide resonator with a loaded Q of ~2000. The frequency stability of the oscillator is $3 \cdot 10^{-5}$ in 24 h.

A protection circuit [7] removes the hf klystron excitation for the pulse duration when a breakdown occurs either in the waveguide or in the accelerator channels. The operating speed of the protection circuit is 0.5 μsec.

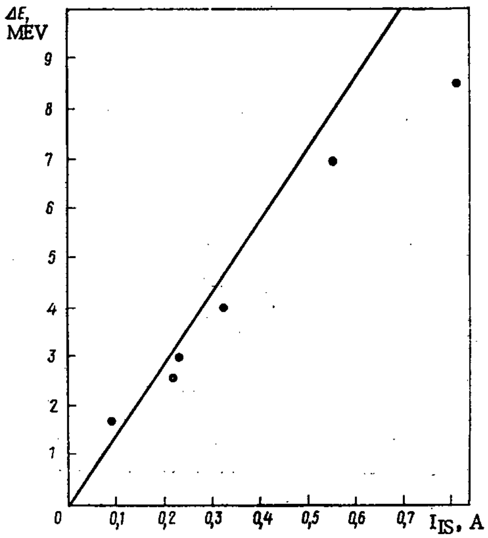

Fig. 2

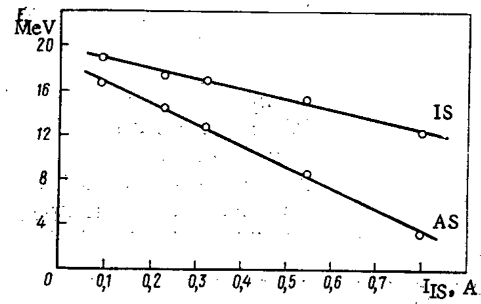

Fig. 3

Fig. 2. Energy loss of injector beam traversing the accelerator section.

Fig. 3. Variation of electron energy with increasing current load in injector (IS) and accelerator (AS) sections without hf power applied to the latter.

The klystron-type buncher-resonator [8] reduces energy scattering and increases the accelerating system output current. The power applied to it from injector waveguide is 20 kW.

The accelerator is evacuated by TÉN-30 titanium electrical-discharge pumps with an air evacuation rate of 30-40 liters / sec. Evacuation points are provided at the electron gun, at the junction between the injector and accelerator section, at the injector input, at the injector and accelerator section waveguides, and at the accelerator output. AIN-50 titanium sublimation pumps with a nitrogen and air evacuation rates of 100 and 40 liters / sec, respectively, and providing a maximum vacuum of 10^{-7} mm Hg are included for accelerating the start of the electrical-discharge pumps after the system is filled with atmospheric air and for aging with hf power applied.

A prevacuum of 10^{-2} mm Hg needed for the start of titanium pumps is provided by a VN-1MG mechanical pump. Evacuation takes place through a forevacuum manifold with a nitrogen cold trap. To accelerate the activation of the electron gun cathode, its evacuation unit contains three TÉN-30 pumps. Forevacuum is measured with thermocouple vacuum gauges; high vacuum is determined by measuring the current of TÉN-30 electrical-discharge pumps calibrated with ionization gauges. The increase of TÉN-30 current in case of breakdown is used to block the vacuum system. The vacuum system provides a maximum vacuum of 10^{-7} mm Hg or less at the evacuation points and 10^{-6} mm Hg at points most distant from the pumps. Measuring equipment including a Faraday cylinder, an inductive current sensor, and a magnetic spectrometer is mounted in the space between the injector and accelerator sections.

A difficulty associated with the extraction of the beam to the target has been encountered with average currents higher than 500 μA. Target foils of various materials (aluminum, tantalum, Kh18N10T steel, copper, nickel, titanium) strongly oxidized when heated by the beam and were rapidly damaged.

Reduction of energy flux density by increasing the beam diameter on the foil considerably prolonged the latter's useful life. The beam spreader is a graphite disk 35 mm in diameter and 0.28 mm thick in an aluminum mounting. The disk was placed about 9 cm in front of the exit foil. The outside surface of the electron guide at the point of the beam spreader was water cooled.

Testing Results

The basic characteristics of an injection accelerator obtained with KIU-12A klystron pulse amplifiers have been reported before [9]. The use of higher-power KIU-53 klystrons made it possible to increase the pulse repetition rate to 100 pulses per second and the average current to 1 mA (see Table 1). The energy control range of the injector accelerator of 19-8 MeV is obtained by changing the current load and not by varying the hf power applied to the injection section. Reduction of the hf power level significantly reduces the capture of

TABLE 1. Injector Accelerator Parameters

Energy, MeV	
at I = 1 A	8
I = 0	19
Maximum pulse current, A	1
Maximum average current, mA	1
Pulse duration, μsec	4; 7; 10
Pulse repetition frequency, sec^{-1}	100; 50; 25; 12.5 6.25; 3.125; single
Energy spread at 0.5 level for I = 1 A, %	6, 7
Beam diameter at I = 1 A, %	1, 5
Divergence, rad	$3 \cdot 10^{-3}$
Hf power at accelerator input, MW	9, 6
Maximum electron efficiency, %	83

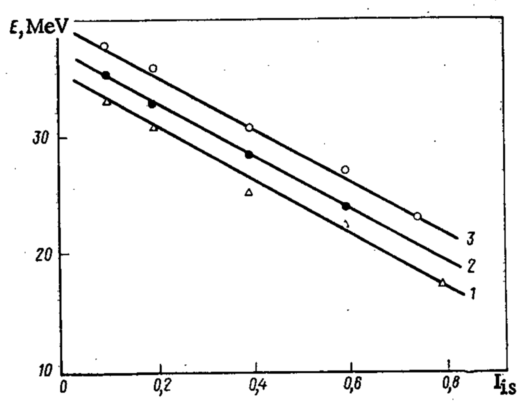

Fig. 4. Loading characteristics of the accelerator for different hf power levels at the section entrance: 1) 6 MW, 2) 8 MW, 3) 10 MW.

electrons into the acceleration process which results not only in a loss of efficiency but also in an undesirable deterioration of the accelerator spectral characteristics. Adjustment of the accelerator section makes it possible smoothly to vary the energy from 3.4 MeV (with maximum current loading and without hf power in the section) to 40 MeV at low currents and with acceleration in the section. When accelerated electrons pass through an "empty" (i.e., without hf energy) accelerating section, their interaction with the iris waveguide structure causes an energy loss ΔE given by the expression

$$\Delta E = JR_{sh}L\left(1 - \frac{1-e^{-\alpha L}}{\alpha L}\right), \tag{1}$$

where J is the accelerated electron current; R_{sh}, section shult resistance; L, section length; and α, attenuation factor. The energy loss increases the beam divergence because of a reduction of the longitudinal component of the electron momentum while its transverse component remains unchanged.

If r_0 is the beam radius at the section entrance, the radius at the exit will be

$$R = r_0 + \int_0^L \left(\frac{dr}{dz}\right) dz. \tag{2}$$

Here

$$\frac{dr}{dz} = \frac{P_r}{\frac{E}{c}\left[1 - \frac{JR_{sh}z}{E}\left(1 - \frac{1-e^{-\alpha z}}{\alpha z}\right)\right]}, \tag{3}$$

where P_r is the transverse component of the momentum of an electron leaving the injector accelerator and c is the velocity of light. The denominator in (3) describes the change of the longitudinal momentum component while the beam tranverses an "empty" section.

Solving the integral in (2), we have

$$R = r_0 + \delta_0 L \sqrt{\frac{E}{2JR_{sh}\alpha L^2}} \ln \frac{1+\sqrt{\frac{JR_{sh}\alpha L^2}{2E}}}{1-\sqrt{\frac{JB_{sh}\alpha L^2}{2E}}}, \tag{4}$$

where $\delta_0 = cP_r/E$ is the initial beam divergence at the entrance to the section. Electron energy at the entrance and exit of the section was measured by magnetic spectrometers; the current was measured by Faraday cylinders. Figure 2 shows the measured (dots) and theoretical (continuous curve) energy loss of a beam of accelerated electrons traversing the section as a function of current. Figure 3 shows the variation of energy as a function of current load in the injector (IS) and accelerator (AS) sections.

Calculations using expression (4) indicate that for a current of 0.8 A the beam radius at the section exit does not exceed the iris aperture. Consequently, such an injector current would pass through an "empty" section without loss. Experimental results were in good agreement with theoretical ones. This has been confirmed both by direct current measurements and by finding the γ-radiation field along the section. With currents higher than 0.8 A we observed at the end of the section a drastic increase of gamma radiation level caused by some of the electrons hitting the waveguide iris. Figure 4 shows loading characteristics of the accelerator. The current dependence of energy was determined at different hf power levels at the entrance to the accelerating section with a fixed power of 9.5 MW applied to the injector section input. Experimental and theoretical results are indicated by dots and solid curves respective. Maximum electron efficiency of the accelerator was the same as of the injector, i.e., 83%. With increasing currents the energy spectrum halfwidth increases from 1 to 4.2%. Maximum beam power was 16 kW (0.8 A at 20 MeV).

LITERATURE CITED

1. V. A. Vishnyakov et al., in: Problems of Atomic Science and Engineering. The Physics of High Energy and Atomic Nucleus [in Russian], Vol. 1 (1), Kharkov Physicotechnical Institute (1972), p. 19.
2. G. D. Kramskoi et al., Zh. Tekh. Fiz., 42, No. 11, 2054 (1969).
3. V. I. Beloglazov et al., in: Problems of Atomic Science and Engineering. Linear Institute Accelerators [in Russian], Vol. 1 (4), Kharkov Physicotechnical (1977), p. 17.
4. V. A. Vishnyakov et al. [1], p. 74.
5. V. B. Mufel' and K. I. Antipov [3], p. 17.
6. V. I. Beloglazov et al., in: Problems of Atomic Science and Engineering. Linear Institute Accelerators [in Russian], Vol. 1 (2), Kharkov Physicotechnical (1976), p. 18.
7. E. P. Vasil'ev et al., in: Problems of Atomic Science and Engineering. The Physics of Higher Energies and Atomic Nucleus [in Russian], Vol. 4 (6), Kharkov Physicotechnical Institute (1976), p. 55.
8. V. A. Vishnyakov et al., ibid. (1973), p. 11.
9. V. A. Vishnyakov et al., At. Energ., 42, No. 3, 231 (1977).

CALCULATION OF GAMMA POWER OF HOT CIRCUITS WITH NONFISSIONABLE MATERIALS

N. I. Rybkin, E. S. Stariznyi,
and A. Kh. Breger

UDC 621.039.553:621.039.573

The parameters of hot circuits with liquid-phase process materials [1, 2] are usually calculated on the basis of average thermal neutron flux densities ($\bar{\varphi}$) and process material velocity ($\bar{v}$) in the activity generator. This is valid for a highly developed turbulent material flow (Re ≫ 2300) since in such conditions the flow velocity is nearly the same as the average flow rate (except for the velocity in a thin boundary layer which can be neglected). Thus, in case of turbulent flow, the average specific activity of the process material at the activity generator exit calculated from the average thermal neutron flux density or obtained taking into account its distribution in the activity generator are practically the same. It has been found however, that the conditions of flow in activity generators of power reactors with complex hydraulic circuits [3] are laminar (Re < 2300). Two competing effects are observed in activity generators with laminar flow: a parabolic cross-sectional flow rate profile in the fluid and a nonuniform neutron flux density distribution caused by self-shielding of internal layers of the liquid. It is important to note that in low flow-rate regions the process material is activated by a neutron flux of higher density. Thus, if flow conditions in the activity generator are laminar, the γ-radiation power in the hot circuits calculated from the average flow rate and the average thermal neutron flux density can contain an appreciable error.

To evaluate the effect of velocity profile and nonuniform neutron flux density distribution on the specific activity of process material at the activity generator output, we use the well-known balance equation for radioactive nuclei in activation zone of a nuclear reactor:

$$dN_i/dt = \Sigma_{\text{act}}\varphi - \lambda_i N_i, \tag{1}$$

where N_i is the concentration of radioactive nuclei of the i-th isotope of the process material* in the hot circuit, λ_i is decay constant of the isotope, t denotes time, $0 \le t \le t_p$, t_p is the time the process material stays in the activity generator. Consider a hot circuit in which the activity generator and irradiator elements have the form of cylinders with radius R. Taking into account the flow rate profile in a cylindrical tube we have

$$t_p(r) = V_p R^2/2G(R^2 - r^2),$$

where V_p is the process material volume in the activity generator; G, volumetric flow rate; and r, moving radius ($0 \le r \le R$).

The radial density distribution function of the thermal neutron flux in an activity generator placed in a moderator with uniformly distributed thermal neutron sources can be written in the P_1 approximation as

$$\varphi(r) = K[I_0(r/L) + \lambda_c \xi \Sigma_s], \tag{2}$$

and the mean density in the activity generator cross section, as

$$\bar{\varphi} = K[(2L/R)I_1(R/L) + \lambda_c \xi \Sigma_s], \tag{3}$$

where I_0 and I_1 are Bessel functions of an imaginary argument; L, thermal neutron diffusion length in the process material of the hot circuit; $\lambda_c = 1/\Sigma_c$; Σ_c and Σ_s, macroscopic neutron absorption and scattering cross sections by the process material nuclei.

The solutions of (1) for $t = t_p$ and $R/L \le 2$ are the following recurrent relations for average concentrations of radioactive nuclei†:

*The subscript i is henceforth omitted since the discussion concerns one isotope only.
†The flow in the connections is assumed to be turbulent since the time the process materials stays in them is such that, as a rule, Re ≫ 2300 [1].

Translated from Atomnaya Énergiya, Vol. 46, No. 5, pp. 341-342, May, 1979. Original article submitted July 28, 1977.

 0038-531X/79/4605-0392$07.50

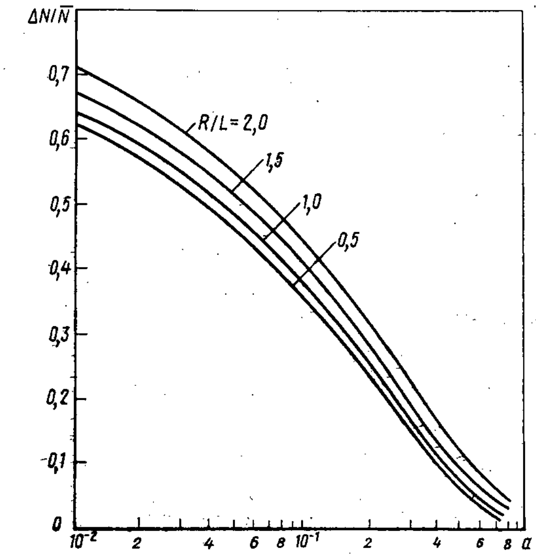

Fig. 1. The function $\Delta N/\overline{N} = f(a,\ R/L)$ for $\overline{N}(0) = N^*(0) = 0$.

a) taking into account the flux density distribution (2),

$$\overline{N}_{n+1} = \overline{N}_n(0) + F_1 - F_2; \tag{4}$$

b) according to the mean density (3),

$$\overline{N}^*_{n+1} = \overline{N}^*_n(0)\exp(-2a) + F_1[1 - \exp(-2a)] \tag{5}$$

(here n is the number of the hot circuit operating run);

$$F_1 = \frac{2\alpha L}{\lambda R} I_1\left(\frac{R}{L}\right);$$

$$F_2 = \frac{\alpha+\beta}{\lambda} E_2(a) + \frac{1}{2}\frac{\alpha}{\lambda}\left(\frac{R}{2L}\right)^2 [(2+a)E_2(a) - \exp(-a)];$$

$$\overline{N}_n(0) = (F_1 - F_2)\frac{1 - [E_2(a)E_2(b)\exp(-\lambda t_k)]^n}{1 - E_2(a)E_2(b)\exp(-\lambda t_k)};$$

$$\overline{N}^*_n(0) = F_1[1 - \exp(-2a)]\frac{1 - \{\exp[-2(a+b)]\exp(-\lambda t_k)\}^n}{1 - \exp[-2(a+b)]\exp(-\lambda t_k)};$$

$$a = \lambda V_p/2G; \quad b = \lambda V_y/2G;$$
$$\alpha = K\Sigma_{act}; \quad \beta = K\Sigma_{act}\lambda_c\xi\Sigma_s,$$

where V_y is the volume of process material in the irradiator; t, time the material stays in the connections; E_2, integral exponential function; and K, a dimensional factor.

Analysis of expressions (4) and (5) indicates that for given process material characteristics and nuclear reactor parameters $\overline{N}$ and $\overline{N}^*$ are determined by the magnitude of Re during the motion of fluid in the activity generator and irradiator and by the number of the hot circuit operating runs.

Figure 1 shows the function $\Delta N/\overline{N} = (\overline{N} - \overline{N}^*)/\overline{N}$ for the case when $\overline{N}(0) = \overline{N}^*(0) = 0$ (first hot circuit run) for different R / L. The figure shows that for $a \ll 1$ (elongated velocity profile) $\Delta N/\overline{N}$ increases considerably. The dependence on R / L is at the same time weak. In such a case the dependence of $\Delta N/\overline{N}$ on the number of hot circuit runs can be considered for a = b (optimum ratio of activity generator and irradiator capacities [2]) and for R / L. Expanding the function $I_1(R/L)$ into a series and neglecting the second term in the expression for F_2 for $\lambda t_k > 0$ to within ~10%, a convenient practical expression for $\Delta N/\overline{N}$ at $a \geq 0.1$ for the n-th hot circuit operating run is

$$\frac{\Delta N}{\overline{N}} = 1 - \frac{1 + E_2(a)}{1 - \exp(-2a)}\,\frac{1 - \exp(-4an)}{1 - E_2^{2n}(a)}. \tag{6}$$

For $a < 0.1$, expression (6) gives an error >10%, and in this case $\Delta N/\overline{N}$ should be determined from the relations (4) and (5). Obviously, when $0.1 \leq a < 1$, $\Delta N/\overline{N}$ has a maximum at n = 1. In transitional conditions of the nuclear reactor and hot circuit (activity saturation of the hot circuit or changing the nuclear reactor power) $\Delta N/\overline{N}$ decreases when the number of operating runs increases. In case of activity saturation ($n \to \infty$), $\Delta N/\overline{N}$ depends, if only weakly, on a and amounts to ~10%.

Thus, when using liquid-phase process materials with high thermal neutron absorption cross sections (ten to hundreds of barns) and short (of the order ≤1 h) half-lives of produced isotopes, the γ-radiation power of the hot circuit should be calculated taking into account the hydrodynamic conditions of flow of the process material.

In conclusion, the authors thank N. P. Syrkus for useful discussions.

LITERATURE CITED

1. A. Kh. Breger et al., Principles of Radiation-Chemistry Equipment Design [in Russian], Atomizdat, Moscow (1967).
2. A. S. Dindun, V. V. Gavar, and É. Ya. Tomson, Hot Circuits as Sources of γ Radiation [in Russian], Zinatne, Riga (1969).
3. A. Kh. Breger et al., At. Energ., 37, No. 1, 60 (1974).

PERFORMANCE OF AN IRRADIATION LOOP CONTAINING NONFISSILE MATERIAL

N. I. Rybkin, A. Kh. Breger, E. S. Stariznii, and N. P. Syrkus

UDC 621.039.573

Various types of circulation have been employed in new or updated irradiation loops in research reactors [1]: direct-flow (Fig. 1a-c) or with hydraulic decoupling (d-h), with further subdivision in terms of the branching in one or more stages (a, d, and h), in addition to any other differences in the parts within the reactor (generation in one or several stages, as in a-d, g, and h) or in the number of irradiation units (a, c, d, f, g, h). Each of these different schemes has its advantages and disadvantages. For example, a direct-flow scheme is simple to design and gives a high external yield factor η_γ for the γ radiation [2], but it does result in flow instability in branched and multiple-irradiation systems and cannot be used if the difference in height between the source and the irradiation unit is much in excess of 10 m on account of the lack of pumps giving appropriate pressures. Schemes with hydraulic decoupling are free from some of the disadvantages of direct-flow schemes but have lower values for η_γ, and therefore the optimality of any particular scheme must be considered in terms of reliability, stability, and efficiency, and this requires a detailed examination for each particular design. Here we employ an optimality criterion based on the loss of γ-ray flux in a hydraulic system relative to a direct-flow one:

$$r=1-\eta_{\gamma h}/\eta_{\gamma d}.$$

The extraction (yield) factor for a loop that includes l reactor sections and m irradiation sections is:

$$\eta_\gamma=\sum_{j=1}^{m} A_j\Big/\sum_{i=1}^{l} N_i,$$

where A_j is the steady-state activity of the working substance in irradiator j and N_i is the number of active nuclei formed in 1 sec in section i.

A published method [3] enables us to show that

$$A_j=M_j\,(1-\widetilde{\lambda}_j)\,BS,$$

where

$$B=\sum_{i=1}^{l} N_{0i}\,(\Phi_{i1}-\Phi_{i2}\widetilde{\lambda}_i);$$

$$N_{0i}=\frac{G_{pi}\varphi_i\Sigma_{\text{act}}}{\varphi_i\,(\sigma_{a2}-\sigma_{a1})+\lambda};$$

Translated from Atomnaya Énergiya, Vol. 46, No. 5, pp. 342-344, May, 1979. Original article submitted July 27, 1978; revision submitted December 11, 1978.

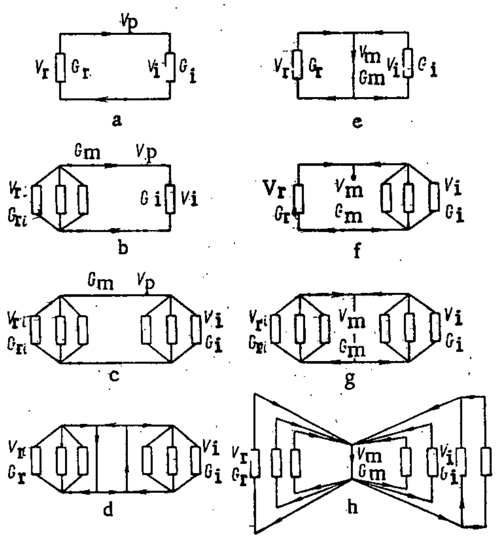

Fig. 1

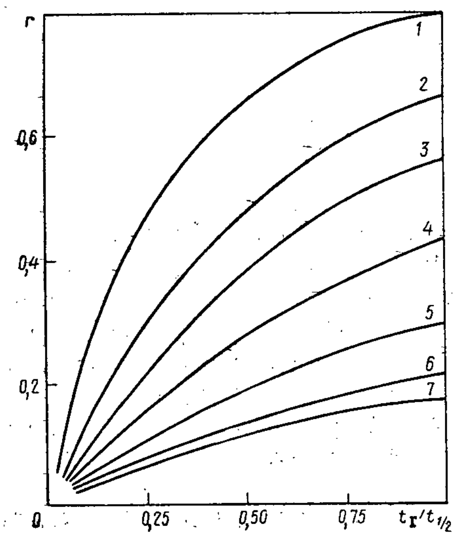

Fig. 2

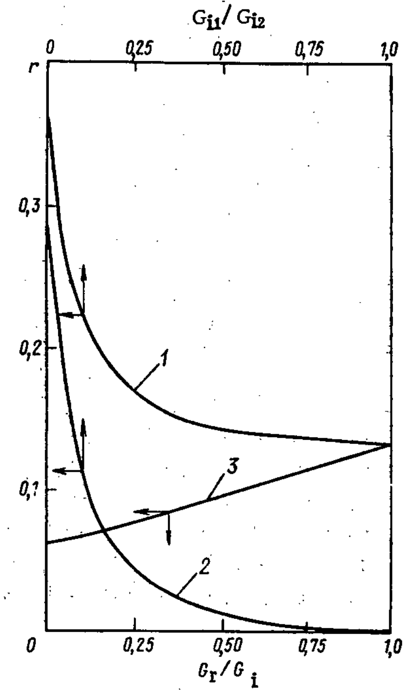

Fig. 3

Fig. 1. Designs of irradiation loop.

Fig. 2. Curves for γ-ray flux loss: $r = f(t_r/T_{1/2}, G_i/G_r)$ for $G_i/G_r = 0.1$ (1); 0.2 (2); 0.3 (3); 0.4 (4); 1.0 (5); 2.0 (6); 5.0 (7).

Fig. 3. Curves for γ-ray flux loss in an RBMK reactor: 1) $r_h = f(G_{i1}/G_{i2}, G_i/G_r = 1)$; 2) $r_d = f(G_{i1}/G_{i2}, G_i/G_r = 1)$; 3) $r_h = f(G_r/G_i, G_{i1}/G_{i2} = 1)$ for $t_r/T_{1/2} = 0.282$, $t_p/t_r = 0.427$, $V_{i1} = V_{i2} = V_r$.

$$S_d = \frac{\left(\sum_{i=1}^{l} L_i\Phi_{i1}\right)^{\tau/T_c}}{\sum_{i=1}^{l} L_i\Phi_{i1} - \left(\sum_{j=1}^{m} M_j\tilde{\lambda}_j\right)\left(\sum_{i=1}^{l} L_i\Phi_{i2}\tilde{\lambda}_i\right)\tilde{\lambda}_{ij}}$$

(for a direct-flow scheme) and

$$S_h = \frac{\left(\sum_{i=1}^{l} L_i\Phi_{i1} + \sum_{j=1}^{m} M_j\right)^{\tau/T_c}}{\sum_{i=1}^{r} L_i\Phi_{i1} - \sum_{i=1}^{l} L_i\Phi_{i2}\bar{\lambda}_i + \sum_{j=1}^{m} M_j + \sum_{j=1}^{m} M_j\bar{\lambda}_j}$$

(for a hydraulic-decoupling scheme).

Here Σ_{act} is the macroscopic thermal-neutron activation cross section for the working substance; φ_i, thermal-neutron flux density; σ_{a1}, σ_{a2}, thermal-neutron absorption cross sections for the target and product nuclides; λ, decay constant; $L_i = G_{ri}/G_m$, $M_j = G_{ij}/G_m$; G_{ri}, G_{ii}, G_m, volume flow rates in the reactor, in the irradiator, and in the mixing section; Φ_{1i}, Φ_{i2}, $\bar{\lambda}_i$, $\bar{\lambda}_j$, $\tilde{\lambda}_i$, $\tilde{\lambda}_j$, $\tilde{\lambda}_{ij}$, exponential functions whose exponents are $-\varphi_i\sigma_{a1}t_{ri}$, $-\varphi_i\sigma_{a2}t_{ri}$, $-\lambda T_{ri}$, $-\lambda T_{ij}$, $-\lambda t_{ri}$, $-\lambda t_{ij}$, $-\lambda t_{pij}$, respectively; t_{ri}, t_{ij}, t_{pij}, times spent by the working substance in the reactor, the irradiator, and the pipelines; τ, loop working time; $T_c = (\Sigma V_{ri} + \sum_j V_{ij} + \sum_{ij} V_{pij})/G_m$, circulation time; V_r, V_i, V_p, volumes of the working substance in the reactor, irradiator, and pipelines; and $T_{ri} = t_{ri} + t_{pi} + t_m$; $T_{ij} = t_{ij} + t_{pj} + t_m$; t_m, t_{pi}, t_{pj}, times spent by the working substance in the mixer (volume V) and in the pipelines before and after the mixer (Fig. 1):

$$N_{ri\,d} = N_{0i}\left(\sum_{i=1}^{l} L_i\Phi_{i1}\right)^{\tau/T_c}(\Phi_{i1} - \Phi_{i2}\tilde{\lambda}_i);$$

$$N_{ri\,h} = N_{0i}\left(\sum_{i=1}^{l} L_i\Phi_{i1} + \sum_{j=1}^{m} M_j\right)^{\tau/T_c}(\Phi_{i1} - \Phi_{i2}\tilde{\lambda}_i).$$

Quantitative evaluation of the effects of the mode of operation on r can be based on schemes with one reactor section ($l = 1$) and one irradiator ($m = 1$).

Figure 2 shows values for $r = f(t_r / T_{1/2}, G_i / G_r)$ for the case $V_i = 2V_r$ and $t_p = 0$ (data have also been obtained for $t_p \neq 0$). These results show that at high circulation speeds, i.e., for $t_r / T_{1/2} \ll 1$, we have that $G_i / G_r > 1$ and $r \lesssim 0.1$, and under such conditions a loop with hydraulic decoupling shows little effect on the γ-ray recovery factor. However, r increases considerably with $t_r / T_{1/2}$, especially for $G_i / G_r \lesssim 1$, and it becomes irrational to use a hydraulic-decoupling scheme, at least from the energy viewpoint. The results are largely analogous if an irradiator system ($m \geq 2$) is used.

The effects of uneven distribution of the working material between the irradiators on the γ-ray yield factor are only slight.

Figure 3 shows an example of the behavior of r for loops in an RBMK reactor [4]. In hydraulic decoupling with two irradiators and equal flow rates in the reactor sections, the result for r was about 0.13 for $G_{i_1} = G_{i2}$ ($V_m \to 0$) (curve 1), which corresponds to a loss of 14 kW of γ-ray power.* If the flow rate through the irradiators is increased to the point where $G_{i_1} = G_{i_2} > G_r$, there is a fall in r (curve 3), while for a direct-flow scheme with the same relationships and the same capacities for the major units one gets only a slight change in r for flow rates in the irradiators within the range $0.25 \lesssim G_{i_1} / G_{i_2} \lesssim 1$, and only for $G_{i_1} / G_{i_2} < 0.25$ is there an appreciable rise in r (curve 2). Therefore, the detailed engineering design of the system has to be considered in optimizing such an irradiation loop.

LITERATURE CITED

1. A. S. Dindun, V. V. Gavar, and É. Ya. Tomson, Radiation Loops as γ-Ray Sources [in Russian], Zinatne, Riga (1969).
2. A. Kh. Breger, Yu. S. Ryabukhin, and F. A. Makhlis, Dokl. Akad. Nauk SSSR, 136, 671 (1961).
3. E. S. Stariznii and A. Kh. Breger, Izotopy SSSR, No. 38, 19 (1974).
4. A. Kh. Breger et al., At. Energ., 37, No. 1, 60 (1974).

*With such a loop operating for 7000 h/yr, the loss corresponds to about 10^5 kW · h/yr of γ-ray energy or (assuming a cost of about 5 rubles/kW · h) a loss of about 0.5 million rubles per year.

SELF-ABSORPTION FACTOR OF γ RADIATION IN FUEL ASSEMBLIES

V. A. Voronina, Yu. N. Kazachenkov, and V. D. Simonov

UDC 539.122.539.166.3

One of the methods of determination of the isotopic composition of irradiated nuclear fuel is by γ spectrometry of fission products [1]. Of particular practical importance is the isotopic composition of entire fuel assemblies. Fuel assemblies are analyzed with the aid of high-resolution Ge(Li) detectors with a sensitive volume of several cubic centimeters placed at a distance of 3-5 m from the assembly. A collimator with a slit not longer than 5 mm is placed in front of the detector [2].

Besides measuring the γ-radiation intensity, to determine the composition of radioactive fission products it is also necessary to find the self-absorption factor of the assembly. The expression for self-absorption of γ quanta of energy E in a fuel assembly with γ sources uniformly distributed in a volume V has the form

$$K(E) = \frac{\iiint_V [dv/4\pi l^2(\mathbf{r})] \exp\left[-\int \mu(E, \mathbf{r})\, dr\right]}{\iiint_V dv/4\pi l^2(\mathbf{r})}, \tag{1}$$

where $\mu(E, \mathbf{r})$ is the γ quanta attenuation at point $\mathbf{r}$ and $l(\mathbf{r})$ is the distance from point $\mathbf{r}$ to the detector.

Translated from Atomnaya Énergiya, Vol. 46, No. 5, pp. 344-346, May, 1979. Original article submitted January 30, 1978.

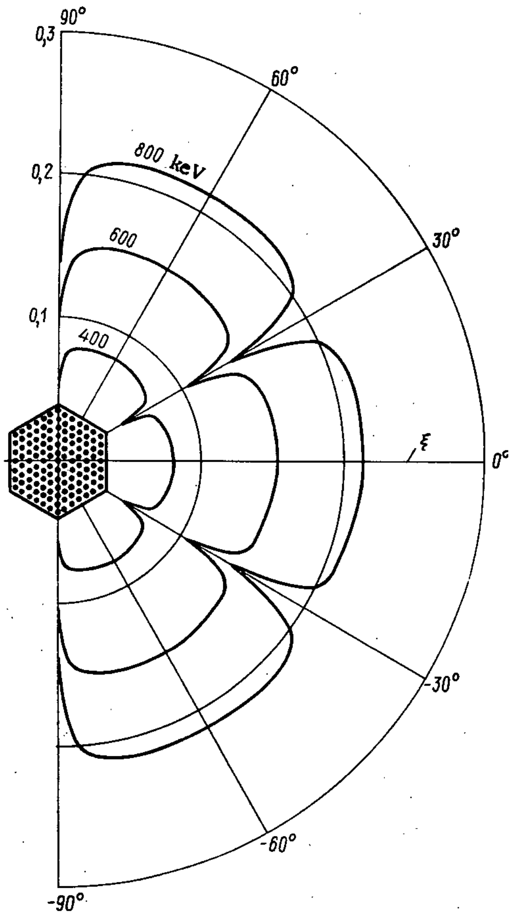

Fig. 1. Angular distribution of γ radiation self-absorption factor in VVÉR-440 fuel assemblies.

The specific features of γ spectrometers allow the following assumptions to be made: γ quanta incident on the detector are parallel to a line ξ drawn from the center of the detector to the center of the fuel assembly cross section; the distance from the detector to any point of the cross section of the i-th fuel element of the assembly is equal to the distance l_i to its center; the detector has a point sensitive volume; the γ-radiation intensity bounded by the slit height is constant. For cylindrical fuel elements expression (1) gives then:

$$K(E,\alpha)=\frac{\sum\limits_i \frac{\chi_i(E,\alpha)}{l_i^2(\alpha)}\int\limits_{-r}^{r}\exp\left[-\mu_1(E)\left(\sqrt{R_2^2-x^2}-\sqrt{R_1^2-x^2}\right)\right]J_i(E,x)\prod\limits_{\substack{|x_{i'}-x_i|\leqslant r\\ y_{i'}<y_i}}\Psi\left[E,\,x+x_i(\alpha)-x_{i'}(\alpha)\right]dx}{\sum\limits_i \frac{1}{l_i^2(\alpha)}\int\limits_{-r}^{r}\int\limits_{-\sqrt{r^2-x^2}}^{\sqrt{r^2-x^2}}\varphi_i(x,y)\,dy\,dx}, \tag{2}$$

where

$$J_i(E,x)=\begin{cases}\int\limits_{-\sqrt{r^2-x^2}}^{\sqrt{r^2-x^2}}\varphi_i(x,y)\exp\left[-\mu(E)\left(y+\sqrt{r^2-x^2}-2\sqrt{r_0^2-x^2}\right)\right]dy, & |x|<r_0,\\ \int\limits_{-\sqrt{r^2-x^2}}^{\sqrt{r^2-x^2}}\varphi_i(x,y)\exp\left[-\mu(E)\left(y+\sqrt{r^2-x^2}\right)\right]dy, & r_0\leqslant|x|\leqslant r;\end{cases}$$

$$\Psi(E,x)=\begin{cases}\exp\left[-2\mu_1(E)\left(\sqrt{R_2^2-x^2}-\sqrt{R_1^2-x^2}\right)-2\mu(E)\left(\sqrt{r^2-x^2}-\sqrt{r_0^2-x^2}\right)\right], & |x|<r_0,\\ \exp\left[-2\mu_1(E)\left(\sqrt{R_2^2-x^2}-\sqrt{R_1^2-x^2}\right)-2\mu(E)\sqrt{r^2-x^2}\right], & r_0\leqslant|x|\leqslant r,\\ \exp\left[-2\mu_1(E)\left(\sqrt{R_2^2-x^2}-\sqrt{R_1^2-x^2}\right)\right], & r<|x|<R_1,\\ \exp\left[-2\mu_1(E)\left(\sqrt{R_2^2-x^2}\right)\right], & R_1\leqslant|x|\leqslant R_2,\\ 1, & |x|>R_2;\end{cases}$$

$\varphi_i(x, y)$ is the cross-sectional distribution function of γ sources in the i-th fuel element; α, angle between the normal to the surface closest to the detector and the line ξ, i.e., the angle of turn of the fuel assembly with respect to the detector; $x_i(\alpha)$ and $y_i(\alpha)$, coordinates of the center of the i-th fuel element after the assembly

TABLE 1. Relative Contribution of γ Radiation of Fuel-Element Semirings Facing the Detector (α = 0), %

E, keV	No. of fuel-element semirings		
	1	2	3
400	68	92	96
600	53	78	87
800	45	69	80

TABLE 2. Self-Absorption Factor for Various γ Source Distributions (α = 0)

Factor	E, keV				
	500	1000	1500	2000	3000
K	0,120	0,263	0,341	0,379	0,411
K_1	0,124	0,267	0,344	0,382	0,414
K_2	0,127	0,271	0,348	0,385	0,417

has been turned through and angle α in a fixed system whose axis of ordinates is directed along the line ξ; μ(E) and μ_1(E), linear γ quanta attenuation factors of the fuel element core and casing, respectively; $\chi_i(E, \alpha)$, γ-radiation attenuation factor of the i-th fuel element in the fuel assembly jacket; and r, r_0 and R_2, R_1, outside and inside radii of the i-th fuel element core and casing, respectively.

Expression (2) provides information on the specific features of γ radiation of fuel assemblies. Figure 1 shows the angular dependence of the self-absorption factor of a hexagonal fuel assembly of the VVÉR-440 reactor [3] calculated for γ quanta with an energy of 400, 600, and 800 keV using the data of [4] and assuming a uniform distribution of γ sources in the fuel. Most significant screening is observed in the direction of the fuel assembly edge (α = 30°, 90°, . . .) where the fuel elements follow each other closely. Table 1 lists the relative contribution of the outside hexagonal semirings of fuel elements to the radiation reaching the detector. In spectrometric measurements the detector "sees" mainly the fuel elements closest to it while the contribution of the more screened fuel elements increases with increasing γ-quanta energy. For example, when the energy increases from 400 to 800 keV, the relative contribution of the most screened portion of the assembly increases from 4 to 20%. The effect of γ sources distribution inhomogeneity across the VVÉR-440 fuel assembly on the self-absorption is illustrated in Table 2 which list the self-absorption factor for a uniform distribution of γ sources (K), and for radiation intensity of the fuel element of the outside hexagonal semiring increased by 10% (K_1) and 20% (K_2). The inhomogeneity is less pronounced at high γ quanta energies. In all considered cases the change in the self-absorption factor did not exceed 2% at energies higher than 1500 keV.

Expression (2) can be used to calculate the γ radiation self-absorption factor for any fuel assemblies with cylindrical fuel elements and for any γ source distribution in the fuel. The derived expression can be easily extended to other γ-radiation sources of a complex heterogeneous structure provided their dimensions are much less than the distance to the observation point.

LITERATURE CITED

1. O. A. Miller et al., At. Energ., 27, No. 4, 281 (1969).
2. H. Graber et al., Kernenergie, 17, No. 3, 73 (1974).
3. F. Ya. Ovchinnikov et al., Operation of Reactor Units of the Novovoronezh Atomic Power Plant [in Russian], Atomizdat, Moscow (1972).
4. E. Storm and H. Israel, γ Radiation Interaction Cross Sections (for Energies from 0.001 to 100 MeV and Elements 1-100) [Russian translation], Atomizdat, Moscow (1973).

TEMPERATURE FIELD AT THE SURFACE OF THE PERIPHERAL ASSEMBLY FUEL ELEMENTS IN A NUCLEAR REACTOR WITH A LIQUID-METAL COOLANT

B. P. Shulyndin

UDC 621.039.534

To ensure reliable operation of nuclear-reactor fuel elements, certain thermophysical fuel-element characteristics must not exceed the limiting permissible values. Therefore, one of the problems of thermohydraulic nuclear-reaction calculation is to determine the temperature distribution at the fuel-element surface. The solution of this problem is particularly important for the piles of fast reactors with liquid-metal coolant, since they are characterized by large values of the thermal stress, small values of the relative fuel-element lattice step h (i.e., the ratio of the lattice step to the fuel-element diameter d), and also significant differences in the cooling of internal and peripheral fuel elements.

Accurate determination of the temperature field at the fuel-element surfaces in the pile by solving the differential equations of hydrodynamics and heat transfer for spiral fuel-element spacing is impossible; the use of approximate methods is necessary.

In the thermohydraulic calculation of reactors with liquid-metal coolant, the principle of approximate thermal modeling of the fuel-elements is found to be effective [1]; it offers the possibility of extending experimental results obtained on models to real piles [2] and also of calculating the temperature nonuniformity at the fuel-element surface in a regular lattice. In the latter case, the results obtained by calculation for "plane" conditions of heat-carrier flow (when the axial coolant velocity is constant in the pile cross section) and for Prandtl-value numbers $Pr \to 0$ [3] are used in describing the real turbulent flow conditions [4].

In the present work, a method is proposed for calculating the temperature distribution at the surface of the peripheral fuel elements in the cubic assembly of a reactor with liquid-metal coolant; the surrounding space is divided into five elementary cells, for each of which the values of the mean temperature and heat-carrier velocity are known in a series of cross sections of the pile. The method rests on the use of a generalized principle of approximate thermal modeling in each cell.

In [3] monograms are given for the calculation (for "plane" flow conditions) of the relative temperature nonuniformity over the fuel-element perimeter $\theta(h, \varepsilon_{k_0})$ and the coefficient $Z(h, \varepsilon_{k_0})$ taking into account the deviation from cosinusoidal form of the temperature distribution over the perimeter. They are obtained separately for triangular and square lattices. Here ε_{k_0} is the thermal-similarity parameter calculated for the k_0-th number of the fundamental harmonic in the Fourier-series expansion of the temperature field [1, 3]. The use of the principle of approximate thermal modeling is based on the possibility of generalizing the characterized nomograms in the form $\theta(y, \varepsilon_{k_0})$, $Z(y, \varepsilon_{k_0})$, regardless of the type of lattice.

The geometric nonuniformity parameter of the cell, y, is the ratio between the mean distance from the fuel-element surface to the nearest adiabatic-limit line (ALL) in the cell (in regular cells, the line of points equidistant from the fuel elements) and the minimum distance. In this notation, the periodicity of the temperature field over the fuel-element perimeter has no effect on θ and Z, as well as the similarity parameter ε_{k_0}.

The generalized dependences obtained may be approximated, with an error not exceeding ±3%, by the relations

$$\theta = 0.23 \exp\left[7.35\cdot 10^{-2}\frac{y-5{,}9}{y-1{,}049}\right] - 0{,}76\exp\left[0.4\frac{y-5.9}{y-1{,}049}\right]\lg\varepsilon_{k_0}; \tag{1}$$

$$Z = 1{,}01 - 0.307\exp\left[0{,}262\frac{y-5.9}{y-1{,}049}\right]\lg\varepsilon_{k_0}. \tag{2}$$

These relations are valid for $k_0 = 4$ (a square lattice) and $k_0 = 6$ (a triangular lattice). It may therefore be supposed that they are valid for any part of the fuel-element perimeter in an irregular cell that falls between

Translated from Atomnaya Énergiya, Vol. 46, No. 5, pp. 347-348, May, 1979. Original article submitted March 22, 1978.

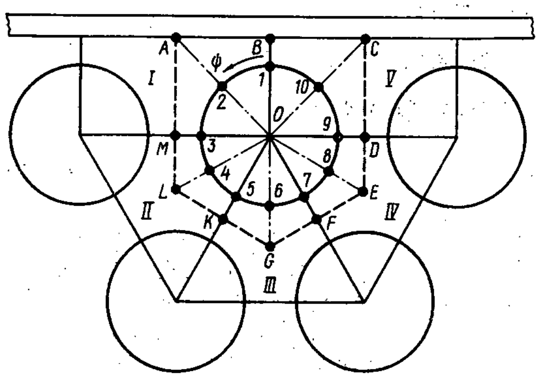

Fig. 1

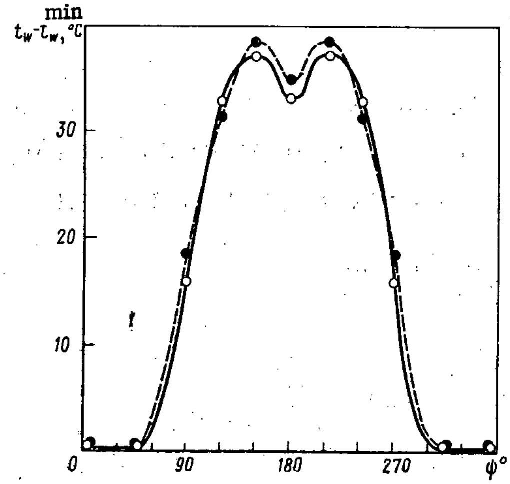

Fig. 2

Fig. 1. Surroundings of a lateral fuel element of a cubic assembly: I-V) cells; 1-10) calculation points.

Fig. 2. Temperature distribution over the perimeter of a lateral fuel element of a BOR-60 pile at a height of 0.24 m from the active-region inlet: ●) experiment [2]; ○) calculation.

the directions from the center of the fuel element to the ALL points most and least distant from the fuel-element surface, i.e., for the part of the perimeter between the points of relative temperature minima and maxima on the fuel-element surface. This assumption allows the relative values of the temperature maxima and minima to be determined, after which the temperature distributions are "matched" by the simple averaging of temperature values at the boundaries of the calculation regions. Note that in such calculations k_0 should be understood to be the ratio between the angle π and the angle between the directions from the center of the fuel-element to the points of relative temperature maxima and minima. As a result, the calculation procedure described may be used to obtain values of the surface temperature for each peripheral fuel element at 10 points of its parameter.

Determining y in the absence of displacement medium in the peripheral cells, it may be assumed without particular error that the adiabatic-limit lines in the directions of the assembly casing are the internal perimeter of the casing. The parameter y must be calculated for each calculation region within which the distance from the fuel-element surface to the ALL varies monotonically. For example, for a lateral fuel element of a cubic assembly, these calculation regions are the areas OBC, OCD, ODE, etc. (Fig. 1).

The presence of a displacement medium in the peripheral cells may be easily taken into account by adjusting the nonuniformity parameter y according to the following approximate relation, which takes into account the change in mean distance from the fuel-element surface to the ALL

$$y = y_0 \frac{2\sqrt{(F - F_D)/\pi} - d}{2\sqrt{F/\pi} - d}, \tag{3}$$

where y_0 is the geometric nonuniformity parameter for a calculation region without displacement medium; F, cross-sectional area of the region with no displacement medium; F_D, area of the region occupied by displacement medium.

Thermal interaction between adjacent cells is taken into account using some effective nonuniformity y_e instead of the geometric parameter y in Eqs. (1) and (2)

$$y_e = 1 + (y - 1)\exp\left(-15\frac{\lambda_{fi}\,|t_{i+1} - t_{i-1}|}{\Delta\Pi_i \bar{q}}\right), \tag{4}$$

where t_{i+1} and t_{i-1} are the mean heat-carrier temperatures in the cells adjacent to the given cell i; λ_{fi}, thermal conductivity of the heat carrier in cell i; $\Delta\Pi_i$, length of the fuel-element perimeter within cell i; $\bar{q}$, mean thermal load of the fuel-element surface. Equation (4) is derived using an assumption regarding the influence on the temperature nonuniformity of the ratio between the heat fluxes perpendicular and parallel to the fuel-element perimeter.

The correctness of Eq. (4) is confirmed in that, using Eq. (4) and the numerical value of 15 for the coefficient, good agreement is obtained between the calculated results and experimental data for piles differing widely in their geometric parameters and cooling parameters [2, 5, 6].

Thus, the method developed for the calculation of the temperature field at the surface of peripheral fuel elements reduces to the following. Using one of the existing methods (e.g., the methods of [6, 7]), in each pile cross section considered, the mean values of the heat-carrier axial velocity and temperature over the height in each cell surrounding the peripheral fuel element and the fuel-element surface temperature are determined. The geometric and effective nonuniformity parameters of the calculation regions and the values of θ and Z for plane heat-carrier flow are determined using Eqs. (1)-(4). The value of θ is multiplied by the correction factor $\varkappa$, taking into account the deviation from planar of the turbulent conditions of liquid flow, which is calculated from the relation in [4]; for peripheral cells, the relative lattice step is replaced by some effective value of the step of a triangular lattice, in the elementary cells of which the proportion of coolant is the same as in the given peripheral cell.

For each calculation region, the values of the fuel-element surface temperature at the points of relative maxima (t_W^{max}) and minima (t_W^{min}) are calculated

$$t_W^{max} = \bar{t}_{Wi} + \frac{Z\theta}{Z+1}\,\frac{d\bar{q}}{2\lambda_{fi}}; \tag{5}$$

$$t_W^{min} = \bar{t}_{Wi} - \frac{\theta}{Z+1}\,\frac{d\bar{q}}{2\lambda_{fi}}, \tag{6}$$

where $\bar{t}_{Wi}$ is the mean fuel-element surface temperature within the cell. At the temperatures of the region, the temperature values are averaged.

The method developed has been used to calculate the temperature field at the surface of corner and side fuel elements of piles with liquid-metal coolant for which thermophysical investigations on models have been carried out [2, 5], and agreement between calculation and experiment is found to be good (Fig. 2).

LITERATURE CITED

1. P. A. Ushakov, in: Liquid Metals [in Russian], Atomizdat, Moscow (1967), p. 137.
2. V. I. Subbotin et al., At. Energ., 28, No. 6, 489 (1970).
3. P. A. Ushakov et al., Preprint FÉI-163, Obninsk (1969).
4. M. Kh. Ibragimov and A. V. Zhukov, At. Energ., 24, No. 6, 520 (1968).
5. A. V. Zhukov et al., in: Liquid Metals [in Russian], Atomizdat, Moscow (1967), p. 170.
6. V. I. Subbotin et al., Hydrodynamics and Heat Transfer in Atomic Power Stations (Principles of Calculation) [in Russian], Atomizdat, Moscow (1975).
7. V. E. Minashin et al., Thermophysics of Nuclear Reactors with Liquid-Metal Coolant and Methods of Electrical Modeling [in Russian], Atomizdat, Moscow (1971).

ACTIVATION COMPONENT OF THE RESPONSE OF A SELF-POWERED NEUTRON DETECTOR TO THERMAL AND EPITHERMAL NEUTRONS

O. Érben

UDC 539.1.074.8

One has to determine the depression and self-screening coefficients in theoretical calculation of the activation component of the response of an SPN β-emission detector to thermal and epithermal fluxes s_{th} and s_{epi}, where these fluxes are Φ_{th} and φ_{epi}, respectively, while the coefficients are G_{th} and G_{epi}; one also has to calculate the probabilities ε_{th} and ε_{epi} that β particles from these sources will produce signals.

The current I_β due to β decay of activated atoms in the emitter is

$$I_\beta = s_{th}\Phi_{th} + s_{epi}\varphi_{epi}, \tag{1}$$

i.e.,

$$I_\beta = k_1 G_{th}\varepsilon_{th}\Phi_{th} + k_2 G_{epi}\varepsilon_{epi}\varphi_{epi}. \tag{2}$$

The constants k_1 and k_2 include the nuclear-physics constants of the emitter material.

The overall activation component for a silver SPN is the sum of components related to $^{107-110}Ag$ and the corresponding β decays; as the activation cross sections of rhodium and silver are high, it is not possible to use simple approximate relationships for G_{th} (emitter radius ≥ 0.02 cm), while G_{epi} differs substantially from G_{th} for rhodium or ^{109}Ag on account of the large resonance integrals for these materials. Therefore, G_{th} and G_{epi} have been calculated via the Apollo program [1], which solves the kinetic equation for neutron transport in 99 energy groups for thermal reactors. Since the resonance integral for ^{51}V is small, the results were incorporated into a single group for vanadium SPN and into two groups (thermal and epithermal) for rhodium and silver devices [2]. The calculations gave functions that describe the distribution of the β-particle sources over the cross section of the emitter as

$$S_j(r) = \frac{1 + b_j r^2}{\pi r_e^2 [1 + (b_j r_e^2/2)]}, \quad j = \text{th, epi}, \tag{3}$$

where r_e is the emitter radius; r, distance from the axis of the emitter; and b_{th}, b_{epi}, parameters defined by the calculations (Table 1), which were performed for the environment of the ISIS research reactor: fuel with 93% enriched ^{235}U, moderator and coolant – water at 40°C. Data have also been given [2] from analogous calculations for cobalt SPN.

The method of determining ε_{th} and ε_{epi} has been described [3], and here we describe only the basis of the solution and the results. By r_e and ρ_e we denote the radius and density of the emitter, while r_{ii}, r_{ie}, ρ_i are the internal and external radii and density of the insulator. Let the S(r) defined above describe the distribution of the β-particle sources over the cross section of the emitter and take the form $\int_0^{r_e} 2\pi r S(r) dr = 1$; then B(E) [4] characterizes the energy spectrum from β decay of maximum decay energy $E_{\beta max}$ and takes the form $\int_0^{E_{\beta max}} B \times (E) dE = 1$. Let p(r, E) be the probability that a β particle emitted at a distance r from the axis of the emitter with energy E will make a contribution to the detector signal. Then

$$\varepsilon_j = \int_0^{r_e} 2\pi r S_j(r) \int_0^{E_{\beta max}} B(E)\, p(r, E)\, dE\, dr, \quad j = \text{th, epi}. \tag{4}$$

Nuclear Research Institute, Řež, Czechoslovakia. Translated from Atomnaya Énergiya, Vol. 46, No. 5, pp. 349–352, May, 1979. Original article submitted March 27, 1978.

TABLE 1. Depression and Self-Screening Coefficients and Parameters b_{th} and b_{epi} for SPN

r_e, cm	Emitter material	G_{th}	G_{epi}	b_{th}, cm^{-2}	b_{epi}, cm^{-2}
0,020	Vanadium	0,972		7	
	Rhodium	0,758	0,250	309	3385
	Silver 107	0,888	0,912	96	66
	Silver 109	0,889	0,285	95	3735
0,025	Vanadium	0,970		6	
	Rhodium	0,724	0,234	260	2950
	Silver 107	0,866	0,825	80	45
	Silver 109	0,867	0,259	80	2740
0,040	Vanadium	0,957		3,86	
	Rhodium	0,599	0,178	173	1325
	Silver 107	0,800	0,721	51	22
	Silver 109	0,801	0,170	51	656
0,050	Vanadium	0,942		3,3	
	Rhodium	0,535	0,156	150	950
	Silver 107	0,754	0,676	43	16
	Silver 109	0,756	0,149	43	470
0,075	Vanadium	0,922		2,28	
	Rhodium	0,418	0,122	110	457
	Silver 107	0,663	0,604	29	8,7
	Silver 109	0,664	0,132	29	261
0,100	Vanadium	0,901		1,74	
	Rhodium	0,335	0,102	66	277
	Silver 107	0,585	0,557	23	5,6
	Silver 109	0,587	0,111	23	120

Then Warren's theory [5] indicates that β particles coming to rest in the insulator set up a potential whose peak value lies at radius r_p; therefore, a β particle that enters the part of the insulator bounded by r_p is returned to the emitter by this potential and does not influence the detector signal, while the same applies for a particle that comes to rest in the emitter. This probability is given by

$$p(r,\ E)=(1/4\pi)\int_{\varphi}\int_{\vartheta}\sin\vartheta\, d\vartheta\, d\varphi. \tag{5}$$

The integration is carried over the solid angle bounding the region r_p of the insulator through which a β particle can pass without absorption (Fig. 1). A β particle emitted at a distance r and moving in the direction defined by the angles ϑ and φ passes from the point of origin to the point of maximum potential along a path of length $\overline{OA}$ in the material and of $\overline{A'B}$ in the insulator. Published equations [6] are used to define the range for the β particle. Let $f_e(E)$ or $f_i(E)$ be the range of a β particle of energy E in the material of the emitter or insulator, respectively, while $F_e(R)$ is the inverse of $f_e(E)$. To facilitate the calculations, the range of a particle in the emitter is replaced by the mean equivalent range in the emitter material, i.e., we introduce a constant K:

$$K=[1/(E_{\beta\max}-0{,}1)]\int_{0{,}1}^{E_{\beta\max}}[f_e(E)/f_i(E)]\, dE. \tag{6}$$

We determine the β-particle ranges and transform the limits of integration in such a way that $p(r, E) \neq 0$ to get

$$\varepsilon_j=\frac{1}{\pi}\int_{r_{\min}}^{r_e} 2\pi r S_j(r)\int_{E_{\min}}^{E_{\beta\max}} B(E)\int_{-\pi/2}^{\varphi B}\Psi(\varphi)\, d\varphi\, dE\, dr, \tag{7}$$

TABLE 2. Characteristics and Symbols for SPN Used in Experiments

Insulator radius, cm	Vanadium		Rhodium		Silver	
	V1	V2	R1	R2	S1	S2
r_e	0,02718	0,05319	0,02581	0,05058	0,02476	0,04958
r_{ii}	0,03	0,06	0,03	0,06	0,03	0,06
r_{ie}	0,0555	0,0995	0,0555	0,0995	0,0555	0,0995

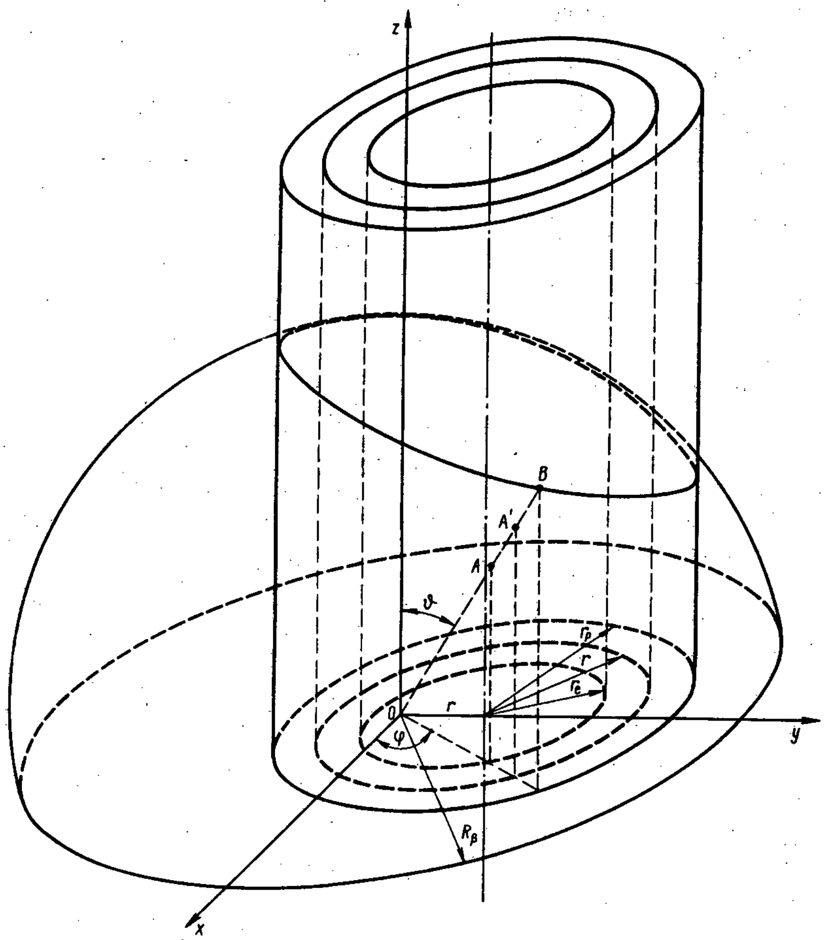

Fig. 1. Schematic representation of an SPN and of the β-particle range.

TABLE 3. Probability of a β Particle Producing a Signal

SPN	Nuclide	$E_{\beta\ max}$, MeV	β-particle source	ε
V1	^{52}V	2,47	th+epi	0,665
V2	^{52}V	2,47	th+epi	0,432
R1	^{104}Rh	2,44	th	0,379
			epi	0,398
R2	^{104}Rh	2,44	th	0,196
			epi	0,222
S1	^{108}Ag	1,00	th	0,079
			epi	0,079
		1,64	th	0,232
			epi	0,232
	^{110}Ag	2,21	th	0,382
			epi	0,401
		2,87	th	0,532
			epi	0,545
S2	^{108}Ag	1,00	th	0,028
			epi	0,028
		1,64	th	0,103
			epi	0,102
	^{110}Ag	2,21	th	0,186
			epi	0,208
		2,87	th	0,290
			epi	0,310

where

$$j=\text{th, epi}; \tag{8}$$

$$\Psi(\varphi)=\sqrt{1-t^2};$$

$$t=\frac{1}{f_e(\tau)}\{\rho_e r\sin\varphi+\rho_e\sqrt{r_e^2-r^2\cos^2\varphi}+K\rho_1\sqrt{r_p^2-r^2\cos^2\varphi}-K\rho_1\sqrt{r_{1i}^2-r^2\cos^2\varphi}\}; \tag{9}$$

TABLE 4. Activation Component of SPN Sensitivity

Detector	s_{th}, 10^{-21} A/ neutron/cm^2·sec		s_{epi}, 10^{-21} A/ neutron/cm^2·sec	
	theor.	expt.	theor.	expt.
V1	0,691	0,736	0,382	0,0577
V2	1,68	1,53	0,931	1,48
R1	8,71	8,24	20,9	22,3
R2	13,0	12,1	30,3	27,6
S1	3,52	3,50	15,5	13,9
S2	6,50	6,56	20,6	20,3

TABLE 5. Thermal and Epithermal Neutron Flux Densities as Defined by Activation ($\mp 3\%$)

Irradiation site	Φ_{th}, 10^{10} neutrons/cm^2·sec	φ_{epi}, 10^{10} neutrons/cm^2·sec
Core	3,507	0,338
First peripheral part	2,238	0,0546

TABLE 6. Proportion of Activation Component in Total Signal from Sensitive Part of Detector

SPN	I_β/I_t core	I_β/I_t first peripheral part	SPN	I_β/I_t core	I_β/I_t first peripheral part
V1	1,004	0,973	R2	0,832	0,870
V2	0,968	0,931	S1	0,933	0,942
R1	0,931	0,954	S2	0,864	0,873

TABLE 7. Values of I_β in 10^{-10} A

SPN	Core		First peripheral part	
	theor.	expt.	theor.	expt.
V1	0,255	0,260	0,157	0,165
V2	0,621	0,587	0,381	0,351
R1	3,761	3,643	2,063	1,970
R2	5,583	5,166	3,074	2,857
S1	1,758	1,696	0,872	0,861
S2	2,976	2,986	1,567	1,582

$$\tau = E/m_0c^2; \tag{10}$$

$$\tau_{max} = E_{\beta max}/m_0c^2; \tag{11}$$

$$r_{min} = \max\ \{0;\ r_e - 1/\rho_e [f_e(\tau_{max}) - K\rho_1 (r_p - r_{11})]\}; \tag{12}$$

$$E_{min} = \min\ \{E_{\beta max};\ m_0c^2 F_e [(r_e - r)\rho_e + K\rho_1 (r_p - r_{11})]\}; \tag{13}$$

$$\varphi_B = \begin{cases} \pi/2 & \text{for } \tau \geqslant \tau_{cr1} \\ \text{solution to (15)} & \text{for } \tau_{cr2} < \tau < \tau_{cr1} \\ -\pi/2 & \text{for } \tau \leqslant \tau_{cr2}; \end{cases} \tag{14}$$

$$f_e(\tau) = \rho_e r \sin\varphi_B + \rho_e \sqrt{r_e^2 - r^2\cos^2\varphi_B} + K\rho_1 \sqrt{r_p^2 - r^2\cos^2\varphi_B} - K\rho_1 \sqrt{r_{11}^2 - r^2\cos^2\varphi_B}; \tag{15}$$

$$\tau_{cr1} = F_e [\rho_e (r_e + r) + K\rho_1 (r_p - r_{11})]; \tag{16}$$

$$\tau_{cr2} = F_e [\rho_e (r_e - r) + K\rho_1 (r_p - r_{11})]; \tag{17}$$

where m_0c^2 is the electron rest energy.

The probability that a β particle would produce a signal was determined for each type of SPN separately. The theoretical calculations were checked on detectors having Al_2O_3 insulators of density 3.74 g/cm^3 and emitter lengths of 8.5 cm (Table 2). Tables 3 and 4 give the probabilities of signals and the activation components of the response for SPN; the values of s_{th} and s_{epi} given in Table 4 are from (1) as deduced from the observed I_β and measured Φ_{th} and φ_{epi} for the core and the first peripheral part (Table 7).

The theoretical calculations were checked by irradiating SPN in the ISIS research reactor at the Nuclear Research Institute in Scalay [2, 7, 8] (Table 5). The fall in the detector signal after emergency reactor shutdown served to define the components of the signal arising from β decay of the activated atoms, as well as the contribution from the interaction between the capture and other γ rays from the reactor on the one hand and the detector material on the other (Table 6). The currents given in Table 7 were derived from the theoretical s_{th} and s_{epi} and the measured Φ_{th} and φ_{epi} with an error of ±5%. Theory and experiment are in satisfactory agreement. There is a substantial discrepancy over s_{epi} for the vanadium SPN, which is due to the nonuniform production of the detector signal by the thermal and epithermal neutrons (about 5% of the signal in a vanadium SPN in the core is due to the epithermal neutrons, and about 2% in the first peripheral part of the core in ISIS). Therefore, more precise determination of s_{th} and s_{epi} requires experiments with SPN placed at several points in the reactor where the neutron spectra differ substantially.

This method of determining s_{th} and s_{epi} for SPN gives values in which the burnup of the emitter material may be neglected. Data have been presented [9] on the effects of rhodium burnup on the sensitivity of these SPN.

LITERATURE CITED

1. A. Hoffmann et al., APOLLO, Rapport SERMA "S" 1193, CEN, Saclay (1973).
2. O. Erben, "The determination of self-powered neutron detector sensitivity on thermal and epithermal neutron flux densities," Jad. Energ. (in press).
3. O. Erben, "The determination of beta particle escape efficiency of self-powered neutron detectors," Jad. Energ. (in press).
4. B. S. Dzhelepov et al., Beta Processes: Functions for Analysis of β-Ray and Electron-Capture Spectra [in Russian], Nauka, Leningrad (1972).
5. H. D. Warren, Nucl. Sci. Eng., 48, No. 2, 331 (1972).
6. T. Tabata et al., Nucl. Instrum. Methods, 103, No. 1, 85 (1972).
7. O. Erben, C. Le Tanno, and C. Morin, Collectron: Étude de la Sensibilité, Rapport CEA-CEN/S (in press).
8. O. Erben, Some Properties and Applications of SPN Detectors. Ustav. Jad. Vlast. Report 4376-R, T (1978).
9. O. Erben, "The influence of rhodium burn-up on the sensitivity of rhodium self-powered neutron detectors," Jad. Energ. (in press).

NUMBER OF K-EMISSION PHOTONS GENERATED BY MONOENERGETIC ELECTRONS AND β PARTICLES

F. P. Teplov, V. P. Sytin,
and A. I. Melovat-skaya

UDC 539.121.7

The determination of the number of K-emission photons originating in the ionization of the K shell by electron or β-particle bombardment has considerable scientific and practical importance as, e.g., in the design and application of radionuclide sources of ionizing radiation [1], the study of interaction of radiation and matter, the evaluation of the fraction of characteristic radiation in x-ray emission spectra. The known expressions from which the number of K-emission photons generated by monoenergetic electrons or β particles can be computed either are of a particular nature [2] or have been derived under assumptions that do not provide reliable results [1, 3].

The number of K-emission photons generated in material with an atomic number Z by an electron with an initial energy E is given by

$$N_k=\int_{E_k}^{E} \omega_k\sigma(E, Z)\frac{1}{dE/dx}\,dE, \tag{1}$$

where E_k is the energy of the K-absorption band edge; ω_k, K-fluorescence yield; $\sigma(E, Z)$, ionization cross section of the K shell; and dE/dx, loss of electron energy per unit trajectory.

Expression (1) has been applied to elements with atomic numbers 13-92 and for electron energies not exceeding $U_0 = E/E_k = 20$. We have used expressions for ω_k and $\sigma(E, Z)$ adopted from [4, 5], respectively, and the Bethe–Bloch equation for dE/dx [6]. The obtained results are listed in Table 1.

By analyzing the obtained numerical values, it is possible to derive an approximate function for the number of K-emission photons generated by monoenergetic electrons:

$$N_k=0.263\omega_k Z^{-1.11}(U_0-1-\ln U_0)^{1.12} \tag{2}$$

The results obtained using Eq. (2) differ from those cited in Table 1 by not more than ±10%. The values of N_k have been used to find the number of K-emission photons excited by beta particles of radionuclides. The energy spectra of radionuclide β emission were split into a definite number of intervals assuming that all β particles within an interval have the same energy. The obtained results are shown in Table 2.

Translated from Atomnaya Énergiya, Vol. 46, No. 5, pp. 352-354, May, 1979. Original article submitted May 15, 1978.

0038-531X/79/4605-0406$07.50

TABLE 1. Number of K-Emission Photons, Photons / Electrons

U_0	Al	Zr	Sn	Lo	W	Pb	U
1,5	0,18	2,1	1,8	1,7	1,4	1,2	1,1
2,5	1,5	16	16	14	11	10,1	9,2
5	6,9	84	80	75	63	53	48
10	22	260	250	230	200	170	160
15	39	460	440	410	340	310	270
20	58	660	640	590	500	450	410

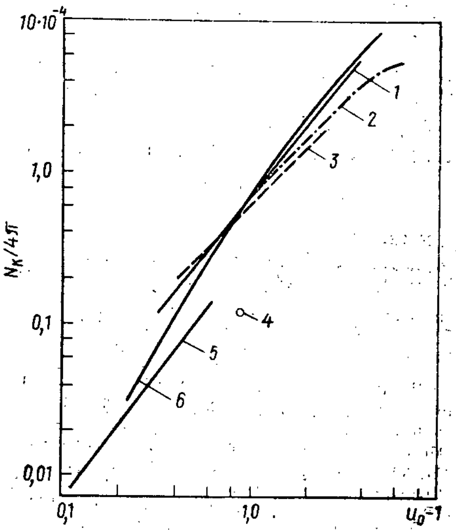

Fig. 1. Number of copper K-emission photons generated by electrons: 1-5) experimental results of several authors; 6) obtained from Eq. 2.

TABLE 2. Number of K-Emission Photons Generated by β Particles, Photons /β Particle

Element	^{147}Pm	^{90}Sr	^{85}Kr	^{204}Tl	^{32}P	^{90}Y
Sn	$1,5\cdot10^{-3}$	$1,5\cdot10^{-2}$	$2,2\cdot10^{-2}$	$1,8\cdot10^{-2}$	—	—
	$(4\cdot10^{-3})$		$(2\cdot10^{-2})$			
W	$1,1\cdot10^{-4}$	$2,3\cdot10^{-3}$	$4\cdot10^{-3}$	—	$1,9\cdot10^{-2}$	$2,7\cdot10^{-2}$
Pb	$4,3\cdot10^{-5}$	$1,5\cdot10^{-3}$	$2,5\cdot10^{-3}$	—	$1,3\cdot10^{-2}$	$1,9\cdot10^{-2}$
	$(6\cdot10^{-4})$		$(2\cdot10^{-3})$			$(7\cdot10^{-3})$
U	$5,6\cdot10^{-6}$	$7\cdot10^{-4}$	$1,2\cdot10^{-3}$	$1\cdot10^{-3}$	$7,3\cdot10^{-3}$	$1,2\cdot10^{-2}$

Calculations for radionuclides with a maximum β spectrum energy $E_\beta > 0.2$ MeV and for elements with $Z \geq 50$ gave the following approximating function:

$$N_{ks} = 3.16\cdot10^{-3}\,[(U_m - 1 - 1.3\ln U_m)\,S_\beta]^{1.31}, \qquad (3)$$

where $U_m = E_\beta / E_k$, $S_\beta = (E_{mq}/E_\beta)^2$, E_{mq} is the mean-square β spectrum energy. The difference between the N_{ks} values obtained from Eq. (3) and those listed in Table 2 does not exceed ±20%.

The obtained results were compared with published theoretical and experimental data. Figure 1 shows the number of K-emission photons in copper as a function of electron energy, and also the data obtained from Eq. (2) which is seen to be in good agreement with known data. Results calculated in [3] are shown in Table 2 within parentheses. It is seen that they do not agree with the results obtained in this work, i.e., the assumptions made in [3] as to the K-shell ionization cross section and electron energies do not provide satisfactory results in the calculation of K-emission photons generated by β particles. The reliability of the results obtained here is ensured by the high accuracy of the relationships on which our calculations are based and by the good agreement of the calculated results with known experimental data.

LITERATURE CITED

1. S. V. Rumyantsev et al., Low-Energy Radiation Sources for Nondestructive Testing [in Russian], Atomizdat, Moscow (1976).
2. W. Hink, Z. Phys., 177, No. 4, 424 (1964).
3. I. Filosofo et al., in: Production and Application of Radioactive Isotopes [in Russian], Atomizdat, Moscow (1960), p. 54.
4. Alpha, Beta, and Gamma Spectroscopy [in Russian], No. 4, Atomizdat, Moscow (1969).
5. A. Arthurs and B. Moiseiwitsch, Proc. Soc., No. A247, 550 (1958).
6. Alpha, Beta, and Gamma Spectroscopy [in Russian], No. 1, Atomizdat, Moscow (1969).

Declassified and Approved For Release 2013/02/12 : CIA-RDP10-02196R000800010005-1

VISCOSITIES OF MOLTEN MIXTURES OF URANIUM TETRAFLUORIDE WITH ALKALI FLUORIDES

V. N. Desyatnik, A. I. Nechaev, and Yu. F. Chervinskii

UDC 532.133:546.161

Measurements have been made over a wide temperature range and over the entire composition range on the viscosities of molten lithium fluoride, potassium fluoride, uranium tetrafluoride, and binary mixtures of these; damped rotational oscillation of a cylindrical crucible filled with a liquid was employed [1]. The coefficient of variation of the kinematic viscosity was 2.0%. Molybdenum crucibles were used in purified argon. The initial salts were dried chemically pure lithium and potassium fluorides, while the anhydrous uranium tetrafluoride was produced by a standard method [2]. The results for the alkali fluorides are in good agreement with published values [3].

The molar viscosity μ in erg · sec / mole was calculated from the results; also, the activation energy E for viscous flow was calculated in each case. Table 1 gives the results as the coefficients in the equations for the temperature dependence of the viscosity, along with the standard deviations S of the observed viscosities from the fitted equations.

An existing model for the structure of an ionic liquid [4] indicates that alkali-halide melts can be considered as mixtures of associated particles, free ions, and vacancies. The complexing agents are the alkali-metal cations, which are surrounded by the larger polarizable halide ions. Exceptions must be made for potassium, rubidium, and cesium fluorides, in which complexes based on fluorine are favored by energy considerations. These latter complexes should be particularly characteristic of molten halides of polyvalent metals, since elementary cations and anions are unlikely in such media. Alkali-metal cations differ in size and charge from the cations of uranium tetrafluoride, and mixing of such compounds should result in the preferential formation of groups based on U(IV), which is highly polarizable. The molar viscosity is directly related to the structure of the melt and should reflect the interaction occurring on mixing.

Isotherms for 1230°K were drawn up in order to determine the effects of the composition; the molar viscosity varies with the composition for mixtures of lithium fluoride with potassium fluoride, but the deviation from additivity is slight, which may indicate that there are no marked changes in the structure (Fig. 1).

In the $LiF-UF_4$ system, particularly at low levels of uranium tetrafluoride, the structured units involved in the viscous flow are elementary lithium cations in the second coordination sphere, $LiF_n^{(n-1)}$ ions, and

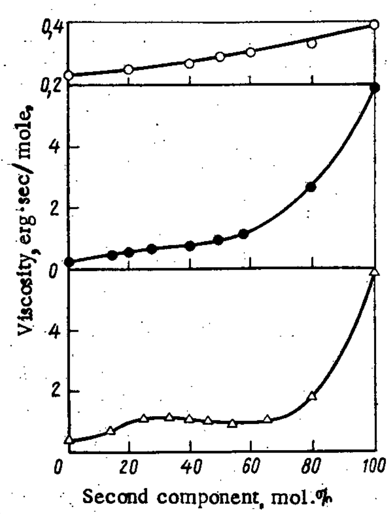

Fig. 1. Molar-viscosity isotherms for the following melts: LiF−KF (○); LiF−UF (●); and $KF-UF_4$ (Δ).

Translated from Atomnaya Énergiya, Vol. 46, No. 5, pp. 354-355, May, 1979. Original article submitted May 29, 1978; revision submitted December 4, 1978.

 0038-531X/79/4605-0408$07.50

TABLE 1. Viscosities of Molten Salt Mixtures

Second component mol.%	$\lg \mu = A + B/T$		$S \cdot 10^3$	E, cal/mole	Temp., °K
	$-A$	B			
			LiF—KF		
0,0	1,6284	1223	0,16	5596	1139—1282
20,0	1,6512	1268	0,23	5802	1039—1320
40,0	1,7075	1381	0,51	6319	926—1297
50,0	1,6798	1408	0,69	6443	820—1308
59,8	1,5949	1342	0,48	6141	923—1306
79,9	1,3203	1038	0,37	4750	1139—1306
100,0	1,3729	1189	0,34	5440	1144—1305
			$LiF-UF_4$		
15,0	1,1514	940	0,63	4301	1052—1284
20,0	1,0921	994	1,28	4548	977—1293
27,5	1,0546	968	0,43	4429	864—1268
39,9	0,9431	938	1,35	4292	943—1281
50,0	0,9377	1126	1,31	5152	1054—1283
57,8	0,9361	1226	3,38	5610	1077—1295
79,3	1,2426	2059	3,73	9421	1255—1302
			$KF-UF_4$		
14,0	0,9971	988	0,88	4521	1111—1278
24,9	0,8333	1068	2,33	4887	1211—1278
33,2	0,9422	1241	2,04	5678	1159—1270
40,0	0,8697	1135	1,38	5192	1073—1275
46,0	0,7893	1002	2,62	4585	1101—1267
53,6	0,7505	893	2,71	4085	1072—1253
66,4	0,7196	981	1,58	4489	1090—1252
78,9	1,2800	1886	2,92	8630	1205—1327
100,0	2,0444	3455	3,31	15 809	1323—1428

probably also UF_6^{2-}. As the uranium tetrafluoride concentration increases, the alkali-metal complexes are replaced by uranium ones. The viscosity increases slightly as a consequence.

In the $KF-UF_4$ system, the viscosity has a turning point in the composition range corresponding to the congruently melting compound $2KF \times UF_4$ [5], which is evidently due to the heightened stability of the uranium complexes in this composition range. The second coordination sphere in that case contains mainly elementary alkali-metal cations. Any further increase in the uranium tetrafluoride content causes the alkali cations in the second coordination sphere to be replaced by complex uranium cations such as UF_2^{2+} or UF_3^+, which is accompanied by a considerable increase in the viscosity, and the maximum value corresponds to pure uranium tetrafluoride.

The variation in the activation energy of viscous flow with the composition confirms this view of the momentum-transport mechanism. This energy increases considerably at high uranium tetrafluoride contents, evidently on account of the increased number of large uranium cation complexes in the second coordination sphere, which cause difficulties in momentum transfer.

The concentration dependence of the molar viscosity in each of the systems containing uranium tetrafluoride indicates accentuated interaction between the ions and more complicated structures, particularly on going from systems containing lithium fluoride to ones containing potassium fluoride.

LITERATURE CITED

1. E. G. Shvidkovskii, Some Aspects of the Viscosity of Molten Metals [in Russian], Gostekhteorizdat, Moscow (1955).
2. J. J. Katz and E. Rabinowitch, The Chemistry of Uranium, Part 1, The Element: Its Binary and Related Compounds, Peter Smith.
3. M. V. Smirnov et al., Zh. Fiz. Khim., 48, No. 2, 467 (1974).
4. M. V. Smirnov, Potentials of Molten Chlorides [in Russian], Nauka, Moscow (1973), p. 201.
5. G. Janz et al., J. Phys. Chem. Ref. Data, 3, No. 1, 1 (1974).

DETERMINATION OF FUEL BURNUP IN VVÉR-440 ASSEMBLIES WITH AN "ARAGONIT" RADIATION METER

O. A. Miller, L. I. Golubev,
G. A. Kulakov, and Yu. V. Efremov

UDC 621.039.516.22

The IAEA safeguards and supervision of nuclear materials require measurement of fuel burnup in fuel assemblies of water-cooled–water-moderated (VVÉR) reactors. The necessity of carrying out such measurements directly at the storage of irradiated fuel assemblies has been pointed out before [1]. Such measurements have been carried out at the fuel storage of the fourth unit of the Novovoronezh Atomic Power Plant by taking the γ radiation spectra of exposed fuel assemblies under a layer of water with the aid of the "Aragonit" radiation meter.

The measuring stand, set up in a water pool, consists of a tube surrounded by lead shield $\approx$80 mm thick and closed at the bottom. The lead shield has a hole into which is placed a collimator 50 mm in diameter, about 2 m long, with a 50 × 5 mm aperture.

The measured assembly was placed under water near the collimator and radiation spectra were taken at eight points spaced by $\approx$300 mm. The "Aragonit" meter was lowered down the tube so that the Ge(Li) detector faced the collimator (Fig. 1).

The "Aragonit" radiation meter is a γ detection unit including a planar germanium–lithium semiconductor detector with an active volume of 9.3 cm^3. The intrinsic energy resolution of the detector at the 1333-keV line was 2.8 keV with supply voltage V = 2200 V and a differentiation time equal to 2 μsec; the photopeak/compton ratio at this energy was 6.8. The detector output signal was preamplified by a charge-sensitive preamplifier with a noncooled main stage. The preamplifier noise level for zero input capacitance was 12 eV + 49 eV/pF; its conversion factor was 200 mV/MeV, the maximum count rate for 1333-keV energy quanta was $2 \cdot 10^{14}$ per second, the overall resolution was 3.3 keV at V = 2200 V and $\tau = 2\ \mu$sec. The detector operating temperature was maintained in cryostat submerged in a special dewar vessel with a shielded-vacuum thermal insulation and filled with liquid nitrogen. The capacity of the dewar vessel was 1.2 liters. The time for total evaporation of liquid nitrogen from the vessel with the cryostat submerged in it was 21 h for an ambient temperature of 25°C.

The detector block was a 1250-mm-long cylindrical bullet with a maximum diameter of 100 mm composed of three independent coupled units: the detector in cryostat, the cylindrical dewar vessel, and the amplifier in a protective case. Such a construction facilitated handling and storage of the detector block since the detector can be cooled during transportation with the aid of commercial ASD-16 dewar vessels. With such an arrangement the detector block could be held for 5-8 days without liquid nitrogen refilling in a conventional package.

The stand was used to analyze type VVÉR-440 fuel assemblies. Initial enrichment was 1.6%, average burnup was found to be 12 kg/ton U, holding time after exposure was 3 years. The γ spectra clearly indicated the presence of 605 (^{134}Cs), 624 (^{106}Ru), 662 (^{137}Cs), 796 and 802 (^{134}Cs) keV lines and certain other.

The relative distribution of burnup along the fuel assembly height was determined from the photon count rate at the ^{137}Cs photopeak (Fig. 2). The burnup nonuniformity factor K_z was found to be 1.40 ± 0.1.

The fuel burnup in the assembly was found from the ratio of count rates at ^{134}Cs (605 keV) and ^{137}Cs (662 keV) at eight points along the assembly (Fig. 3). The deviation of the obtained values from the experimental curve did not exceed ±12%.

The measurements proved the possibility of determining fuel burnup in irradiated fuel assemblies by means of the "Aragonit" radiation meter in a stand mounted directly in the spent-fuel storage pool of the atomic plant.

Translated from Atomnaya Énergiya, Vol. 46, No. 5, pp. 356-357, May, 1979. Original article submitted June 29, 1978; revision submitted September 11, 1978.

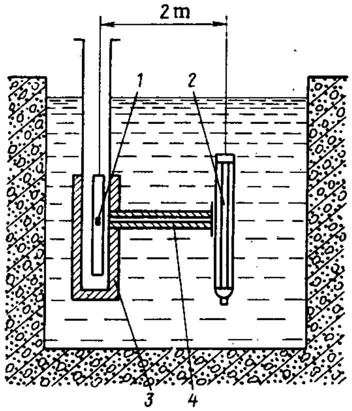

Fig. 1

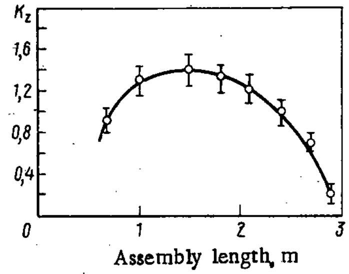

Fig. 2

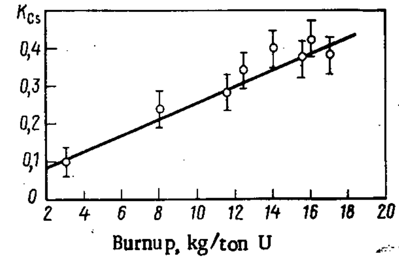

Fig. 3

Fig. 1. Measurement of fuel assemblies in a storage pool: 1) Ge(Li) detector; 2) fuel assembly; 3) lead shield; 4) collimator.

Fig. 2. Height distribution of fuel burnup: ——) calculated, O) experimental.

Fig. 3. Experimental $^{134}Cs\,/\,^{137}Cs$ ratio as a function of fuel burnup: ——) calculated, O) experimental.

LITERATURE CITED

1. S. A. Skvortsov et al., Proc. IAEA Symp. on the Safeguarding of Nuclear Materials, IAEA, Vol. 1, Vienna (1976), p. 187.

MINIMIZATION OF ENERGY DISTRIBUTION INHOMOGENEITIES IN A NUCLEAR REACTOR

V. V. Pobedin and V. D. Simonov

UDC 621.039.512.45

Minimization of energy distribution inhomogeneities in the reactor core is one of the tasks of the intra-reactor fuel control system. For a known fuel composition, minimization consists in determining the layout of fuel assemblies which gives the minimum energy distribution inhomogeneity factor in the reactor core.

Let there be I different combinations $\rho_1, \rho_2, \ldots, \rho_I$ of neutron physical characteristics of N fuel assemblies $(I \leq N)$ forming the reactor core and let the vector ρ_0 describe its composition:

$$\rho_0 = \{\underbrace{\rho_1, \rho_1, \ldots,}_{N_1} \underbrace{\rho_2, \rho_2, \ldots, \ldots,}_{N_2} \underbrace{\rho_I, \rho_I, \ldots}_{N_I}\}$$

$$\sum_{i=1}^{I} N_i = N.$$

Let x_n denote the coordinate point (or group of points) corresponding to the n-th cell of the core. The core layout, i.e., the correspondence $\{x_n \to \rho_i\}$, is described by an N dimensional vector $\rho = \{\rho_{i_1}, \rho_{i_2}, \ldots, \rho_{i_N}\}$ belonging to the set of all possible permutations of the components of vector ρ_0 $(i_n = 1, 2, \ldots, 1)$.

If operator $L(\rho)$ corresponds to the boundary problem of neutron transport in the core, the minimization of energy distribution inhomogeneity can be formulated as follows.

To find $\min \| K(\rho) \|_C$, where $\| K(\rho) \|_C = \max\limits_{r} \left| \frac{\Psi_\rho(r)}{\overline{\Psi}_\rho(r)} \right|$ and the function $\Psi_\rho(\mathbf{r})$, which describes the energy distribution in the core, satisfies the equation $L(\rho)\Psi_\rho(\mathbf{r}) = 0$.

Translated from Atomnaya Énergiya, Vol. 46, No. 5, pp. 357-359, May, 1979. Original article submitted June 4, 1978.

Declassified and Approved For Release 2013/02/12 : CIA-RDP10-02196R000800010005-1

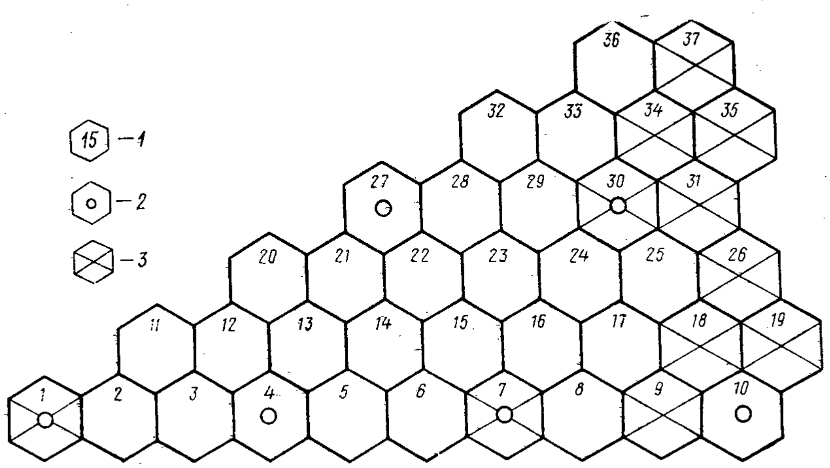

Fig. 1. A 30° sector of the VVÉR-440 core: 1) core cell; 2) cell for SUZ control assembly; 3) cell with fixed fuel assembly.

The object function of this integral optimization problem is the energy distribution inhomogeneity factor $K(\rho)$ and the vector ρ is its control. Let us assume that $K(\rho)$ is an analytic function. Then, in the neighborhood of the point $\bar{\rho}_0 = (\bar{\rho}_1, \bar{\rho}_2, \ldots, \bar{\rho}_N)$ the function can be represented to within $0(\rho_i - \bar{\rho}_0)^2$ in the form $K(\rho) = \sum_{i=1}^{N} f_i(\rho_i)$ and the problem can be solved using the concepts of dynamic programming, i.e., seeking the solution as a result of an N-step process of successive determination of the components $\hat{\rho}_{i_n}$ of the optimal control vector $\hat{\rho}$.

Accordingly, the solution algorithm consists in finding a fuel assembly arrangement trajectory, selecting optimal control at each step of the optimization process. The algorithm includes determination of the base point – "exploratory search" [2] and "search by patterns" [3] – i.e., the determination of the control $\hat{\rho}^{(m)}$ that minimizes the inhomogeneity factor at the step m.

The first minimization step begins with solving the boundary problem for a core with neutron physical characteristics $\bar{\rho}_0$ averaged over the entire core volume. This is followed by the determination of the base point, a point at which alternate variation of vector components within allowable limits produces maximum response in energy distribution:

$$K_{l_{(1)}} = K(\bar{\rho}_0, \ldots, \underbrace{\bar{\rho}_0 \pm \Delta\rho,}_{l_{(1)}} \bar{\rho}_0, \ldots) \longrightarrow \max.$$

For the point thus determined and within the limits of the available collection ρ_i, one then finds a $\hat{\rho}_{i_k}^{(1)}$ such that the vector $\hat{\rho}^{(1)} = \{\bar{\rho}_0, \ldots, \hat{\rho}_{i_k}^{(1)}, \bar{\rho}_0, \ldots\}$ minimizes at this step the inhomogeneity factor $K(\hat{\rho}^{(1)}) = \min\{K(\rho^{(1)})\}$.

The same operations are repeated at the following steps. The sequence of operations is such that the core cells most sensitive to changes in neutron physical characteristics are filled first and the effect of subsequent steps on former ones is leveled out.

Completion of each step determines the location of one fuel assembly and the number of empty cells and coordinate points corresponding to them decreases. The number of remaining fuel assemblies and possible controls also decreases. Thus, the neutron physical characteristics of the core region containing vacant cells must be averaged anew after each step. The last step N gives the minimum energy distribution inhomogeneity factor.

The above algorithm has been implemented as a computer program. The results of its application are illustrated by the example of minimizing the power distribution inhomogeneity in the VVÉR-440 reactor core [4] with a composition corresponding to that of the fifth run.

We have analyzed a 30° sector of core characteristics periodicity with partially inserted absorbers of the SUZ control assembly group (cells 1 and 7 in Fig. 1). The fuel assembly power distribution has been calculated using the BIPR program [5] based on a lattice with a single node in the fuel assembly cross section. Since the neutron physical characteristics of fuel assemblies are entered into this program as functions of fuel burnup,

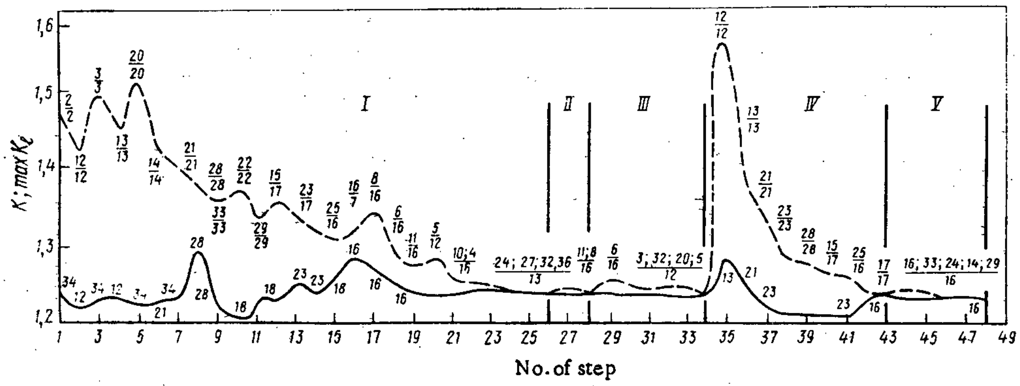

Fig. 2. Sequence of determination of base nodes and variation of the inhomogeneity factor K in the course of optimization: – – –) max K_l (numerator indicates the base node and the denominator, the node of max K_l for a perturbation $\bar{p}_0 \pm \Delta\rho$); ——) K (figures indicate cells with maximum power).

the average concentration of poison in fuel assemblies served as the control. To determine the effect of the initial poison field, the optimization process was divided into several stages.

The first stage began with a core in which trickle-feed fuel assemblies were placed, in accordance with the recommendations [6], at the core periphery and with the fuel portions of the SUZ control assembly group inside the core (see Fig. 1). The remaining region (26 cells) was divided into four zones in accordance with the limitations on fuel assembly relocation that dictate the allowable zone size and the number of fuel assemblies in them and, consequently, also the available controls for each zone [7]. The initial distribution of neutron physical characteristics corresponded to the arrangement of fixed assemblies and to the average poison concentration in the zones.

The base coordinate point (node) at each step was determined simultaneously for all four zones. Figure 2 shows the sequence of $\{\max K_l\}$ values from which the base nodes were selected, the order of fuel assembly insertion in the cells, and the variation of the power distribution inhomogeneity factor K in the course of the optimization process. The core layout was completed with the 26th step (section I) at which the inhomogeneity factor was found to be 1.246. The specificity of its variation with each step depends on the discreteness of control.

At the second stage the initial poison field in the core was formed by dividing the central region (22 cells, with fixed fuel assemblies in cells 4, 10, 27, and 36), obtained at the first stage, into two zones that preserve layout symmetry. These zones include two subzones each with fuel assemblies remaining in the reactor for the same period of time grouped in each subzone. The concentration of poison in each subzone was averaged. Base coordinates were determined individually for each subzone (sections II–V in Fig. 2). The stage ended at the 48th step. The inhomogeneity factor decreased to 1.237 by relocating two fuel assembly pairs with burnups differing by 0.15 and 0.3 kg/ton U.

The next stages were preceded by testing all the possible versions of averaging of the core characteristics. In all cases the results did not differ from that obtained at the first stage by more than the result obtained at the second stage.

LITERATURE CITED

1. G. Hadley, Nonlinear and Dynamic Programming, Addison-Wesley (1964).
2. R. Hook and T. Jeeves, J. Assoc. Computer, 8, 212 (1962).
3. C. Wood, "Application of 'direct search' to the solution of engineering problems," Westinghouse Res. Lab. Sci. Paper 6-41210-1-P1 (1960).
4. V. A. Sidorenko, At. Energ., 43, No. 5, 325 (1977).
5. D. M. Petrunin, E. D. Belyaeva, and I. L. Kireeva, Preprint of the Atomic Energy Institute, IAE-2519, Moscow (1975).
6. K-Fr. Potter, V. Riehn, and G. Suschowk, Kernenergie, 19, No. 4, 116 (1976).
7. V. V. Pobedin and V. D. Simonov, Kernenergie, 12, No. 3, 77 (1978).

FORMATION OF HYDROGEN IN THE RADIOLYSIS OF WATER VAPOR

B. G. Dzantiev, A. N. Ermakov, and V. N. Popov

UDC 541.15:621.039

Recently, in connection with the problem of hydrogen power, new economical ways of synthesizing hydrogen based on water and mineral raw materials has been widely discussed in domestic and foreign literature [1]. One of the possible ways of solving this problem may be the process of thermoradiation dehydrogenation of water vapor (TRDW), using the thermal and radiation components of the power of a nuclear reactor. To evaluate the competitiveness of this method in comparison with others (heat cycles, electrolysis, etc.), data are needed on the yield of hydrogen in the radiolysis of water vapor, especially under conditions of high temperature and dose rate (T, J). The published data on the efficiency of radiation convertion of $H_2O \rightarrow H_2$ are sparse [2] and cover narrow regions of variation of T and J. And yet, from data on the decomposition of H_2O in the presence of organic additives [2], it follows that the yield of atomic hydrogen $G_H = 7 \cdot 100^{-1}$ eV. Then, under conditions excluding losses of hydrogen atoms, in principle it can reach values $G(H_2) \approx G_H \approx 7$. Evidently in this sense an increase in the temperature, when the contribution of the reaction $H + H_2O \rightarrow H_2$ (activation energy $E_1 \approx 1$ eV) increases and the role of nonproductive recombination processes: H + OH, H + H, OH + OH, decreases, is favorable.

In this work we present the results of experimental and theoretical investigations of the radiolysis of water vapor in a broad range of T and J. Irradiation of preliminarily purified distilled and degasified water was conducted on an U-12 pulsed accelerator in the temperature range 300-900°K according to the method described earlier [3, 4]. The radiation dose was monitored by chemical dosimetry ($C_2H_4 \rightarrow H_2$) and by other methods. The temperature of the irradiated samples was recorded with a thermocouple. Hydrogen and oxygen were chromatographically analyzed. The values of $G(H_2)$ were determined according to the slopes of the kinetic curves. It was shown that in the absence of radiation influence, the formation of hydrogen by thermal and thermocatalytic means does not occur within the investigated temperature range.

The initial radiation yield of H_2 in the irradiation of water vapor is a sigmoid function of the temperature (see Fig. 1). At $T \lesssim 150$°C, $G_{min}(H_2) = 1.6$ and does not depend on T. At $T \gtrsim 350$°C, $G_{max}(H_2) = 8$ and also does not vary when the temperature is further increased. The transition from $G_{min}(H_2)$ to $G_{max}(H_2)$ occurs within a relative narrow temperature range ($\Delta T \approx 150$°C). The effective activation energy of the formation of H_2, $E_{eff} \sim 2$ kcal/mole; E_{eff} is not directly correlated with E_1, which is due to competition of the following processes: 1) $H + H_2O$; 2) H + OH; 3) H + H; 4) OH + OH; and 5) $H_2O \rightarrow H_2$.

The kinetic analysis of the radiolysis of water vapor in the linear region of the curves of formation of H_2 can be performed within the framework of a two-radical model (H, OH) and the five equations indicated above. To estimate the efficiency of the decomposition of H_2O as a function of T and J, it is useful to introduce the parameters ξ and r, correspondingly equal to the ratio of the rates W of the reactions $H + H_2O$ and H + OH, and to the concentration ratio [H] / [OH], into consideration:

$$\xi = W_1/W_2 = k_1\,[H_2O]/k_2\,[OH].$$

For pure water vapors $\xi = k_4'/r - k_3'r$, where $k_i' = k_i/k_2$; r = [H] / [OH]. Under these conditions $\eta = [G(H_2) - G^0_{H_2}]/G_H = (\xi + k_3'r)/(1 + \xi + 2k_3'r)$; $G^0_{H_2} = G_5 = 0.5$. A family of curves $G(H_2) = f(T, J)$ for $J = 10^{12}$–10^{20} eV/cm$^3 \cdot$ sec and T = 300-1000°K was obtained using functions of this kind.

A comparison of the calculated curve and the experimental values indicates good agreement of the experimental and theoretical functions $G(H_2) = f(T)$. The value $G(H_2) = 8$ achieved in the work is of the order of G(H) and corresponds to ≈20% conversion of the radiation energy to the desired channel of the reaction of H_2 synthesis. However, this value cannot be considered the limit. In principle the yield of hydrogen can be increased by the conversion of OH radicals to atomic and, correspondingly, molecular hydrogen (selection of the

---

Translated from Atomnaya Énergiya, Vol. 46, No. 5, pp. 359-360, May, 1979. Original article submitted September 1, 1978.

 0038-531X/79/4605-0414$07.50

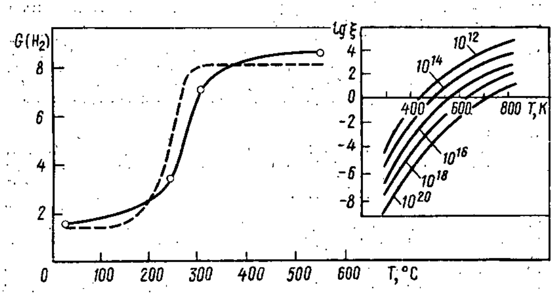

Fig. 1. Experimental dependence (○) of the radiation yield of hydrogen in the irradiation of water vapor on the temperature at $J = 1.3 \cdot 10^{15}$ eV/cm$^3 \cdot$ sec and P_{H_2O} = 760 mm Hg: – – –) theoretical curve of $G(H_2) = f(T)$ for the same dose rate; on inset, calculated functions $\xi = \xi(T, J)$.

physicochemical parameters of radiolysis, introduction of converting additives X = NO, CO, etc.). In the latter case, the realization of a chain process is not excluded: $H + H_2O \rightarrow H_2 + OH$; $OH + X \rightarrow XO + H$. Another possibility of increasing $G(H_2)$ may be associated with a change in the primary spectrum of dissociative ionization of H_2O molecules on account of charge transfer to water molecules from additions of substances with a high ionization potential (N_2, He).

The authors would like to thank V. A. Legasov for formulating the problem and for his interest in the work.

LITERATURE CITED

1. V. A. Legasov, Priroda, 3, 3 (1973).
2. R. Dixon, Radiat. Res. Rev., 2, 237 (1970).
3. B. G. Dzantiev, V. N. Popov, and Yu. N. Smelova, Khim. Vys. Energ., 5, No. 1, 86 (1970).
4. V. I. Gol'danskii et al., At. Energ., 30, No. 3, 262 (1971).

THE 45TH MEETING OF THE SCIENTIFIC COUNCIL OF THE JOINT INSTITUTE FOR NUCLEAR RESEARCH

V. G. Sadukovskii

This meeting was held in January, 1979 in Dubna; the activities of the institute during 1978 were surveyed, along with the current and forward plans. The meeting was opened by the director of the institute, N. N. Bogolyubov, who outlined the work of the executive in implementing the decisions of the council. The directors of the individual laboratories also presented reports on recent researches and development studies carried out in 1978.

The Laboratory of Theoretical Physics (report by D. I. Blokhintsev) has used the quasipotential approach in quantum field theory in examining corrections to the self-modeling behavior in high-energy large-angle scattering amplitudes. A parton picture of exclusive processes has been built up in quantum chromodynamics, and this picture is not a Feynman type. A detailed study has been made of the power-law behavior of the hadron formation cross section for large values of the transverse momentum. Hypotheses on the global duality of quark loops and resonance contributions to spectral sum rules have been used in calculating the electromagnetic radii of charged and neutral kaons along with the structural parameters of the corresponding semilepton decays. The results are in agreement with experiment. Chiral quantum field theory has been employed in completing a description of the major decays of meson octets. Calculations have been performed on the lepton and semilepton decays of D and F mesons. A computer program has been written for performing the Bogolyubov–Parasyuk R operation in scalar theories, i.e., the construction of renormalized-function coefficients for Feynman diagrams in the form of integrals with respect to parameters. A form of quantum electrodynamics has been devised in which the gauge transformations are dependent on a fundamental length. Radiation corrections have also been applied to deep inelastic scattering of neutrinos by nucleons, which are required for the joint Dubna–CERN experiment.

In the area of nuclear theory, a microscopic approach has been devised for research on heavy-ion interactions. A mechanism has been examined for dissipation of the energy of the relative motion of particles, particularly by the production of internal excitations of one-particle and collective types. The Pauli principle has been incorporated into the theory of collective nuclear oscillations, and a quasiparticle–phonon model has been employed, which indicates that corrections for giant resonances applied to the radiation widths of neutron resonances in spherical nuclei can produce good agreement with experiment for E1 and M1 transitions.

The first exact expressions have also been derived for the Green's functions involved in the interactions of electrons with phonons and external electric fields; these have been used in kinetic equations for an electron–phonon system. A general approach has been devised for researching channeling of light and heavy particles in crystals, which employs techniques first devised for examining small systems interacting with thermostats.

The High-Energy Laboratory (report by A. M. Baldin) has completed a research on elastic scattering of protons by protons, deuterons, and helium nuclei in joint Dubna–FNAL experiments on the 500-GeV accelerator in Batavia. In the experiment on forward K-meson scattering at electrons at 250 GeV, a result was obtained for the electromagnetic radius of the K meson.

The NA-4 apparatus has been installed on the SPS-400 accelerator at CERN for joint Dubna–CERN experiments on deep inelastic scattering of muons by H, D, and C targets. Extensive checks have been performed on the equipment during adjustment and a start has been made on processing the beam data.

The processing has been continued on data obtained in experiments with the Institute of High-Energy Physics accelerator at Protvino, which has been operated with the BIS-2 complex, the Ludmila system, and a 2-m propane chamber. Upper bounds have been defined for the partial cross sections for the formation of 17 systems that seem to be likely sources of charmed particles decaying to 2 or 3 charged particles. These estimates lie at the level of 0.1-1.3 μbarn. Researches have also been performed on the inclusive formation

Translated from Atomnaya Énergiya, Vol. 46, No. 5, pp. 361-364, May, 1979.

 0038-531X/79/4605-0416$07.50

of neutral particles and on invariant cross sections and mean π-meson and proton multiplicities, as well as on light isobars and antiisobars in antiproton–proton collisions. A test has been performed on scale invariance in multiplicity (KNO) and on Wrublewski's relation for multinucleon interactions of π mesons with carbon.

The synchrophasotron at the Joint Institute for Nuclear Research has been used in an extensive program of research on relativistic nuclear physics; the DISK-2 system has been used with an 8.6-GeV/sec proton beam in research on the high-order cumulative formation of pions, protons, deuterons, and tritons. The energy spectra of the cumulative particles are of exponential type for an emission angle of 180° for various nuclei and the various curves are similar in shape. Indications have been obtained that superdense states occur in research on dibaryon systems composed of Λ-hyperons and protons, particularly from research with the propane chamber used with a neutron beam of average momentum 7 GeV/sec.

Studies have also been performed to improve the utilization of the synchrophasotron in physics experiments, which have involved upgrading the parameters. The carbon-nucleus flux has been raised to $2 \cdot 10^6$ particles/pulse, and this can now support parallel operation of two physics experiments. A second slow beam-extraction system has been installed for operation of 200-400 MeV/nucleon, and ion radiography has been used with a helium-nucleus beam at 200 MeV/nucleon.

The researches for the nuclotron project and the storage system (UNK) have involved the manufacture and detailed testing of five specimens of pulsed superconducting magnets. Measurements have been made on the energy deposition on irradiating a superconductor in an intense proton beam. New techniques developed in the laboratory have included the design of high-sensitivity detectors based on proportional chambers for the analysis of thin-layer radiochromatograms, the development of new electronic units for interfacing physics experiments to computers, and devices for data acquisition and processing.

The Nuclear-Problems Laboratory (report by V. P. Dzhelepov) has conducted physics researches with the synchrocyclotron, and in particular has completed researches on a new phenomenon observed in the laboratory, viz., the resonant formation of a deuteron–deuteron μ-meson mesomolecule. A germanium–lithium γ-ray spectrometer has been used with the $n + {}^1H \rightarrow {}^2D + \gamma$ reaction to measure the deuteron binding energy with higher precision, and this has provided better values for the neutron rest mass and the mass difference between the proton and neutron. A new technique has also been developed that has provided a complete and consistent set of γ-ray energy standards in the region of 2 MeV, which has reduced the systematic errors arising in previous indirect techniques, while also ensuring considerably improved reliability.

Measurements have also been made on the polarization of the cumulative protons in the scattering of protons by carbon, which have indicated that it is impossible to explain the momentum and angular results via a mechanism involving a high-momentum component of the nucleon motion in ^{12}C.

Data from the MIS system have been processed to yield the semicoherent elastic-scattering cross sections for pions of momentum 40 GeV/sec incident on carbon. Studies have also been made on double pion charge transfer at carbon and on the associative multiplicity occurring in the formation of π^0 mesons in π^-p interactions at 5 GeV/sec. These measurements have been performed with the 1-m propane chamber. In addition, measurements on the $\pi^- p \rightarrow \pi^0\pi^0 n$ reaction at 270 GeV have been completed, and the experiments confirm the pion–pion interaction theory based on deviation from chiral symmetry in the strong interaction. An experiment has also been completed in which μ-mesoatom radiation has been used in determining the elemental compositions of organs. Experiments under the YaSNAPP program have been performed, especially those concerned with neutron-deficient isotopes. Previous systematic studies with the spin system have been continued, especially with transition-region nuclides, by nuclear orientation at very low temperatures.

Major results have also been obtained in various more technological aspects. A very large spectrometer with streamer chambers (the RISK system) has been commissioned in the 70-GeV accelerator beam. Apparatus has been built for examining polarization effects in ecchange pion–proton scattering, which has included the commissioning of the world's largest polarized frozen-proton target for research on polarization effects at high energies. Tests have been completed on the beam from the Serpukhov accelerator for the first design of the Hyperon spectrometer system, which is intended for research on hypercharge-exchange processes in π and K meson beams. A new method has also been developed for researching the parameters characteristic of the superconducting state in metals by means of impurity-muon spin relaxation. The laboratory has also collaborated with the Institute of Nuclear Physics in Rez (Czechoslovakia) on the extraction of the beam from the U-120M accelerator without energy loss.

A large volume of work has also been performed on upgrading the synchrocyclotron to a high-current phasotron. New types of units within the CAMAC standard have also been built.

The Nuclear-Reactions Laboratory (reports by G. N. Flerov and Yu. Ts. Oganesyan) has commissioned a a new accelerator (the U-400 4-m isochronous cyclotron) with many applications in nuclear physics, especially the synthesis of new heavy and superheavy elements. This cyclotron was built entirely within the institute within a very short period. In December, 1978 an intense beam of argon ions of energy 5 MeV/nucleon was produced at the final accelerator radius.

The main efforts of the laboratory in the research field have been concerned with the search for naturally occurring superheavy elements, synthesis of transuranium elements, and nuclear reaction mechanisms. Experiments have been performed on the concentration of a natural spontaneously fissile isotope. The concentration level so far attained provides a basis for detailed studies on the mass and decay. New data have also been obtained on the spontaneous fission of some isotopes of elements 105 and 106. Attempts have been made to synthesize element 108 in the $^{226}Ra + ^{48}Ca$ and $^{208}Pb + ^{58}Fe$ reactions, and upper bounds for the reaction cross sections have been defined. Information has also been obtained on the characteristics of fission in heavy nuclei induced by α particles at energies near the height of the Coulomb barrier. The contributions from the symmetrical and unsymmetrical modes of fission have been distinguished, and it has been concluded that shell effects influence fission in weakly excited heavy nuclei. Researches have also been performed on quasimolecular spectra. A new method has been devised for elucidating the nature of the positrons arising in the collisions of heavy nuclei.

Development studies have also been continued on the application of nuclear-physics methods. Workers from the institute have commissioned a new plant of high throughput for the production of nuclear filters. Also, the microtron in the laboratory has been used in devising methods of routine analysis for various types of material containing trace amounts of rarer elements.

The Neutron-Physics Laboratory (report by I. M. Frank) has obtained evidence on the absolute value and energy trend for the neutron radiative-capture cross section of helium-3, as such data are of major importance for fundamental research on four-nucleon systems. The method developed in the laboratory has been used in early experiments on the isomeric shift of the neutron resonance in uranium-238 in various compounds. This technique has defined the change in the rms radius of the nucleus on excitation up to energies of about 6 MeV. Small-angle neutron scattering has also solved a problem in molecular biology, viz., the distance between antigen binding centers in an immunoglobulin molecule. Measurements also show that temperature and isotopic replacement of hydrogen have little effect on ultracold-neutron storage times, which has a bearing on the focusing of such neutrons in neutron-optics experiments. An energy diagram for the crystalline levels has also been devised for the $PrNi_5$ intermetallide by means of inelastic neutron scattering.

The IBR-2 pulsed reactor has also been commissioned, and careful measurements have been made on all parameters, which have been compared with calculated values. Preparations are far advanced for full-scale operation of the IBR-2, including completion of the installation of the sodium cooling system, many different pneumatic and vacuum tests on the sodium loops, etc. Considerable progress has also been made on the IBR-2 injector, which is an LIU-30 linear electron-induction accelerator. The injector part of the accelerator is being assembled and other equipment is being manufactured. Specialists from the institute and from member-countries have also performed many different studies on the physics equipment needed for research with the IBR-2 and for equipment needed for general purposes in the measuring bay.

The Laboratory of Computing Technique and Automatics (report by N. N. Govorun) has completed the experimental operation of the first network of terminals working into an ES1010 minicomputer and a BÉSM-6. A microcomputer has been built into a VDU processor, and a small batch of graphics VDUs is being built that employ a new storage CRT. Engineering work has also been completed on the interfacing of eight ES5061 units of total capacity 230 megabytes to a BÉSM-6, and extensive debugging of the associated software has already been performed.

New electronic equipment has also been tested for the HPD system, together with six Camet panels for use in software-managed tracktracing. The real-time filtration system for the Spiral equipment has also been completed. A suite of base software has also been written for calibrating and managing the AÉLT-2/160 system, which has also been interfaced to a CDC-6500 computer, and routine measurements have therefore been begun on photographs recorded with the MIS system, while trials have been begun on similar measurements with the RISK photographs.

Software has also been written for data acquisition and hardware monitoring in the BIS-2 by means of an ES1040 minicomputer, along with software for ion radiography and base software for the Dubna–CERN joint muon experiment. Specialists at the laboratory have devised a simple and efficient means of generating applied-program packages for processing queries in a special language within the framework of the Hydra system, as well as software for processing two-dimensional spectra.

Development work has also been continued on new methods of numerical solution for nonlinear problems in physics, particularly those related to the UNK project and the heavy-ion accelerator system (UKTI), in addition to simulation of processes in nuclear physics at relativistic energies and of nonlinear phenomena in field theory.

Software has also been defined for calculations on resonant states within the framework of Schrödinger's equation with a spherically symmetrical Saxon–Woods potential.

The meeting also received reports on the state of developments in the UNK and UKTI projects, as well as the plans of the Division of New Acceleration Methods for 1979 (report by Yu. N. Denisov). Collaboration between Dubna and the Institute of High-Energy Physics over the UNK system has steadily extended on the basis of the agreed program. Collaboration between High-Energy Laboratory and the Division of New Acceleration Methods has shown that it is desirable that the cryostat system for the UNK should include jet (ejector) pumps employing liquid helium. Measurements have been made on the losses in the MO-09 superconducting magnets built at the Institute of High-Energy Physics, as well as on the losses in short specimens of superconducting leads and cables used at that institute in models for magnetic components for the UNK. Measurements have also been made on the radiation heating in superconductors. A suite of four magnetometers has been built for testbed purposes. An excitation source and certain other units for the acceleration section have also been built for beam handling in the U-7000 synchrotron.

Collaboration with the Kurchatov Institute of Atomic Energy and with certain other institutes in the country has led to physical definition of the synchrotron form of the UKTI. Advances in collective acceleration techniques made in the Division of New Acceleration Methods lead one to hope that a collective-acceleration injection system can be built for the UKTI, and researches and developments in this area are being based on the prototype heavy-ion collective accelerator (KUTI). It has proved possible to support stable acceleration of nitrogen ions, and the first trials have been performed on the acceleration of xenon ions. An induction system for accelerating electron-ion rings has been designed and built on the basis of components from the LIU-3000 induction accelerator. Work has also been completed on the first draft for the automatic management system for the KUTI. Trials are also now in hand on the data-presentation system.

Workers at the institute have also designed and built 84 proportional chambers of dimensions 3 × 1.5 m for use in the joint muon experiment with CERN. The parameters of these chambers make them among the best detectors of this class. There has been no instance of failure in 8 months of operation in the muon beam from the 400-GeV proton synchrotron.

The Deputy Director of the institute, D. Kis, presented a report on international collaboration and international relationships of the institute.

The year 1978 was characterized by the further extension of collaboration with other scientific centers; the plans for research and international scientific collaboration have included the definition and execution of joint studies and data exchanges on 143 topics. The institute has been the organizer of eight major scientific conferences and schools, as well as of 18 working conferences. International sections of the institute (the scientific councils and the specialized committees) discussed various problems at their 21st conference in Dubna. Joint studies and exchanges have involved 1010 members of the staff of the institute, which have included many visits to member-countries for collaboration and participation in conferences, which have involved 502 Dubna staff members. Also, Dubna scientists have participated in 107 scientific conferences, symposia, and schools held in various countries. The Dubna plans for 1979 include the organization of six scientific symposia and schools, along with 19 working conferences. The most important of these are as follows: an international symposium on high-energy physics and elementary particles (Poprad, Czechoslovakia), fundamental problems in theoretical and mathematical physics (Dubna), few-body problems in nuclear physics (Dubna), and the international school on high-energy physics organized jointly by Dubna and CERN (Dobogoko, Hungary).

The meeting also confirmed the draft for the general forward plan of the institute up to 1990 together with the major lines of the five-year plan for 1981-1985 (reports by N. N. Bogolyubov).

The main lines of scientific development at the institute up to 1990 include the following: High-energy physics: research for hadron components, the physics of new J/ψ particles, phenomena at high transferred momenta, the causes of parity nonconservation, and checks on basic aspects of quantum field theory. Elementary-particle physics: Here the major topics include the possible observation of deep coupling or a single source for the weak, electromagnetic, and strong interactions at the unitary limit (300 GeV in the center-of-mass system) and the search for a fundamental length, whose discovery would radically alter concepts on space–time geometry. Nuclear physics: Research on major aspects, some of which are related to advances in relativistic nuclear physics, as well as research on highly charged ions (including the relativistic region), which in future should be based on the UKTI, which is designed to produce intense heavy-ion beams (up to uranium). Researches on heavy-iron physics will be further extended with the U-400 isochronous cyclotron. Physics of condensed media: Here nuclear researches will be considerably facilitated by the IBR-2 and the LIU-30 induction accelerators. The commissioning of these systems will give Dubna a leading position in world science, at least up to 1990. Theoretical physics: further advances are planned here, particularly more emphasis on the theory of elementary particles at very high energies, as well as tests on the hypothesis of superdense nuclei. Researches will also be developed on neutron and giant multipole resonances, as well as on scattering theory applied to the structures of solids and biological materials.

The meeting also awarded diplomas to the successful candidates in the annual competition at Dubna. The first prizes were awarded by the council as follows: for the best theoretical study "The effects of rotation on nuclear structure" to I. N. Mikhailov, É. Nadzhakov, and D. Jansen; for the best experimental studies "The experimental basis for the resonant absorption of negative muons by atomic nuclei" to I. Voitkovskaya, V. S. Evseev, T. Kozlovskii, T. N. Mamedov, and V. S. Roganov, and "Giant resonances in the interaction of medium-energy particles with light nuclei" to M. Dmitro, G. R. Kissener, and R. A. Éramzhyan; for the best technological paper "Researches on collective acceleration and design of collective-acceleration prototypes for the Dubna heavy-ion accelerator" to V. P. Sarantsev, G. V. Dolbilov, V. I. Mironov, É. A. Perel'shtein, G. Radonov, A. P. Sumbaev, S. I. Tyutyunnikov, V. P. Fartushnii, A. A. Fateev, and A. S. Shcheulin, and for the best applied study "Design and construction of proton and high-intensity π-meson beam systems and other equipment for use with the synchrocyclotron in the Nuclear-Problems Laboratory at the Joint Institute for Nuclear Research for biomedical purposes" to V. M. Abazov, B. V. Astrakhanov, M. Sh. Vainberg, V. P. Dzhelepov, V. I. Komarov, E. S. Kuz'min, A. G. Molokanov, A. I. Rudeman, O. V. Savchenko, and E. P. Cherevatenko.

CONFERENCE ON THE FIFTH ANNIVERSARY OF THE COMMISSIONING OF LENINGRAD NUCLEAR POWER STATION

A. P. Sirotkin

This conference was held in December 1978 in Sosnovyi Bor and was attended by about 200 representatives of the major organizations involved in the design, construction, engineering support, and operation of nuclear power stations with RBMK reactors; there were 17 papers.

N. M. Sinev opened the conference and dealt with the significance of nuclear power for the European part of the USSR, particularly the role of nuclear power stations with RBMK reactors. Extensive developments on such reactors have provided power systems of unit power 1 million kW. In the early 1980s, there will be 11 such units containing RBMK-1000 reactors, which will provide an annual saving of more than 20 million tons of coal. The progress made in the Leningrad power station was particularly emphasized, since up to Dec. 20, 1978, this had output 45.7 billion kW · h; Sinev emphasized the increasing significance of nuclear power in supplying the country generally, especially certain areas.

The main results from 5 years of operation of this power station were surveyed by A. P. Eperin. The annual output from the power station now constitutes more than 35% of the total supply to the Leningrad area. The power station has also provided the first full evaluation of many scientific and design principles. The experience with the commissioning of the first unit has defined the lines for improving the later units, systems, and processes, and this has halved the time needed to install the second unit and run it at its design power. There has been an ongoing reduction in the unplanned downtime of the unit, along with a reduction in the energy cost. The utilization factor for the design power has risen from 58% in 1974 to 73% in 1978. During this time, the primary efficiency has increased from 30.2 to 31.3%. It has also proved possible to change fuel rods without shutdown, and over 2000 reloading operations had been performed successfully up to Dec. 1, 1978. The design for the first unit included means of replacing spent fuel rods at the center with fresh ones as the main activity migrates toward the periphery.

During the operation, it has been found that the safety margins for operation between routine servicing cycles in the thermal and mechanical sections. The reliability of the station has been improved by planning future sections on a block basis, including division of subsystems and provision of backup for individual units. The sealing in flange joints and sleeves has been improved by use of fusible metals. Improved power distribution has also been shown to be possible, along with better distribution of the flow rates over the drum separators and of the hydraulic coupling between the latter. Some of these deficiencies have been overcome at the power station itself as well as at other power stations containing RBMK reactors, and these measures have provided much improved performance.

More detailed results were presented on the commissioning and operation of the reactors and associated equipment by representatives of various services within the power station. For example, V. V. Sazykin discussed the operation of the Skala system, particularly the need for improved reliability, larger memory volume, and higher processing speed. Yu. O. Sakharzhevskii presented data on creep in the zirconium tubes that indicate that ongoing monitoring is essential. I. A. Varovin presented results on the stability of fuel pins and stated that, as a rule, sealing failures usually occur in the upper pins, whereas the maximum corrosion-deposit formation occurred at 1.5-2 m from the bottom of the core. Changes in the physical characteristics of the reactor during operation were discussed by V. I. Ryabov. The nonuniformity factor for the energy production is about 1.4 along the radius or 1.17-1.2 vertically. The average uranium burnup in the reactors has been 7.5-8 MW · day/kg, and the fast power coefficient of reactivity is negative on account of the characteristics of the fuel and coolant.

V. S. Romanenko considered further improvement in the RBMK, in particular improved stability in the power distribution arising from increase in the ratio of the ^{235}U to the moderator, the use of fuels of elevated density such as uranium silicide, etc.

Translated from Atomnaya Énergiya, Vol. 46, No. 5, pp. 364-365, May, 1979.

0038-531X/79/4605-0421$07.50 ©1979 Plenum Publishing Corporation

Interesting results were also presented by A. L. Gobov from the Chernobyl' nuclear power station, where experience with the first unit at Leningrad has been employed to bring this power station up to nominal power within 8 months after initial loading of the reactor.

During discussions it was pointed out that the 5 years of operation at Leningrad have led to the accumulation of valuable experience, which have defined measures for improving the RBMK reactors, which in part have already been implemented. Successful operation of the Leningrad station and of other such stations represents a major advance in this area of power engineering. This represents the first instance of construction and successful operation of a power reactor of unit output 1 million kW. The major heavy-engineering plants in the country have played a considerable part, and these have been largely responsible for the successful construction and commissioning of units whose actual operation is in accordance with the design parameters. Six units have been commissioned with 4 years of the five-year plan.

ALL-UNION CONFERENCE ON IONIZING-RADIATION PROTECTION OF NUCLEAR ENGINEERING FACILITIES

V. P. Mashkovich

The conference, which was held in Moscow in December 1978, was attended by more than 300 delegates from 85 organizations of various ministries, departments, and the Academy of Sciences of the USSR. At two plenary sessions and 18 section meeting the conference delegates considered more than 250 papers dealing with current problems of ionizing-radiation protection.

The plenary sessions considered the achievements and prospects for the development of the physics of radiation protection, numerical methods of solving the transport equation, the problem of small doses in radiation safety, new "Sanitary regulations for the design and operation of atomic power plants," the problem of optimization of shielding, and the results of calculations performed by various groups of authors employing various programs. At their final session, the delegates discussed ways of enhancing the quality and reliability of the design of shielding for nuclear engineering facilities.

In the section on "Theoretical methods and programs for computer calculation of fields of ionizing radiation" a large proportion of the papers were devoted to the creation of new programs and modernization of existing ones. The section considered problems for one- and two-dimensional shielding geometry and for shielding with inhomogeneities.

Some of the papers dealt with programs for the optimization of shielding and engineering programs for calculating radiation fields.

Let us note some interesting results of research:

principles have been formulated for setting up libraries of program modules for solving radiation protection problems;

the application of group constants in calculations by the Monte Carlo method will make it possible to obtain correct results and the use of biased sampling from distributed sources gives a two- to fourfold advantage in respect of computation time in the calculation of secondary γ radiation by the Monte Carlo method;

a study has been made of the possibility of employing the Ritz variational principle to solve the one-velocity kinetic equation in the self-adjoint form;

by using the method of small perturbations, a numerical method has been developed for taking account of the contribution of secondary radiation to transport problems of γ rays in an infinite medium;

it has been shown that fluctuations in the paths traversed by a fast particle in a thick absorber affect the rms deviation angle and the character of the angular and energy spectrum;

a study has been made of the effect of the field of the space charge on the penetration of fast particles;

Translated from Atomnaya Énergiya, Vol. 46, No. 5, pp. 365-366, May, 1979.

 0038-531X/79/4605-0422$07.50

the concept of quasialbedo has been used to take account of the secondary γ radiation in calculations of the penetration of neutrons into inhomogeneous shielding.

Analysis of the papers presented in this section showed that present-day methods and programs of calculation make it possible to determine, with good approximation, not only the integral but also the differential characteristics of the radiation field in shielding with a complex geometry.

The largest number of papers were read in the section "Differential and integral experimental and theoretical investigations." The information about the propagation of neutrons and γ rays in a medium. It has been ascertained, in particular, that fast neutrons pass through barriers of stainless steel into cylindrical and spherical shields and neutrons from a 14-MeV source into the blanket of a thermonuclear reactor. Interesting studies have been carried out on the energy distributions of neutrons and γ rays emerging from a polyethylene and an iron sphere with a ^{252}Cf at the center. New data have been obtained on factors concerning the accumulation of γ rays for optical and protective glass, behind layered water and lead barriers, and for a two-dimensional shield. The propagation of γ rays in homogeneous and heterogeneous shielding with an extension of up to 20 free path lengths has been investigated.

Studies have been continued on the formation and propagation of secondary γ radiation. These topics have been considered, in particular, for two-dimensional axisymmetric shielding and in three-layer screens.

As before, considerable attention has been paid to the passage of radiation through inhomogeneities in shielding; through shielding with multisectional bend and circular channels, through a sodium line in a heterogeneous shield with randomly distributed inhomogeneities, as well as through equipment as a medium with random distribution of slugs. There have been further developments in the application of the light-modelling method for solving the aforementioned problems.

New information has been obtained on the albedo of γ radiation, including low-energy γ-ray quanta, neutrons, electrons, and positrons, bremsstrahlung behind thick targets for electrons with an energy of 0.01-30 MeV, and the yield of photoneutrons from plane concrete and steel barriers under irradiation with bremsstrahlung from a betatron with a maximum energy of 24 MeV. Part of the papers were devoted to optimization of shielding and the study of radiation fields in air.

Interesting papers were presented on errors in shielding calculations and on the comparison of results of calculations by various programs with the data from fundamental experiments.

The "Nuclear constants" section considered 29 papers. Further improvements have been made in the ARAMAKO system of preparing group constants for calculations of shielding. In particular, this system has been supplemented with the ARAMAKO-G complex for preparing γ-ray group constants. The BND-14 neutron data library has been connected to the ARAMAKO-2F system for calculations of the transport of neutrons with an energy of up to 14 MeV in the shielding of thermonuclear machines. There was a particular discussion of the preparation of small-group constants and group constants for γ rays as applied to the solution of the transport equation in the $D_{L,N}$ approximation, and the preparation of constants for media with a resonance structure, including calculations of shielding by the Monte Carlo method. Studies have been made of the effect of the errors in the interaction cross sections on the results of calculations and the accuracy of measurement of neutron spectra in the reactor shielding and the errors of group approximations were discussed.

Interesting papers were presented in the section "The radiation fields of operating facilities and their analysis." The papers pointed out that irradiation of personnel of atomic power plants with VVÉR-440 commercial water-cooled—water-moderated power reactors (according to the data from operation of the Kolsk atomic power plant) does not exceed 15%, on the average, of the maximum permissible value, with 80% of the personnel irradiation being caused by repair work done on the shutdown reactor. An interesting method for calculating the allowable concentration of radionuclides in the coolant or deposits in the equipment of the atomic power plant was presented.

The section "Protection of nuclear engineering facilities" head many papers on experimental research and calculations on the following atomic plants: Armenian, Novovoronezh, Kursk, and Kolsk.

Twelve papers were devoted to the activation-product contamination and corrosion of the primary circuit of reactors of various types and their role in the creation of the radiation environment of the atomic power plant. Estimates were made of the radiation environment during normal operation of an atomic thermal power plant and the radiation consequences of possible accident situations. Problems were formulated for investigations on shielding for thermonuclear reactors. In particular, the bottleneck in the shielding of such facilities are the inhomogeneities in the shielding which prove to be much than in nuclear reactors.

Part of the papers were devoted to the radiation resistance and aging of shielding materials. Interesting papers were presented on the measurement of the gas release from concrete and polyethylene with fillers under the action of radiation from a reactor. It was shown, e.g., that with a fluence of up to 10^{19} neutrons/cm^2 the principal mechanism of gas formation in concrete is that of radiation-induced decomposition of the bound water.

The main results of investigations and problems for further study were presented in the recommendations adopted by the conference. Some papers will be published on forthcoming issues of this journal.

SOVIET – FRENCH SEMINAR ON SAFETY OF ATOMIC POWER PLANTS WITH WATER-MODERATED – WATER-COOLED REACTORS

A. N. Isaev

The seminar was held at the Fontenay-aux-Roses and Saclay nuclear research centers in France in January 1979. Nineteen papers presented by Soviet and French specialists discussed thermophysical and strength design studies under conditions of maximum theoretical failure, problems of experimental confirmation of computational procedures, the problem of taking account of seismic forces on the building and equipment of an atomic power plant, the approach to the choice of technological schemes for ensuring the safety of atomic power plants, and standardization in ensuring safety.

In France, the complex of these topics is handled within the framework of a structurally unique program of research carried out in the scientific centers of the Commissariat a l'Énergie Atomique. France engages in extensive international collaboration in safety research. She has entered into suitable agreements with the U. S. A., the Federal Republic of Germany, Japan, Switzerland, and Belgium. Although plans call for national design standards in France in the future, at the present time mainly U. S. standards and criteria are employed in analyses of safety. The analyses ascertain such parameters in the development of a failure, caused by loss of coolant, as maximum temperature of fuel-element jacket, oxidation of the jacket, formation of hydrogen, and preservation of the geometry of the active zone, and also investigate the effect of the size, place, shape, and rate of formation of the break in the circuit. To study these problems, French specialists participate in the SATAN VI, WREFLOOD, COCO, and LOCTA VI programs on the primary circuit thermohydraulics. Analysis of the safety of water-moderated–water-cooled reactors in France revealed some errors in the computational programs used by Westinghouse (U. S. A.) in designing the PWR. The local pressure, flow rate, and density arising during leakage of underheated water are analyzed in accordance with the BLOWDOWN II computational program and the vertical and lateral forces are calculated in accordance with the FORCE-2 and LAT-FORCE programs. The following criteria are adhered to when designing the primary circuit: a break in the primary circuit does not result in a break in the steam line, a break in one loop of the circuit does not entail a break in the other loop, and a break in one branch of a loop does not entail a break in the other branch of the same loop.

The basis of most investigations consists of studying the effectiveness of the emergency cooling system. The first-generation computational programs gave conservative estimates whereas second-generation programs, e.g., POSEIDON (analog of the American TRAC program), still overestimate the maximum temperature of the fuel-element jackets (by roughly 100°C) even though they are more physical. An extensive experimental program is being carried out in France as a basis for computational methods: the study of coolant leakage and critical flow rates during decompression (CANON, MOBY DICK, and SUPER MOBY DICK facilities in Grenoble), research on heat exchange during decompression and flooding (OMEGA and ERSEC in Grenoble), the effect of the steam formed on the process of flooding (EPIS in Saclay), and nuclear heating (PHEBUS in Cadarache).

The PHEBUS facility consists of a pool reactor in whose core an experimental high-pressure loop containing the fuel assembly to the tested has been set up. The channel containing the fuel assembly is connected to a safety tube which in turn is connected to a safety jacket containing the experimental equipment. The experiments are designed to study a complex of phenomena which occur in a power reactor during failure due to the loss of coolant and subsequent flooding of the reactor core, as well as to estimate the effectiveness of a

Translated from Atomnaya Énergiya, Vol. 46, No. 5, pp. 366-367, May, 1979.

program for calculating the fuel-element temperature. The reactor control system can simulate an emergency reduction of the power reactor; equipment makes it possible for a circuit containing water at 330°C and 160 kg/ cm^2 to be depressurized in 50 msec and then to simulate energy cooling of the fuel element. The loop with the fuel assembly under study has been designed for a maximum power of 700 kW, with the linear maximum power in the fuel element reaching 570 W/cm. In the experiments the researchers will vary the diameter of the break, its position, the linear power of the energy released by the fuel elements, the internal pressure in the elements, and the flow rate of the low- and high-pressure flooding water.

It was proposed to bring the reactor up to 10 MW in April 1979, and to initially test fuel elements with a ^{235}U enrichment of 20%. Plans call for the power to be raised to 55 MW in the summer of 1979 at which time tests are to begin with new fuel assemblies containing up to 25 fuel elements each. Later, experiments will be conducted with spent fuel which will be supplied from the CAP reactor in Cadarache or from the BR-2 reactor in Belgium. The PHEBUS program which covers a 10-yr period (1973-1983) and is being carried out by French scientists is to cost 261 million francs: capital expenditures, 88 million francs; preparation of experiments, 33 million francs; and execution of experiments and processing of results, 140 million francs.

The mechanical behavior of the elements of the primary circuit during coolant leakage is studied on the AQUITAINE II and SUPER BEC stands in Cadarache, the interaction of steam with concrete is studied on the ECOTRA stand in Grenoble, and leaks between boxes, on the REBECA stand in Cadarache as well. The radiation consequences of failures due to coolant loss are studied on the FLASH facility in Grenoble.

The experiments are linked by a single objective, i.e., refining the theoretical and computational models used to substantiate the safety of atomic power plants and reducing the conservatism in the safety estimates. The margins thus found in the parameters of the processes occurring during a failure, it is proposed, will be used in the near future to ease the operating requirements on existing atomic power plants as well as those in the design stage and not to change the characteristics of atomic power plants or to cut the costs of safety systems.

The introduction of a quantitative probabilistic approach to the analysis of safety is facilitated by the experiments behind done at Fontenay-aux-Roses. In addition to the development of computational methods, the researchers there have developed, and built on the basis of similar devices, a complex of apparatus which gives designers a convenient and efficient working tool for the probabilistic analysis of systems under development. The use of a quantitative probabilistic method for analyzing various emergency cooling systems for new series of French atomic power plants with a block power of 1300 MW (electrical) showed that the probability of an emergency cooling system based on a $2 \times 133\%$ scheme failing is $3 \cdot 10^{-4}$ yr^{-1}, that of a system based on a $3 \times 100\%$ scheme is $2 \cdot 10^{-4}$ yr^{-1}, that of a $4 \times 100\%$ system is 10^{-4}, while a system based on a West German $4 \times 50\%$ scheme has a failure probability of 10^{-3} yr^{-1}. As a result, it was found that it would be most optimal to construct an emergency cooling system based on the $2 \times 133\%$ scheme.

Much space in French investigations is taken up by problems of resistance to earthquakes. On the basis of archival data, the historically most probable earthquake is determined for proposed site of an atomic power plant with account for the distance and intensity of possible earthquake foci. The maximum calculated earthquake is taken to be one number on the scale above the probable earthquake. The equipment and individual components of the equipment of atomic power plants are tested for earthquake resistance at Saclay on two vibration stands – VESUVE and TOURNESOL. The first lifting capacity of 20 tons makes it possible to obtain one-dimensional horizontal displacements of the table holding the equipment being tested while the second lifting capacity of 10 tons makes it possible to obtain a two-dimensional displacement (vertical and horizontal). These stands can reproduce sinusoidal vibrations with a frequency of up to 200 Hz as well as vibrations corresponding to earthquakes that had been recorded to really occur.

When atomic power stations are built in series the designs make allowance for one type of earthquake, with the local spectrum on the site of the plant being compared with a standard; in France, for an atomic power plant with a power of 1300 MW the standard adopted is the American standard spectrum of 0.16 g. The use of series atomic power plant designs for a maximum calculated earthquake of 8 on the seismic scale in regions of increased seismicity is conducive to the production of special antiseismic supports. Up to 2000 such elastic supports, constituting an assembly of alternating layers of stainless steel and an elastic elastomer, are installed beneath the building for an atomic power plant. In the event of an earthquake with a horizontal acceleration of up to 0.2 g, an atomic power plant on such supports withstands the elastic vibrations. In an earthquake of any intensity the elements of the foundation of the building experience an acceleration of no more than 0.2 g since the elastic supports do not transfer to the building any horizontal acceleration greater than 0.2 g and equalize the distribution of accelerations over height. In an earthquake with an acceleration exceeding 0.2 g, the building undergoes a movement on the supports; in the event of an acceleration of more than 0.6 g, this movement can reach 150 mm. The use of elastic supports increases the seismic resistance of the atomic power plant by 1-1.5 numbers on the seismic scale. At the present time such supports are being used (or are to be used) in eight atomic power plants, including the CRUAS atomic power plant under construction in France (four units of 900 MW each).

MEETING OF GROUP OF IAEA ADVISERS ON ATOMIC POWER PLANT SAFETY

O. M. Kovalevich

The 50th meeting of the senior advisers group within the framework of the IAEA Nuclear Safety Standards (NUSS) program on the elaboration of compendia and guides on ensuring the safety of atomic power plants was held in Vienna in December 1978. Before the meeting, the first official publications were prepared, in English, of the five main documents of the program: compendia of regulations "Governmental Organization," "Choice of Site," "Design," "Operation," and "Quality Control." Thus, after 4 years of work the first practical results have been published.

It can now be seen when the program will be completed in accordance with the planned list of documents (roughly by 1981). The future of the program and activity of the organizational mechanism set up by the IAEA for implementing it was discussed with the participation of leading staff members of the IAEA Secretariat. It was acknowledged that one of the next tasks should be to review the published documents of the program with allowance for experience gained from their application in various countries and changes that may have occurred in the approaches to atomic power plant safety.

The most important aspect of the future activity of the IAEA within the framework of the NUSS program is that of extending the range of topics dealt with. In its present form the program encompasses land-based stationary atomic power plants with thermal reactors, intended for energy production.

The discussion showed that it is desirable in future to incorporate fast and research reactors as well as various elements of the nuclear fuel cycle into the program. Differences were specified in the character and purpose of the documents produced within the framework of the NUSS program and similar documents elaborated under other IAEA programs. In accordance with the NUSS program, documents are being drawn up which are in the nature of standardizing technical documentation on a problem which has reached an appropriate level in respect of accumulation of experience and generalization of approaches. The documents of other IAEA programs on this problem are aimed at generalizing the scientific and engineering information and preparing a basis for documents under the NUSS program. Some measures were designated for extending the NUSS program to cover fast reactors.

Two guides were considered at the meeting: SG-02 "Inspection in the course of operation" and SG-S3 "Atmospheric dispersion in the choice of a site for an atomic power plant." The discussion on the first guide showed that inspections have been carried out in various countries and it is difficult to formulate any concrete recommendations. It was therefore resolved to merely make some general comments illuminating the principal aspects of this procedure and to request that the IAEA produce a more detailed technical document outside the framework of the NUSS program.

The SG-3 guide which was adopted reflected various approaches to the calculation of atmospheric dispersion of radioactive products in the event of a discharge from an atomic power plant. The guide, which is quite large (about 130 pp.), is of a concrete technical character in many ways and can serve as a handbook for practical use. In addition to discussing methods of calculating concentrations, it throws light on meteorological investigations on the site, control and measuring instruments and data accumulation, and takes account of extraordinary conditions.

Translated from Atomnaya Énergiya, Vol. 46, No. 5, p. 368, May, 1979.

 0038-531X/79/4605-0426$07.50

CHANGING YOUR ADDRESS?

In order to receive your journal without interruption, please complete this change of address notice and forward to the Publisher, 60 days in advance, if possible.

(Please Print)

Old Address:

name

address

city

state (or country) zip code

New Address

name

address

city

state (or country) zip code

date new address effective

name of journal

Declassified and Approved For Release 2013/02/12 : CIA-RDP10-02196R000800010005-1